The PHILOSOPHICAL MAGAZINE

FIRST PUBLISHED IN 1798

Vol. 42 SEVENTH SERIES No. 326 March, 1951

A Journal of Theoretical Experimental and Applied Physics

PRICE 12s. 0d.
Annual Subscription £6 0s. 0d. payable in advance.

AND PUBLISHED BY TAYLOR & FRANCIS LTD., RED LION COURT, FLEET ST., LONDON, E.C.4.

Early Scientific Publications

DIARY OF ROBERT HOOKE, M.A., M.D., F.R.S.
1672-1680

Edited by **H. W. ROBINSON** and **W. ADAMS**
Recommended for publication by the Royal Society, London

25/-
net

"This vivid record of the scientific, artistic and social activities of a remarkable man during remarkable years has too long remained in obscurity."—Extract from foreword by Sir Frederick Gowland Hopkins, O.M., President of the Royal Society.

MATHEMATICAL WORK OF JOHN WALLIS, D.D., F.R.S.

By **J. F. SCOTT, Ph.D., B.A.**

12/6
net

"His work will be indispensable to those interested in the early history of The Royal Society. I commend to all students of the Seventeenth Century, whether scientific or humane, this learned and lucid book."—Extract from foreword by Prof. E. N. da C. Andrade, D.Sc., Ph.D., F.R.S.
Recommended for publication by University of London

CORRESPONDENCE AND PAPERS OF EDMOND HALLEY

Arranged and Edited by **EUGENE FAIRFIELD MACPIKE**

21/-
net

First published on behalf of The History of Science Society by Oxford University Press. Now re-issued by Taylor & Francis, Ltd.

MEMOIRS OF SIR ISAAC NEWTON'S LIFE

5/-
net

By **WILLIAM STUKELEY, M.D., F.R.S., 1752**
From an Original Manuscript
Now in the possession of the Royal Society, London

HEVELIUS, FLAMSTEED AND HALLEY

12/6
net

Three Contemporary Astronomers and their Mutual Relations
By **EUGENE FAIRFIELD MACPIKE**
Published by arrangement with The History of Science Society

Established
over 150 years

TAYLOR & FRANCIS, LTD.
RED LION COURT, FLEET ST., LONDON E.C.
PRINTERS & PUBLISHERS OF SCIENTIFIC BOOKS

XXIII. *Renormalization of the Meson–Photon–Nucleon Interaction.*

By P. T. Matthews †,
Clare College, Cambridge, England ‡.

[Received October 27, 1950.]

Abstract

It is shown by direct calculation to fourth order in the coupling constants that all divergences, except those arising from the scattering of mesons by mesons, can be removed from the combined interaction of charged spinless mesons, nucleons (scalar interaction) and the electromagnetic field by mass and ' charge ' renormalization. The remaining divergence can be cancelled to this order by assuming a direct interaction between mesons with a suitably chosen coupling constant.

§ 1. Introduction.

Dyson (1949) has put Feynman's (1949) graphical technique for calculating the S-matrix elements in electrodynamics into the Schwinger (1948) Tomonaga (1946) form and has shown that the consistent application of mass and charge renormalization yields a finite theory to any order in the coupling constant. The analogous treatment of the scalar interaction of spinless mesons with nucleons has been given by the author (Matthews 1950 a) and also a summary of the graphical method as applied to charged spinless mesons in the electromagnetic field (1950 b). This latter interaction has been treated independently and in much greater detail by Rohrlich (1950). Here the extent to which renormalization is effective in removing the divergences from the combined interaction of neutrons, protons, charged spinless mesons (scalar interaction) and the electromagnet field is considered by direct calculation to fourth order in the coupling constants e and f. It is shown that for the removal of all divergencies, except those from the scattering of mesons by mesons, by mass and "charge" renormalization certain conditions between the infinite constants, which determine the renormalized charge, have to be satisfied. It is checked that these conditions are satisfied to second order. The remaining divergencies from the scattering of mesons by mesons can certainly be removed, to this order, by the introduction of a direct interaction between mesons with a suitably chosen constant thus leading to a finite S-matrix. (A brief report of these results has been published elsewhere (Matthews 1950 c).)

One of the conditions referred to above occurs in the interaction of spinless mesons with the electromagnetic field. Since the completion of these calculations, more general proofs of it have been given by Dyson (1950) and

† Communicated by the Author.
‡ Now at the Institute for Advanced Study, Princeton, N.J., U.S.A.

by Rohrlich (1950), based on gauge invariance. A similarly general solution has since been given by Salam (1950) of the present problem by a development of the work of Ward (1950). The problem in its complete generality is much complicated by the overlapping of divergent parts similar in principle to the "a" and "b" divergencies in self energy parts discussed by Dyson (1949, § VII) and no proof has yet been given, though there seems little doubt that this scheme does in fact lead to a finite S-matrix up to any order.

§ 2 Primitive Divergents.

The Hamiltonian in the interaction representation of the combined interaction for pseudo-scalar mesons is

$$H=\Sigma H_i, \quad (i=1, 2, 3) \quad . \quad . \quad . \quad . \quad . \quad . \quad . \quad (1)$$

where

$$H_1=\left(\frac{ie}{\hbar c}\right)A_\mu\left(\phi^*\frac{\partial\phi}{\partial x_\mu}-\frac{\partial\phi^*}{\partial x_\mu}\phi\right)-\left(\frac{ie}{\hbar c}\right)^2 A_\mu A_\nu\phi^*\phi\delta_{\mu\nu}, \quad . \quad . \quad . \quad (2)$$

$$H_2=if\bar{\psi}\gamma_5(\tau_-\phi^*+\tau_+\phi)\psi+\delta\lambda\phi^{*2}\phi^2, \quad . \quad . \quad . \quad . \quad . \quad . \quad . \quad (3)$$

$$H_3=ie\bar{\psi}\gamma_\mu\tau_P\psi A_\mu. \quad . \quad . \quad . \quad . \quad . \quad . \quad . \quad . \quad . \quad . \quad . \quad . \quad (4)$$

τ_+ operating on a neutron gives a proton and on a proton gives zero. τ_- is the same operator with the neutron and proton reversed. τ_P gives a proton when operating on a proton and zero when operating on a neutron. The terms required for mass renormalization have not been included. A term in H_1 explicitly dependent on the surface direction has also been omitted. This can be ignored without error if the corresponding term in the P-bracket of two derivatives of ϕ is also ignored (Matthews 1949.) Any scattering effect in which both the real and virtual processes are specified can be represented by a graph. Dotted lines denote photons, wavy lines with double arrow denote mesons, full lines with double arrows denote protons and full lines with single arrows denote neutrons. Thus double arrows signify the movement of charge and for charge to be conserved the double arrowed lines (either full or wavy) must form continuous loops (open or closed). Single arrows determine the motion of neutrons (as opposed to anti-neutrons) and for consistency the nucleon lines must form continuous loops of either single or double arrows. At any vertex with a photon line entering the other two lines must be double arrowed. At a meson–nucleon vertex the nucleon lines must be one double and one single arrow. If these rules are observed the τ-factors can be neglected. The rules for obtaining the corresponding S-matrix element can be summarized as follows (see Dyson (1949), Rohrlich (1950) and Matthews (1950 a and b)):

(i.) Each internal photon line give a factor

$$\hbar c\delta_{\mu\nu}(2\pi)^{-3}\int D_F(p)d^4p.$$

(ii.) Each integral meson line gives a factor

$$\hbar c(2\pi)^{-3}\int \Delta_F(p)d^4p,$$

(iii.) Each internal nucleon line gives a factor

$$(2\pi)^{-3}\int S_p(p)d^4p.$$

(iv.) Each meson–photon 3-vertex gives a factor

$$ie(\hbar c^{-2}(2\pi)^4(p_\mu+p'_\mu)\delta(p-p'+q),$$

where p and p' are the four-vectors of the meson lines entering and leaving the vertex, respectively. (The factor $(p_\mu+p'_\mu)$ arises from the derivatives in H_2.)

(v.) Each meson–photon 4-vertex gives a factor

$$-ie^2(\hbar c)^3(2\pi)^4\delta_{\mu\nu}\delta(p-p'+q-q').$$

(vi.) Each proton–photon vertex gives a factor

$$e(\hbar c)^{-1}(2\pi)^4\gamma_\mu.$$

(vii.) Each meson–nucleon vertex gives a factor

$$f(\hbar c)^{-1}(2\pi)^4\gamma_5.$$

(viii.) Each external photon line gives $A_\mu(k)$, each external meson line entering or leaving the graph gives $\phi(k)$ or $\phi^*(k)$, respectively. Each external nucleon line entering or leaving the graph gives $\bar{\psi}(k)$ or $\psi(k)$, respectively.

(ix.) There is a further numerical factor of $(-1)^{n-l-1}$, where n is the number of nucleon vertices and l is the number of closed nucleon loops. Finally, the whole integral is multiplied by the number of ways the operators can be paired off by interchanging the roles of the two photon operators at the 4-vertices.

The condition for primitive divergent graphs can be derived by Dyson's method (1949) and is

$$(3/2)E_n+E_m+E_p<5, \quad . \quad . \quad . \quad . \quad . \quad . \quad . \quad (5)$$

where E_n, E_m, and E_p are the numbers of external nucleon, meson and photon lines, respectively. Since the nucleon factors appear in H in pairs, E_n in (5) must be either two or zero. If E_n is two then for (5) to be satisfied, either E_m or E_p must be zero. Since the charge bearing lines in any graph form continuous loops, *the number of external charge bearing (double arrowed) lines in any part must be even* †. These considerations together show that the primitive divergents for the three field mixture, in terms of their external lines, are the same as for the separate pairs of interacting fields. They may, however, have different internal structure. Some of the new graphs are illustrated in fig. 1. (It should be noted that these all satisfy the charge conservation and consistency conditions given above).

† In the author's treatment of the meson–nucleon interaction[5] (1950 a), it was wrongly stated that for neutral mesons the divergences from parts with three external meson lines cancel by a type of Furry theorem (Furry 1937). Genuine divergences may arise from this type of graph for neutral mesons, but are definitely excluded for charged mesons by the charge conservation rule.

§3. Renormalization Conditions.

Considerations are now restricted to fourth order in the coupling constants e and f. To calculate the probability of any process one draws all the irreducible graphs of the process to this order. It should be remembered that C-parts (with two external meson and two external photon lines) are divergent. Any such part (except that with a single internal meson line; fig. 2 (a)) is replacable by a 4-vertex and counted as reducible. To obtain the corrections, after mass renormalization, due to the insertions of self-energy, vertex and C-parts, D_F and Δ_F must be replaced by D'_F and Δ'_F defined as

$$D'_F(p)=\left(1+\frac{\alpha}{2\pi}A\right)D_F(p)+D^{(2)}_{F1}(p), \quad . \quad . \quad . \quad . \quad . \quad . \quad (6)$$

$$\Delta'_F(p)=\left(1+\frac{\alpha}{2\pi}C+\frac{\beta}{2\pi}C'\right)\Delta_F(p)+\Delta^{(2)}_{F1}(p), \quad . \quad . \quad . \quad . \quad (7)$$

Fig. 1.

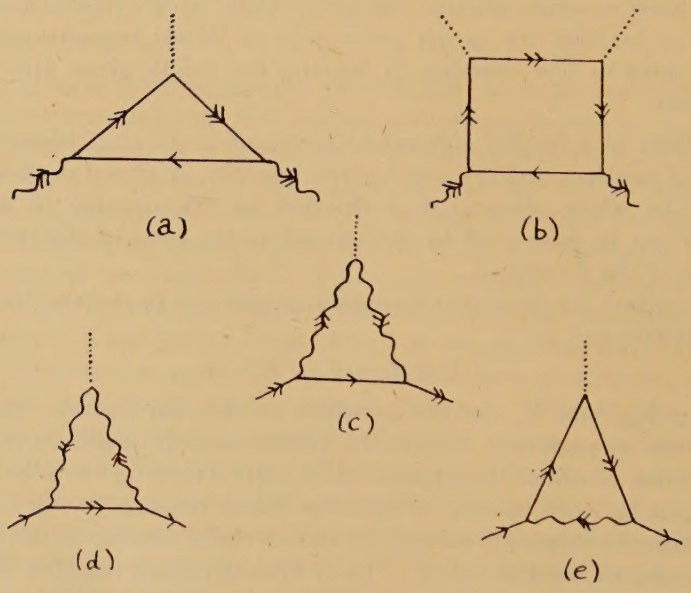

where $\alpha=e^2/4\pi\hbar c$ and $\beta=f^2/4\pi\hbar c$. A, C and C′ are infinite constants defined analogously to those occurring in Dyson's treatment of electrodynamics. $D^{(2)}_{F1}$ and $\Delta^{(2)}_{F1}(p)$ are finite and of second order in the coupling constants. The $S_F(p)$ factors for proton and neutron lines must be replaced, respectively, by

$$S^P_F(p)=\left(1+\frac{\alpha}{2\pi}B+\frac{\beta}{2\pi}B'\right)S_F(p)+S^{P(2)}_{F1}(p), \quad . \quad . \quad . \quad (8)$$

$$S^N_F(p)=\left(1+\frac{\beta}{2\pi}B'\right)S_F(p)+S^{N(2)}_{F1}(p). \quad . \quad . \quad . \quad . \quad . \quad . \quad (9)$$

Also the vertex factors γ_5, γ_μ, $(p_\mu+p'_\mu)$ and $\delta_{\mu\nu}$ must be replaced

$$\Gamma_5(p,p')=\left(1+\frac{\alpha}{2\pi}\mathrm{P}+\frac{\beta}{2\pi}\mathrm{P}'\right)\gamma_5+\Lambda_{51}^{(2)}(p,p'), \quad . \quad . \quad . \quad . \quad . \quad (10)$$

$$\Gamma_\mu(p,p')=\left(1+\frac{\alpha}{2\pi}\mathrm{L}+\frac{\beta}{2\pi}\mathrm{L}'\right)\gamma_\mu+\Lambda_1^{(2)}(p,p'), \quad . \quad . \quad . \quad . \quad . \quad (11)$$

$$\Phi_\mu(p,p')=\left(1+\frac{\alpha}{2\pi}\mathrm{N}+\frac{\beta}{2\pi}\mathrm{N}'\right)(p_\mu+p'_\mu)+\Phi_{\mu 1}^{(2)}(p,p'), \quad . \quad . \quad (12)$$

$$\Theta_{\mu\nu}(p,p',q)=\left(1+\frac{\alpha}{2\pi}\mathrm{R}+\frac{\beta}{2\pi}\mathrm{R}'\right)\delta_{\mu\nu}+\Theta_{\mu\nu 1}^{(2)}(p,p',q), \quad . \quad . \quad . \quad (13)$$

P, P′, L, L′, etc. are infinite constants and the final terms in these equations are all finite. The constants B and L have been calculated explicitly by Karplus and Kroll (1950). The "infinite parts" of the constants C, N and R have been calculated independently by Rohrlich (1950). Also external line factors must be replaced by $(1+\alpha/4\pi\mathrm{A})\mathrm{A}_\mu(k)$, for a photon, $(1+\alpha/4\pi\mathrm{C}+\beta/4\pi\mathrm{C}')\phi(k)$ for a meson, $(1+\alpha/4\pi\mathrm{B}+\beta/4\pi\mathrm{B}')\psi$ for a proton and $(1+\beta/4\pi\mathrm{B}')\ \psi$for a neutron.

Fig. 2.

(a) (b)

The idea of charge renormalization is to express any infinite term occurring in the calculation of a matrix element as a constant infinite multiple of a finite term of lower order and then to show that these infinite multiples can be absorbed by defining the observed coupling constants e_1 and f_1 as double power series in e and f. To see whether this can be done consistently in this case, consider the scattering of photons by mesons. The only irreducible graphs are shown in fig. 2. For renormalization to be effective, the infinite multiples of these graphs arising from the substitutions (7) and (12) into fig. 2 (*a*) and (13) into fig. 2 (*b*) must be the same, since each graph is of order e^2. There are also infinite multiples arising from substitutions in external lines, but since these are the same for both graphs they need not be considered. The required conditions are

$$2\mathrm{N}+\mathrm{C}=\mathrm{R}, \quad . \quad . \quad . \quad . \quad . \quad . \quad . \quad . \quad (14)$$

$$2\mathrm{N}'+\mathrm{C}'=\mathrm{R}'. \quad . \quad . \quad . \quad . \quad . \quad . \quad . \quad . \quad (15)$$

Condition (14) allows for insertions involving mesons and photons only and has been checked by Rohrlich (1950) and by the author (1950 b). Condition (15) arises from the additional parts due to virtual nucleons. (The term $2\mathrm{N}'$ comes from the insertion of fig. 1 (*a*) in the two vertices of fig 2 (*a*),

C′ from a meson self energy part due to virtual nucleons in the internal line of fig. 2 (*a*), and R′ from the insertion of fig. 1 (*b*) in the 4-vertex of fig. 2 (*b*). This condition has also been checked. The required charge renormalization is

$$e_1=e\left[1+\frac{\alpha}{2\pi}\left(\mathrm{N}+\mathrm{C}+\frac{\mathrm{A}}{2}\right)+\frac{\beta}{2\pi}(\mathrm{N}'+\mathrm{C}')\right], \quad . \; . \; . \; (16)$$

since each factor e is associated with a 3-vertex a meson line and half a photon line. As has just been verified, this same renormalization absorbs the factors R and R′ from the C-parts.

If processes involving real protons and photons are now considered, other infinities will arise from the substitutions (6), (8) and (11). These are removed by the charge renormalization

$$e_1=e\left[1+\frac{\alpha}{2\pi}\left(\mathrm{B}+\mathrm{L}+\frac{\mathrm{A}}{2}\right)+\frac{\beta}{2\pi}(\mathrm{B}'+\mathrm{L}')\right]. \; . \; . \; . \; (17)$$

For consistency this must be identical with (16). That is, it is required that

$$\mathrm{B}+\mathrm{L}=\mathrm{N}+\mathrm{C}, \quad . \; . \; . \; . \; . \; . \; . \; . \; (18)$$

$$\mathrm{B}'+\mathrm{L}'=\mathrm{N}'+\mathrm{C}'. \quad . \; . \; . \; . \; . \; . \; . \; (19)$$

In fact it is found that

$$\mathrm{B}=-\mathrm{L}, \quad \mathrm{B}'=-\mathrm{L}', \quad \mathrm{N}=-\mathrm{C}=\mathrm{R}, \quad \mathrm{N}'=-\mathrm{C}'=\mathrm{R}'. \; . \; . \; (20)$$

This means that the whole effective charge renormalization comes from photon self energy parts which are the same for both meson–photon and proton–photon effects, thus leading to the same charge renormalization for both.

For meson–nucleon effects the infinities arising from the substitutions (7), (8), (9) and (10) can be removed by the renormalization

$$f_1=f\left[1+\frac{\alpha}{2\pi}\left(\frac{\mathrm{B}}{2}+\frac{\mathrm{C}}{2}+\mathrm{P}\right)+\frac{\beta}{2\pi}\left(\mathrm{B}'+\frac{\mathrm{C}'}{2}+\mathrm{P}'\right)\right]. \; . \; . \; (21)$$

This can be made independently of (16).

A further possible source of divergence is from graphs with one photon and two neutron external lines (fig. 1 (*d*) and (*e*)). Since no (finite) single vertex of this type exists no renormalization is possible.

However, though each graph diverges separately, the total is finite and no difficulty arises. These graphs lead to the finite neutron magnetic moment which has been discussed in this framework by Case (1949)).

The only remaining divergencies are those from the scattering of mesons by mesons (M-parts), with four external meson lines. This can occur either through virtual nucleons, (f^4), or virtual photons, (e^4), and in each case gives a genuine divergence. To this order these divergences can be cancelled by a suitable choice of the constant in the direct interaction $\delta\lambda\phi^{*2}\phi^2$. This device has been considered more generally by the author (1950 a) for the meson–nucleon interaction and by Rohrlich (1950) for the meson–photon interaction. The former treatment was very incomplete because secondary infinities from parts such as fig. 3 were not considered.

Rohrlich's development is more thorough but there are difficulties when such parts appear inside self energy parts which are not dealt with in detail. This point will be discussed further in a forthcoming paper by Mr. A. Salam.

The whole of the discussion is also applicable to scalar mesons. (It is only necessary to replace $(\gamma_5)_{\alpha\beta}$ by $-i\delta_{\alpha\beta}$.)

Fig. 3.

Acknowledgments.

The author would like to thank Professor W. Pauli for suggesting this problem and for his continued interest, also Dr. N. Kemmer and Mr. A. Salam for stimulating discussions and Drs. F. Rohrlich and D. Feldman for helpful criticism.

APPENDIX.

The calculation of the infinite constants was performed by the methods due to Feynman (1949) as employed by Karplus and Kroll (1950). The "infinite parts" of all the constants can be expressed in terms of

$$\mathrm{I}=\frac{1}{i\pi^2}\int\frac{d^4k}{k^2+\mu^2}$$

and are

$$\mathrm{A}=-\tfrac{3}{2}\mathrm{I},\quad \mathrm{P}=\tfrac{1}{2}\mathrm{I},\quad \mathrm{P}'=0,$$
$$\mathrm{N}=-\mathrm{C}=\mathrm{R}=-\mathrm{I},\qquad \mathrm{B}=-\mathrm{L}=\tfrac{1}{2}\mathrm{I},$$
$$\mathrm{N}'=-\mathrm{C}'=\mathrm{R}'=\mathrm{I},\qquad \mathrm{B}'=-\mathrm{L}'=\tfrac{1}{4}\mathrm{I}.$$

(It is readily seen that the single and double arrows cannot be inserted consistently in the graph of this order corresponding to P′. This is not true for higher orders.)

References.

Case, K. M., 1949, *Phys. Rev.*, **76,** 1.
Dyson, F. J., 1949, *Phys. Rev.*, **75,** 486, 1736; 1950, Private communication.
Feynman, R. P., 1949, *Phys. Rev.*, **76,** 749, 769.
Furry, W., 1937, *Phys. Rev.*, **51,** 125.
Karplus, R., and Kroll, N. M., 1950, *Phys. Rev.*, **77,** 536.
Matthews, P. T., 1949, *Phys. Rev.*, **76,** 1254; 1950 a, *Phil. Mag.*, **41,** 185; 1950 b, *Phys. Rev.*, **80,** 292; 1950 c, *Ibid.*, **80,** 292.
Rohrlich, F., 1950, *Phys. Rev.*, **80,** 666.
Salam, A., 1950, *Phys. Rev.*, **79,** 910.
Schwinger, J., 1948, *Phys. Rev.*, **74,** 1439; **75,** 651.
Tomonaga, S., 1946, *Prog. Theor. Phys.*, **1,** 27.
Ward, J. C., 1950, *Phys. Rev.*, **77,** 293; **78,** 182.

XXIV. *A Generalization of Reversion Formulæ with their Application to Non-linear Differential Equations.*

By A. C. Sim,
Standard Telecommunication Laboratories Ltd.*

[Received January 11, 1951.]

Summary.

The formulæ for algebraic reversion are extended to revert a class of non-integral power series, and also generalized to revert series in which the coefficients contain operators. These formulæ are shown to have a simple and powerful application to non-linear differential equations, which they expand into an infinite sequence of linear equations.

§1. Introduction.

The studies of semiconductors and saturable iron-cored coils are two of many important fields in modern physics and engineering which lead to non-linear problems of practical importance. Such problems occur also, for example, in aerodynamic and navigational theories, in the analysis of electronic circuits, and in nuclear physics. A comprehensive survey of the theory of non-linear mechanics has been published by Minorsky (1947), from which it is clear that the number of methods which are not restricted to one type of problem is very small, and most of the remainder are concerned with non-linear oscillatory equations. The method of reversion described herein is applicable to a wide variety of equations, of which some appear otherwise intractable, provided the equations are expansible in powers of the unknown quantity.

The existing reversion formulæ are applicable only to algebraic equations, and are used extensively for the calculation of roots. The problem may be defined as follows. Given the series

$$\lambda = \sum_{r=1}^{\infty} a_r . y^r, \qquad \ldots\ldots\ldots \quad (1)$$

the coefficients A_r in the reverted series expansion

$$y = \sum_{r=1}^{\infty} A_r . \lambda^r \qquad \ldots\ldots\ldots \quad (2)$$

have to be found. Van Orstrand (1910) has published a very full account of such formulæ and their applications. In addition, a special type of series occurring in the theory of Bessel functions and having the form

$$\{y^{-1} + a_1 y + a_3 y^3 + \ldots . \} = \lambda \qquad \ldots\ldots \quad (3)$$

has been reverted by Bickley and Miller (1943).

* Communicated by Professor D. Gabor.

If the series (1) and (2) converge * it is clear that (2) is a solution of the equation (1), but not necessarily the only solution. In fact it is the solution which vanishes as λ approaches zero, and is, in general, the smallest real solution. If equation (1) possesses no real solution (2) will diverge.

The reversion formulæ may be obtained in two ways, of which the most obvious is the substitution of (2) into (1). The quantities A_r are then found by equating the coefficients of λ^r on each side of the equation. A more elegant approach, due to Harkness and Morley (1898), involves differentiating (2) with respect to y and multiplying each side by λ^{-r}. This gives

$$\lambda^{-r}=d\lambda/dy\{A_1\lambda^{-r}+\ldots.+rA_r\lambda^{-1}+\ldots.\}. \quad . \quad . \quad . \quad . \quad (4)$$

It is then argued that the relation $\lambda^n \,.\, d\lambda/dy=(n+1)^{-1} \,.\, d\lambda^{n+1}/dy$ is true for all n except $n=-1$; and since λ^{n+1} is a power series in y, its derivative cannot contain a term proportional to $\lambda^{-1} \,.\, d\lambda/dy$, because this can only arise from the differentiation of $\log \lambda$. It follows therefore, from (4), that the coefficient of y^{-1} in the power series expansion of λ^{-r} is rA_r, and hence

$$rA_r=\text{coefficient of } y^{-1} \text{ in } \{a_1y+a_2y^2+\ldots.\}^{-r}. \quad . \quad . \quad . \quad (5)$$

It is clear that the evaluation of (5) will assume that the coefficients a_r commute, and this method therefore fails in general when operators are involved.

§2. Reversion.

The series (1) and (3) described above are special cases of the non-integral power series

$$\{a_0y^{(1+n\alpha)}+a_1y^{(1+\overline{n+1}\alpha)}+\ldots.+a_ry^{(1+\overline{n+r}\alpha)}+\ldots.\}=\lambda\phi(x). \quad . \quad (6)$$

This series is the most general one that can be reverted. The coefficients a_r may be any functions of x, d/dx, or any other operator, but they must be independent of y. The real quantity α is quite arbitrary; n is an integer—positive, negative, or zero , and λ is a constant.

In the reversion of (6) it is most convenient to consider $y^{(1+n\alpha)}$ as the unknown quantity. Inspection shows that the reverted series will be in powers of y^m where $m=\alpha/(1+n\alpha)$, so that the solution may be assumed to have the form

$$y^{(1+n\alpha)}=\lambda\sum_{r=0}^{\infty}A_r \,.\, \lambda^{mr}. \quad . \quad . \quad . \quad . \quad . \quad . \quad . \quad . \quad (7)$$

In determining A_r the extended multinomial theorem is required. This may be written in the form

$$\{u_1k+u_2k^2+\ldots+u_rk^r+\ldots\}^{\nu}=\sum_{r=0}^{\infty}\sum_{p}\frac{\Gamma(1+\nu)}{\Gamma(1+q)}\cdot\frac{u_2^{p_2}\ldots u_r^{p_r}}{p_2!\ldots p_r!}\cdot u_1^qk^{(\nu+r)},$$

$$. \quad . \quad . \quad (8)$$

---

* Harkness and Morley (1893) have shown that the reverted series (2) converges in the same domain as the original series (1).

where the exponents q and p_r assume all values which satisfy the two relations

$$(p_2+p_3+\ldots.+p_r)=(\nu-q),$$
$$(p_2+2p_3+\ldots.+(r-1)p_r)=r.$$

It should be noted that p_r and $(\nu-q)$ are positive integers, and when ν is negative, the ratio $\Gamma(1+\nu)/\Gamma(1+q)$ in (8) should be replaced by

$$(-1)^{(\nu-q)}.\Gamma(-q)/\Gamma(-\nu).$$

By direct substitution of (7) into (6) using (8), the reversion coefficients are found to be given by

$$\begin{aligned}
a_0.A_0&=\phi(x),\\
a_0.A_1&=-a_1.A_0^{(1+m)},\\
a_0.A_2&=-\{a_1.(1+m)A_0^mA_1+a_2.A_0^{(1+2m)}\},\\
a_0.A_3&=-\{a_1.(1+m)[mA_0^{(m-1)}A_1^2/2\,!+A_0^mA_2]\\
&\quad+a_2.(1+2m)A_0^{2m}A_1+a_3.A_0^{(1+3m)}\},\\
a_0.A_4&=-\{a_1.(1+m)[m(m-1)A_0^{(m-2)}A_1^3/3\,!+mA_0^{(m-1)}A_1A_2+A_0^mA_3]\\
&\quad+a_2.(1+2m)[2mA_0^{(2m-1)}A_1^2/2\,!+A_0^{2m}A_2]\\
&\quad+a_3.(1+3m)A_0^{3m}A_1+a_4.A_0^{(1+4m)}\},
\end{aligned}$$

and the general term

$$\left.\begin{aligned}
a_0.A_r&=-\sum_{s=1}^{r}a_s.\sum_p\frac{\Gamma(2+ms)}{\Gamma(1+p_0)}.A_0^{p_0}.\frac{A_1^{p_1}\ldots A_{r-s}^{p_{r-s}}}{p_1!\ldots p_{r-s}!},\\
\text{where}\quad&(p_1+p_2+\ldots.+p_{r-s})=(1+ms-p_0)\\
\text{and}\quad&(p_1+2p_2+\ldots.+(r-s)p_{r-s})=(r-s).
\end{aligned}\right\}\quad\ldots\quad(9)$$

Note that $(1+ms-p_0)$ is always a positive integer.

In the general term of (9) when $(1+ms)$ is negative the ratio

$$\Gamma(2+ms)/\Gamma(1+p_0)$$

should be replaced by $(-1)^{(1+ms+p_0)}.\Gamma(-p_0)/\Gamma(-1-ms)$.

In general, the formulæ given by (9) represent a sequence of linear ordinary differential, or integro-differential equations determining the functions A_r. The equation $a_0.A_0=\phi(x)$ is referred to as the *generating equation* and its solution A_0 is termed the *generating function* since the complete solution is expressed in terms of it. The generating function is a first approximation to the true solution and the generating equation is a linear approximation of the original non-linear equation.

It may be noted that if the coefficients a_r commute a simplified formula can be obtained by the method of Harkness and Morley. It is then convenient to change the notation, writing the series in the form

$$z^\beta\{a_0+a_1z+\ldots.+a_rz^r+\ldots.\}=\lambda,\quad\ldots\quad(10)$$

in which β has replaced $(n+\alpha^{-1})$ and z is written for y^{α}. The function $\phi(x)$ is now included in λ. Any arbitrary power of z may be found in this case so that a solution may be assumed in the form

$$z^s=(\lambda/a_0)^{sm}\sum_{r=0}^{\infty} B_r\lambda^{rm}, \quad . \quad . \quad . \quad . \quad . \quad . \quad . \quad . \quad (11)$$

where s is quite arbitrary but real, and m now represents β^{-1}. The coefficients A_r for this series are found to be

$$B_0=1, \quad B_1=-sm\,.\,a_0^{-(1+m)}a_1,$$

$$B_2=sm\{(1+\overline{2+s}\,.\,m)a_0^{-2(1+m)}a_1^2/2\,!-a_0^{-(1+2m)}a_2\},$$

$$B_3=-sm\{(1+\overline{3+s}\,.\,m)(2+\overline{3+s}\,.\,m)a_0^{-3(1+m)}a_1^3/3\,!$$
$$-(1+\overline{3+s}\,.\,m)a_0^{-(2+3m)}a_1a_2+a_0^{-(1+3m)}a_3\},$$

$$B_4=sm\{(1+\overline{4+s}\,.\,m)(2+\overline{4+s}\,.\,m)(3+\overline{4+s}\,.\,m)a_0^{-4(1+m)}a_1^4/4\,!$$
$$-(1+\overline{4+s}\,.\,m)(2+\overline{4+s}\,.\,m)a_0^{-(3+4m)}a_1^2a_2/2\,!$$
$$+(1+\overline{4+s}\,.\,m)a_0^{-2(1+2m)}(a_1a_3+a_2^2/2\,!)-a_0^{-(1+4m)}a_4\},$$

and the general term

$$\left.\begin{aligned} B_r=s/(s+r)\sum_p \frac{(-1)^{(p_0-rm)}\,.\,\Gamma(p_0+sm)}{\Gamma(\overline{s+r}\,.\,m)}\,.\,a_0^{-p_0}\,.\,\frac{a_1^{p_1}\ldots a_r^{p_r}}{p_1!\ldots p_r!}, \\ \text{where} \quad (p_1+p_2+\ldots+p_r) \;=(p_0-rm, \\ (p_1+2p_2+\ldots+rp_r) \;=r. \end{aligned}\right\} \quad . \quad . \quad . \quad (12)$$

In this case when $(s+r)m$ becomes negative the quantity

$$(-1)^{(p_0-rm)}\,.\,\Gamma(p_0+sm)/\Gamma(\overline{s+r}\,.\,m)$$

must be replaced by the ratio $\Gamma(1-\overline{s+r}\,.\,m)/\Gamma(1-p_0-sm)$.

Whilst Van Orstrand has dealt adequately with the application of reversion formulæ to equations not involving operators, it may be noted that the extended form of equation given by (10) offers alternative forms of solution, and will also yield results when applied to some equations containing fractional powers. For example, the equation

$$(x^3+c_2x^2+c_1x)=c_0$$

reverts to a series in powers of c_0. It may be, however, that c_0 is very large and c_1 is the smallest coefficient. Division of the equation by x gives $(x^2+c_2x-c_0x^{-1})=-c_1$ which may also be reverted, producing a more convergent series. It is also possible, using (12) to revert the equation $(c_ax^a+c_bx^b)=c_0$ for any values of a and b provided they are real.

§3. Non-Linear Equations.

To apply the general reversion formulæ (9) to a non-linear differential equation, the equation must first be expanded in an ascending or descending power series of the unknown function y—the coefficients being expressed in terms of x and $D=d/dx$, and arranged so that they contain no negative powers of D. If a general solution is required, the *generating coefficient* a_0, which is the first one in the series, must be of the highest degree in D so that the generating equation has the same order as the equation to be solved.

The set of equations given by the reversion formulæ (9) are all similar in form to the generating equation, although the functions of x on the right-hand side become progressively more complicated as r increases. Each equation, therefore, will give rise to the same number of arbitrary constants. For a complete solution of the equation to be reverted, a *general* solution of the generating equation must be found, whilst only *particular* solutions of the remaining equations for A_r are required. The choice of these particular solutions affects not only the form of the series obtained, but also the ease with which the arbitrary constants are determined from the boundary conditions of the problem, and the convergence and complexity of the reverted series.

If the reverted solution of an equation does not contain sufficient arbitrary constants, or does not converge in a convenient range, the form of solution may frequently be improved by a change of variable. In all applications, therefore, every conceivable form of the expanded equation should be considered, to decide which one is most advantageous. Convergence of the reverted solution must be examined in each individual case, since a general discussion does not appear to be possible. Because of the complexity in deriving a large number of terms of the reverted series, it is usually easiest to check its accuracy and convergence by substituting the few terms obtained into the equation, and examining the remainder which results. Even this procedure can be very formidable, in which case a numerical substitution into the equation affords the only practical verification.

§4. Equations with Initial Boundary Conditions.

It is generally the case that the arbitrary constants in the solution of a non-linear equation are so woven within it that their determination becomes a difficult task. In this section it will be shown that when the generating equation is linear with constant coefficients, as is frequently the case in practise, a form of solution can always be found by reversion which makes the calculation of arbitrary constants from initial conditions as easy as in the case of a linear equation. This is achieved by choosing the particular solutions for the functions A_r so that they all vanish (and also their first $n-1$ derivatives where n is the order of the equation), when the independent variable is zero. The constants can then be rigorously calculated by regarding the generating function as the complete solution for the

purpose. The particular form of the generating function thus obtained can then be used for the derivation of the subsequent terms in the series until sufficient accuracy is obtained from them.

It is now assumed that the generating coefficient a_0 is a polynomial in powers of $D=d/dx$ with constant coefficients. If the degree of this polynomial (equal to the order of the non-linear equation), is n, the inverse of a_0 may be expanded into partial fractions. Let these partial fractions have the form

$$a_0^{-1}=\left\{\sum_{q=1}^{n-R}\frac{\gamma_q}{(D+\alpha_q)}+\sum_{s=1}^{t}\sum_{q=1}^{r_s}\frac{\delta_{q,s}}{(D+\beta_s)^q}\right\}, \quad . \ . \ . \quad (13)$$

in which $-\alpha_1$, $-\alpha_2$, ... , are the non-repeating zeros of a_0, and $-\beta_1$, $-\beta_2$, ... , are t roots which are repeated r_1, r_2, ... , t, times. The coefficients γ_q and $\delta_{q,s}$ are constants depending on the polynomial coefficients which are not defined here. The quantity R is the difference between the degree of the polynomial and the number of non-repeating roots, *i.e.* $R=\Sigma r_s$.

The reversion functions A_r are all defined by the operation of the collection of operators given by (13) on a function of x which is known or can be explicitly determined. Let $f(x)$ represent this function for a particular A_r. It is desired to find a particular solution to this operation which will vanish with its first $n-1$ derivatives when x is zero, then $D^u \,.\, a_0^{-1} \,.\, f(x)$ is required for $u=0, 1, \ldots, n-1$.

With the aid of the contracting notation

$$\delta_s(\beta_s-\delta_s)^u \equiv \sum_{q=1}^{u}\frac{(-1)^{q-1}\,.\,u!}{(u-q)!\,q!}\,.\,\beta_s^{(1+u-q)}\,.\,\delta_{q,s}, \quad . \ . \ . \quad (14)$$

it can be found by means of simple algebraic manœuvres that

$$\sum_{q=1}^{r}\frac{D^u\delta_{q\,s}}{(D+\beta_s)^q}=\delta_s\sum_{q=1}^{u}(\delta_s-\beta_s)^{q-1}\,.\,D^{u-q}+(\delta_s-\beta_s)^u\sum_{q=1}^{r}\left\{\frac{\delta_s}{D+\beta_s}\right\}^q \quad . \ . \quad (15)$$

Thus in the determination of A_r the only operations that need to be considered are $D^q \,.\, f(x)$ and $(D+\beta_s)^{-q} \,.\, f(x)$. The first of these is simply a repeated differentiation, whilst the second is readily interpreted using the operator shifting theorem. A solution which vanishes when x is zero can thus be written

$$(D+\beta_s)^{-q} \,.\, f(x)=e^{-\beta_s x}\int_0^x dx\int_0^x dx \ldots (q \text{ times}) \int_0^x e^{\beta_s x} \,.\, f(x) \,.\, dx. \quad . \quad (16)$$

Since a_0 is defined to be a polynomial of degree n in D, if a_0^{-1} is expanded in powers of D^{-1} the series obtained will commence with a term in $D^{\,n}$. But, by expanding the right-hand side of (13) in powers of D^{-1} some terms containing lower powers are obtained. By equating the two expansions it follows that the coefficients of $D^{\,k}$ in the expansion of (13) for $k=1, \ldots, n-1$, are zero. In the notation of (14) this result can be found to be

$$\left\{\sum_{q=1}^{n-R}\alpha_q^k\gamma_q+\sum_{s=1}^{t}(-1)^k\delta_s(\delta_s-\beta_s)^k\right\}=0 \quad k=0, 1, \ldots, (n-2). \quad (17)$$

It now follows from (13) and (15) that

$$[\mathrm{D}^u . \mathrm{A}_r]_{x=0} = \left\{ \sum_{k=0}^{n-1} \sum_{q=1}^{n-\mathrm{R}} (-1)^k \alpha_q^k \gamma_q \mathrm{D}^{(u-1-k)} . f(x) + \sum_{s=1}^{t} \delta_s \sum_{k=0}^{u-1} (\delta_s - \beta_s)^k \mathrm{D}^{(u-1-k)} . f(x) \right\}_{x=0}$$

$$u=0, 1, \ldots, (n-1) \quad r \neq 0. \quad . \quad . \quad . \quad (18)$$

Finally, from (17) and (18) it is seen that if a solution for A_r is obtained in this special case that vanishes when $x=0$, then its first $(n-1)$ derivatives will also vanish when $x=0$, *i. e.*

If $\mathrm{A}_r=0$ *when* $x=0$, *then*

$$(d^u \mathrm{A}_r / dx^u)_{(x=0)} = 0 \text{ for } u=1, 2, \ldots, (n-1), \quad . \quad . \quad . \quad (19)$$

when a_0 *is a polynomial of* nth *degree in* D *with constant coefficients.*

§5. A Special Equation.

Apart from the general power series (6), it is possible to revert the equation

$$\mathrm{P} . y = \{\phi(x) + f(y)\} \quad . \quad . \quad . \quad . \quad . \quad . \quad . \quad (20)$$

when $f(y)$ is any function of x and y, but $\phi(x)$ is independent of y as before. P is any operator. Note that it is not possible to extract a common factor λ in this case. This form of reversion may be useful when the equation is not expansible in powers of y, since the procedure does not demand this. To solve the equation a solution may be assumed to exist in the form

$$y = \{\mathrm{P}^{-1} . \phi(x) + \mathrm{F}(x)\} \quad . \quad . \quad . \quad . \quad . \quad . \quad . \quad (21)$$

and this may be substituted into (20). A power series in $\mathrm{F}(x)$ is then obtained by expanding $f(y)$ using Taylor's theorem. The resulting series can then be reverted by means of the formulæ already derived in § 2 of this paper. The final reverted solution is then

$$y = \sum_{r=0}^{\infty} \mathrm{C}_r \quad . \quad . \quad . \quad . \quad . \quad . \quad . \quad . \quad . \quad (22)$$

in which

$$\begin{aligned} \mathrm{P} . \mathrm{C}_0 &= \phi(x), \\ (\mathrm{P} - f') . \mathrm{C}_1 &= f(\mathrm{C}_0), \\ (\mathrm{P} - f') . \mathrm{C}_2 &= f'' . \mathrm{C}_1^2 / 2 !, \\ (\mathrm{P} - f') . \mathrm{C}_3 &= \{f'' . \mathrm{C}_1 \mathrm{C}_2 + f''' . \mathrm{C}_1^3 / 3 !\} \text{ etc.} \quad . \quad . \quad . \quad (23) \end{aligned}$$

with the abbreviation $f^r \equiv \left[\frac{\partial r}{\partial x^r} . f(y) \right]_{y=\mathrm{C}_0}$.

A similar set of formulæ may be derived for the case when (20) is without operators, and it is easy to verify that the result is equivalent to that obtained by Lagrangian expansion (Whittaker and Watson 1950).

§6. Illustrations.

(1) Semiconducting materials are sometimes used for shunting switches to reduce transients in the breaking of inductive circuits. In the circuit of fig. 1, an inductive coil is represented by resistance R and inductance L in series, and it is supplied from a battery of voltage E. The switch S is shunted by a non-linear resistor possessing the characteristic $V=KI^c$, where V is the voltage across it, I the current through it, and K and c are constants. The equation satisfied by the current may be written

$$I_0=\{D\,.\,I+I+aI^c\}, \quad . \quad . \quad . \quad . \quad . \quad . \quad . \quad . \quad (24)$$

where the constant a represents the ratio K/R, and the operator D is equivalent to $L/R\,.\,d/dt$. I_0 is the initial value of I, equal to E/R.

Fig. 1.

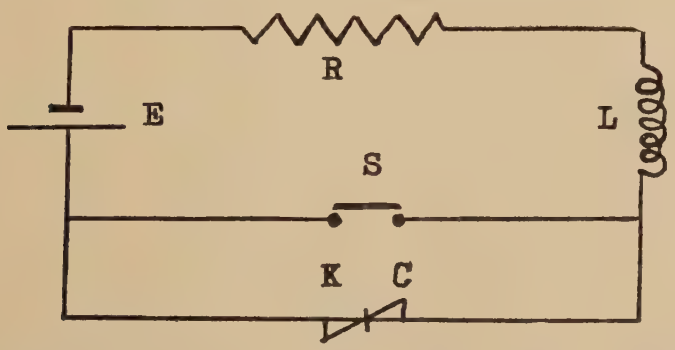

This equation has the special form discussed in § 4. The generating equation is $(D+1)\,.\,I=I_0$ so that the generating function is

$$I_0(1-\exp[-Rt/L])+A\exp[-Rt/L],$$

where A is a constant. Regarding this as the complete solution for the purpose of determining A, it is found that the exponential terms vanish, so that in this case the generating function is simply I_0. From this and equation (9), the next term in the reverted series is $-(D+1)^{-1}\,.\,aI_0^c$, and the series is found to be

$$I=\{I_0-aI_0^c(1-\exp[-Rt/L])+ca^2I_0^{(2c-1)}(1-\exp[-Rt/L](1+Rt/L))\ldots\}. \quad . \quad . \quad . \quad (25)$$

As in the case of algebraic reversion, if the unknown quantity I is replaced by a known approximate solution plus a new dependent variable, the reverted series will then converge more rapidly. In this problem it is known that the initial value of I is I_0, so that the substitution of $(I'+I_0)$ for I should improve convergence. This transforms the equation to

$$\{(D+1)\,.\,I'+a(I'+I_0)^c\}=0. \quad . \quad . \quad . \quad . \quad . \quad . \quad (26)$$

Defining parameters p and q by

$$p=[1+ac\mathrm{I}_0^{(c-1)}] \qquad q=ac(c-1)\mathrm{I}_0^{(c-2)}/2$$

and expanding the second term in (26) by the binomial theorem puts the equation in a suitable form for reversion

$$\{(\mathrm{D}+p)\mathrm{I}'+q\mathrm{I}'^2+\ldots\}=-a\mathrm{I}_0^c. \quad . \quad . \quad . \quad . \quad . \quad (27)$$

Reversion of this series produces a series more rapidly convergent when a and c are large, and no less convergent when they are small

$$\mathrm{I}=\{\mathrm{I}_0-ap^{-1}\mathrm{I}_0^c(1-\exp[-p\mathrm{R}t/\mathrm{L}])$$
$$-a^2p^{-3}q\mathrm{I}_0^c(1-\exp[-2p\mathrm{R}t/\mathrm{L}]-2\mathrm{R}t/\mathrm{L}\,.\exp[-p\mathrm{R}t/\mathrm{L}])\ldots\}. \quad (28)$$

Fig. 2.

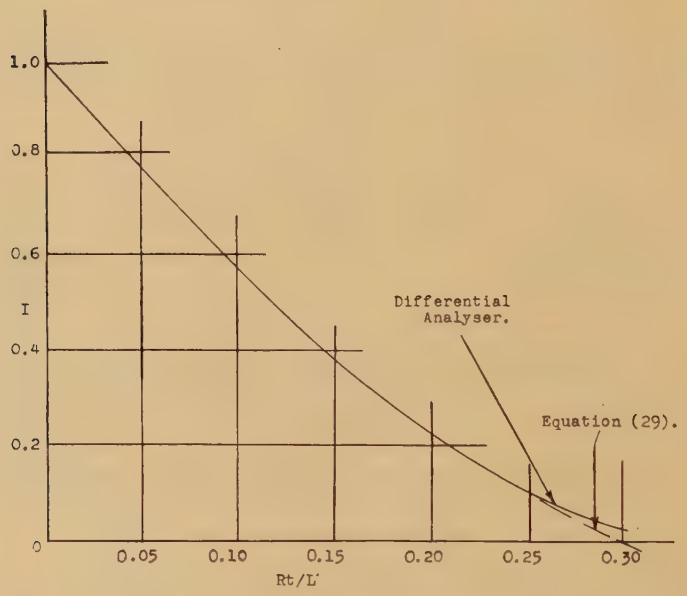

This problem has been analysed by Fairweather and Ingham (1941) using a differential analyser, and it is interesting to compare equation (28) with their results. As a particular numerical case, let $c=0{\cdot}2$, $\mathrm{K}=240$, $\mathrm{R}=50$ and $\mathrm{E}=50$. Then $\mathrm{I}_0=1$, $a=4{\cdot}8$, $p=1{\cdot}96$, and $q=-0{\cdot}384$. Equation (28) then assumes the form

$$\mathrm{I}=\{1-2{\cdot}45(1-\exp[-1{\cdot}96\mathrm{R}t/\mathrm{L}])$$
$$-1{\cdot}182(1-3{\cdot}92\exp[-1{\cdot}96\mathrm{R}t/\mathrm{L}]-\exp[-3{\cdot}92\mathrm{R}t/\mathrm{L}])\ldots\}. \quad (29)$$

In fig. 2 a plot of this expression is compared with the curve obtained on the differential analyser.

(2) The functional equation* $f(x+1)=e^{f(x)}$ may be written in the form $e^{\mathrm{D}}\,.f(x)=e^{f(x)}$, and with $y=f(x)$ this may be expanded into the series

$$\{(e^{\mathrm{D}}-1)\,.\,y-y^2/2\,!-y^3/3\,!\ldots\}=1. \quad . \quad . \quad . \quad . \quad . \quad (30)$$

* This problem was communicated by Professor K. W. Miller of the Armour Research Foundation, Chicago, Ill.

A solution of this equation is required that vanishes when $x=0$. Using the expansion

$$(e^{D}-1)^{-1}=D^{-1}\{1-D/2+D^2/12 \ldots -(-1)^n D^{2n} \cdot B_n/(2n)!\},$$

where B_n is the nth Bernoulli number, the generating function is seen to be $A_0=(e^{D}-1)^{-1} \cdot 1=(x+a)$ where a is a constant, and in this case $a=0$. Proceeding with the reversion leads to

$$y=f(x)=\{x+x(1-x)[(1-2x)/12+(2-13x+17x^2-8x^3)/240 \ldots]\}. \quad . \quad (31)$$

(3) The performance of an anharmonic oscillator satisfies the equation

$$\{(D^2+a^2) \cdot y+by^2\}=0. \quad . \quad . \quad . \quad . \quad . \quad . \quad . \quad (32)$$

For a general solution the generating function is $A \cos (ax+c)$ where A and c are constants. Reversion then produces the series

$$y=\{A \cos (ax+c)-bA^2/2a^2[1-\cos (ax)+\cos (ax+2c)/3 -\cos 2(ax+c)/3-\sin (2c) \cdot \sin (ax)] \ldots\}. \quad . \quad . \quad . \quad (33)$$

(4) The Thomas–Fermi equation of atomic theory is, in dimensionless form,

$$\frac{d^2\phi}{dx^2}=x^{-1/2} \cdot \phi^{3/2} \quad \text{with} \quad \phi(0)=1, \quad \phi(\infty)=0. \quad . \quad . \quad . \quad (34)$$

Referring to the general expression (6), it is seen that for this case

$$a_0=D^2, \qquad \alpha=\tfrac{1}{2}, \qquad n=0, \qquad m=\tfrac{1}{2}, \qquad a_1=-x^{-1/2}$$

and all the remaining a_r are zero. ($\phi(x)$ in (6) is zero.)

The generating function is clearly of the form $(b+ax)$. If b is put equal to 1 to satisfy the first boundary condition, the subsequent functions A_r must be chosen so that they vanish when x is zero. Thus

$$\begin{aligned} A_1&=\int_0^x \int_0^x x^{-1/2} \cdot (1+ax)^{3/2} \cdot dx\, dx \\ &=a^{-3/2}\{z(1+z^2)^{1/2}[z^4/6+2z^2/3-1/8] \\ &\quad +(1+6z^2)/8 \cdot \log [z+(1+z^2)^{1/2}]\} \quad . \quad . \quad . \quad . \quad (35) \end{aligned}$$

in which $z^2=ax$.

This function is cumbersome to handle in the evaluation of A_2, and it is convenient to approximate by assuming that z is small. (35) may then be shown to yield the power series

$$A_1 \approx a^{-3/2}\{4z^3/3+2z^5/5+3z^7/70+\ldots\}. \quad . \quad . \quad . \quad . \quad (36)$$

This approximation may be used to extend the solution until further terms are small compared with z^7. Proceeding in this way a power series is obtained for $\phi(x)$

$$\phi(x)=\{1+ax+4x^{3/2}/3+2ax^{5/2}/5 +x^3/3+3a^2x^{7/2}/70+2ax^4/15 \ldots\}. \quad . \quad . \quad (37)$$

This series is identical with that obtained by Baker (1930) by a method of successive approximations. If the full form for A_1 given by (35) is retained, and an approximate form of A_2 is used a series will be found that converges more rapidly than (37).

It is interesting to note that an alternative solution can be found by solving (34) for $\phi^{3/2}$ instead of ϕ. In this case the parameters are

$$a_0=D^2, \qquad \alpha=5/2, \qquad n=-1, \qquad m=-5/3, \qquad a_1=-x^{-1/2}.$$

§7. Conclusion.

It has been shown that it is possible to revert series involving certain fractional powers of the unknown variable, and that the coefficients in these series need not be algebraic. The application of reversion to non-linear differential equations has been found to be simple, and applicable to a wide variety of problems. It is particularly suited to problems with initial boundary conditions. It suffers from the presence of "secular terms" in common with other series methods (Minorsky 1947), and is not usually suitable when the non-linear terms are large.

The author is grateful for permission to publish this work, from Standard Telecommunication Laboratories Ltd., and also from the British Thomson-Houston Company Ltd. where the work was commenced.

References.

Baker, E. B., 1930, "The Application of the Fermi–Thomas Statistical Model to the Calculation of Potential Distributions in Positive Ions", *Phys. Rev.*, **36,** 630.

Bickley, W. G., and Miller, J. C. P., 1943, "Notes on the Reversion of a Series", *Phil. Mag.* [7], **34,** 35.

Fairweather, A., and Ingham, T., 1941, "Subsidence Transients in Circuits Containing a Non-linear Resistor, with Reference to the Problem of Spark-quenching", *J. Instn. Elect. Engrs.*, **88,** Pt. I, 330.

Harkness, J., and Morley, F., 1893, *Treatise on the Theory of Functions* (London: Macmillan and Co.), p. 116; 1898, *Introduction to Analytic Functions* (London: Macmillan and Co.), p. 144.

Minorsky, N., 1947, *An Introduction to Non-linear Mechanics* (Ann Arbor: J. W. Edwards and Co.).

Van Orstrand, C. E., 1910, "Reversion of Power Series", *Phil. Mag.*, [6] **19,** 366.

Whittaker, E. T., and Watson, G. N., 1950, *A Course of Modern Analysis* (Cambridge: University Press), p. 133.

XXV. *The Boundary Layer in Three Dimensional Flow.*—Part I. *Derivation of the Equations for Flow along a General Curved Surface.*

By Professor L. Howarth, F.R.S.,
Department of Mathematics, University of Bristol*.

[Received January 9, 1951.]

Summary.

The general equations of boundary layer flow along a curved surface S are set up in an appropriate system of orthogonal coordinates and the importance of the curvatures in the general case is made evident.

It is shown that, for a general flow, the necessary and sufficient condition for the curvatures to disappear from the equations of flow is that the boundary layer should be along the surface of a cylinder or a plane.

The form assumed by the equations when S is a surface of revolution is derived.

In Part II. there will be a discussion of the flow in the vicinity of a stagnation point on a general surface.

The Coordinate System.

Let us denote the equation of the given surface S by

$$\chi(x, y, z)=0. \quad . \quad . \quad . \quad . \quad . \quad . \quad . \quad . \quad . \quad (1)$$

This surface together with all parallel† surfaces constitutes a Lamé family of surfaces‡

$$\zeta(x, y, z)=\text{const.} \quad . \quad . \quad . \quad . \quad . \quad . \quad . \quad . \quad (2)$$

It follows that two families of surfaces

$$\xi(x, y, z)=\text{const.} \quad \text{and} \quad \eta(x, y, z)=\text{const.} \quad . \quad . \quad . \quad . \quad (3)$$

exist such that the three families ξ, η, ζ form a triply orthogonal family. The intersections of the original surface with the members of ξ and η are the lines of curvature of S§ and the surfaces $\xi=$ const., $\eta=$const. are, fact, the developables formed by the normals along the lines of curvature on S‖.

---

* Communicated by the Author.

† See Weatherburn ' Differential Geometry ', p. 158. " A surface which is at a constant distance along the normal from another surface S is said to be parallel to S ".

‡ *Op. cit.*, p. 207 or p. 218. Ex. 2.

§ Weatherburn, *op. cit.*, p. 211. Dupin's Theorem.

‖ *Op. cit.*, p. 207.

If h_1, h_2, h_3 are the length elements in our coordinate system then, by definition h_3 is a function of ζ only. We can, without loss of generality, take it to be unity, ζ then representing distance measured normal to S.

The Equations of Motion.

In terms of these coordinates, denoting by u, v, w the corresponding velocity components,

$$\text{div } \mathbf{V} = \frac{1}{h_1 h_2}\left[\frac{\partial}{\partial \xi}(h_2 u) + \frac{\partial}{\partial \eta}(h_1 v) + \frac{\partial}{\partial \zeta}(h_1 h_2 w)\right], \quad \ldots \quad (4)$$

$$\text{curl } \mathbf{V} = \frac{1}{h_2}\left[\frac{\partial w}{\partial \eta} - \frac{\partial}{\partial \zeta}(h_2 v)\right], \frac{1}{h_1}\left[\frac{\partial}{\partial \zeta}(h_1 u) - \frac{\partial w}{\partial \xi}\right], \frac{1}{h_1 h_2}\left[\frac{\partial}{\partial \xi}(h_2 v) - \frac{\partial}{\partial \eta}(h_1 u)\right]. \quad \ldots \quad 5)$$

The components of acceleration are

$$\left.\begin{aligned} &\frac{\partial u}{\partial t} + \frac{u}{h_1}\frac{\partial u}{\partial \xi} + \frac{v}{h_2}\frac{\partial u}{\partial \eta} + w\frac{\partial u}{\partial \zeta} + \frac{uv}{h_1 h_2}\frac{\partial h_1}{\partial \eta} - \frac{v^2}{h_1 h_2}\frac{\partial h_2}{\partial \xi} + \frac{wu}{h_1}\frac{\partial h_1}{\partial \zeta}, \\ &\frac{\partial v}{\partial t} + \frac{u}{h_1}\frac{\partial v}{\partial \xi} + \frac{v}{h_2}\frac{\partial v}{\partial \eta} + w\frac{\partial v}{\partial \zeta} - \frac{u^2}{h_1 h_2}\frac{\partial h_1}{\partial \eta} + \frac{uv}{h_1 h_2}\frac{\partial h_2}{\partial \xi} + \frac{wv}{h_2}\frac{\partial h_2}{\partial \zeta}, \\ &\frac{\partial w}{\partial t} + \frac{u}{h_1}\frac{\partial w}{\partial \xi} + \frac{v}{h_2}\frac{\partial w}{\partial \eta} + w\frac{\partial w}{\partial \zeta} - \frac{u^2}{h_1}\frac{\partial h_1}{\partial \zeta} - \frac{v^2}{h_2}\frac{\partial h_2}{\partial \zeta}. \end{aligned}\right\} \quad (6)$$

On making the usual boundary layer assumptions, with the additional assumption that h_1, h_2 and *all* their first derivatives are O(1), we have the following equations of motion

$$\frac{\partial u}{\partial t} + \frac{u}{h_1}\frac{\partial u}{\partial \xi} + \frac{v}{h_2}\frac{\partial u}{\partial \eta} + w\frac{\partial u}{\partial \zeta} + \frac{uv}{h_1 h_2}\frac{\partial h_1}{\partial \eta} - \frac{v^2}{h_1 h_2}\frac{\partial h_2}{\partial \xi} = -\frac{1}{\rho h_1}\frac{\partial p}{\partial \xi} + \nu\frac{\partial^2 u}{\partial \zeta^2}, \quad (7)$$

$$\frac{\partial v}{\partial t} + \frac{u}{h_1}\frac{\partial v}{\partial \xi} + \frac{v}{h_2}\frac{\partial v}{\partial \eta} + w\frac{\partial v}{\partial \zeta} + \frac{uv}{h_1 h_2}\frac{\partial h_2}{\partial \xi} - \frac{u^2}{h_1 h_2}\frac{\partial h_1}{\partial \eta} = -\frac{1}{\rho h_2}\frac{\partial p}{\partial \eta} + \nu\frac{\partial^2 v}{\partial \zeta^2}, \quad (8)$$

$$\frac{\partial p}{\partial \zeta} = \text{O}(1) \quad \ldots \quad (9)$$

and the equation of continuity is

$$\frac{1}{h_1 h_2}\left[\frac{\partial}{\partial \xi}(h_2 u) + \frac{\partial}{\partial \eta}(h_1 v)\right] + \frac{\partial w}{\partial \zeta} = 0. \quad \ldots \quad (10)$$

The length elements h_1, h_2 are not completely arbitrary; the Lamé relations, in our case, lead to the following results:—

(i.) $\frac{1}{h_2}\frac{\partial h_1}{\partial \eta}$ and $\frac{1}{h_1}\frac{\partial h_2}{\partial \xi}$ are each functions of ξ and η only,

(ii.) h_1 and h_2 are each of the form $\text{F}(\xi, \eta) + \zeta \text{G}(\xi, \eta)$,

(iii.) $$\frac{\partial}{\partial \xi}\left(\frac{1}{h_1}\frac{\partial h_2}{\partial \xi}\right) + \frac{\partial}{\partial \eta}\left(\frac{1}{h_2}\frac{\partial h_1}{\partial \eta}\right) + \frac{\partial h_1}{\partial \zeta}\frac{\partial h_2}{\partial \zeta} = 0. \quad \ldots \quad (11)$$

Furthermore, if K_1 is the principal curvature on the surface ξ=const. in the direction of the parameter η (the curve ζ=const. on this surface) and K_2 is similarly the principal curvature on the surface η=const. in the direction of the parameter ξ.

$$K_1=-\frac{1}{h_1h_2}\frac{\partial h_2}{\partial \xi} \quad \text{and} \quad K_2=-\frac{1}{h_1h_2}\frac{\partial h_1}{\partial \eta}. \quad . \quad . \quad . \quad (12)$$

The surfaces ξ=const. and η=const. being developables, their other principal curvatures are zero, of course.

Also if K_a and K_b are the principal curvatures of the surface ζ=const. in the directions ξ and η increasing

$$K_a=-\frac{1}{h_1}\frac{\partial h_1}{\partial \zeta}, \qquad K_b=-\frac{1}{h_2}\frac{\partial h_2}{\partial \zeta}. \quad . \quad . \quad . \quad . \quad (13)$$

Therefore, in terms of the curvatures K_1, K_2, the equations of motion (7), (8), and (10) may be written

$$\frac{\partial u}{\partial t}+\frac{u}{h_1}\frac{\partial u}{\partial \xi}+\frac{v}{h_2}\frac{\partial u}{\partial \eta}+w\frac{\partial u}{\partial \zeta}-K_2uv+K_1v^2=-\frac{1}{\rho h_1}\frac{\partial p}{\partial \xi}+\nu\frac{\partial^2 u}{\partial \zeta^2}, \quad . \quad (14)$$

$$\frac{\partial v}{\partial t}+\frac{u}{h_1}\frac{\partial v}{\partial \xi}+\frac{v}{h_2}\frac{\partial v}{\partial \eta}+w\frac{\partial v}{\partial \zeta}+K_2u^2-K_1uv=-\frac{1}{\rho h_2}\frac{\partial p}{\partial \eta}+\nu\frac{\partial^2 v}{\partial \zeta^2}, \quad . \quad (15)$$

$$\frac{1}{h_1}\frac{\partial u}{\partial \xi}+\frac{1}{h_2}\frac{\partial v}{\partial \eta}+\frac{\partial w}{\partial \zeta}-K_1u-K_2v=0, \quad . \quad . \quad . \quad . \quad (16)$$

where the values of h_1, h_2, K_1 and K_2 may, to the orders of approximation involved, be taken in the surface S. As in two dimensional theory, we must suppose p prescribed, in virtue of (9), by the flow outside and then equations (14)–(16) are the equations which serve to determine u, v, w.

Uniqueness.

Considering the field of flow as a whole, the system of orthogonal coordinates we have set up is clearly not unique. For example, for an ellipsoid the confocal system is an obvious alternative. Nevertheless, since by Dupin's theorem the curves of intersection of a triply orthogonal family are lines of curvature on each it follows that, however we set up the orthogonal coordinate system, the surfaces ξ=const. and η=const. must intersect the surface S in its lines of curvatures. Hence, no matter how we choose our triply orthogonal family to contain S, the various possibilities for the families ξ=const. and η=const. must all touch the families we have chosen along the lines of curvature of S. Since we are concerned in boundary layer theory only with the immediate vicinity of S our equations represent the unique form for an orthogonal coordinate system, apart that is, from the choice of scales for ξ and η.

The general flow along the surface of a right circular cone of semi-angle α makes an instructive illustration. The coordinate system we have developed consists of

(i.) cones parallel to the given cone;

(ii.) cones orthogonal to the given cone;

(iii.) meridian planes.

In cylindrical polar coordinates r, ϕ, z we may express these families as

$$\xi=\phi, \quad \eta=z\cos\alpha+r\sin\alpha, \quad \zeta=z\sin\alpha-r\cos\alpha, \quad . \quad . \quad (17)$$

so that

$$h_1=\eta\sin\alpha-\zeta\cos\alpha=r, \quad h_2=h_3=1, \quad . \quad . \quad . \quad . \quad (18)$$

$$K_1=0, \qquad K_2=-\frac{1}{h_1}\sin\alpha. \quad . \quad . \quad . \quad (19)$$

Spherical polar coordinates R, θ, ϕ with corresponding velocity components U, V, W would be an obvious alternative system. In the comparing the two we should have

$$u=W, \quad v=U\cos(\theta-\alpha)-V\sin(\theta-\alpha), \quad w=U\sin(\theta-\alpha)+V\cos(\theta-\alpha)^*$$
$$. \quad . \quad . \quad (20)$$

and at the surface of the cone

$$\frac{1}{h_1}\frac{\partial}{\partial\xi}=\frac{1}{R\sin\alpha}\frac{\partial}{\partial\phi}, \quad \frac{\partial}{\partial\eta}=\frac{\partial}{\partial R}, \quad \frac{\partial}{\partial\zeta}=\frac{1}{R}\frac{\partial}{\partial\theta}, \quad . \quad . \quad (21)$$

It can then be verified that the two sets of equations are identical.

Discussion.

The presence of the terms K_1 and K_2 in eqns. (14)–(16) makes manifest the importance of curvature in the general problem, though it should be noted that the significant curvatures are not the principal curvatures of S but the non-zero principal curvatures of the two orthogonal familes ξ and η. In this respect, the theory differs from the two dimensional theory where curvature effects, so long as the curvatures are not very large or change very rapidly, disappear from the equations. We may, in consequence, in three dimensional boundary layer flow expect effects additional to those we might reasonably associate with the addition of an extra dimension.

When K_1 and K_2 both vanish we have what is clearly an exceptional case in this respect and it is of some interest to determine the surfaces so defined. Although the vanishing of K_1 and K_2 refers only to values at the surface S, it can readily be established that they must in consequence vanish everywhere on the developables. Hence the developables $\xi=$const. and $\eta=$const. are planes.

Furthermore, we may now establish that one of these families consists of parallel planes. For, suppose, if possible, that two members of $\xi=$const. are non-parallel planes. Any member of $\eta=$const. must then, since it is orthogonal to both the chosen planes, meet them and must have

* Since differentiations have to be carried out it is obviously insufficient to consider surface values of u, v, w only.

a normal whose direction cosines are uniquely defined by the direction cosines of their normals. In other words, the family η=const. must consist of parallel planes. Hence we infer that at least one of the families ξ=const. and η=const. must consist of parallel planes. Suppose it is η=const. We can then without loss of generality express the equations of the two systems in the forms.

$$z=\eta, \quad . \quad . \quad . \quad . \quad . \quad . \quad . \quad . \quad . \quad . \quad . \quad (22)$$

$$y=xf(\xi)+g(\xi). \quad . \quad . \quad . \quad . \quad . \quad . \quad . \quad . \quad . \quad (23)$$

Suppose the third family is expressed by

$$F(x, y, z)=\zeta. \quad . \quad . \quad . \quad . \quad . \quad . \quad . \quad . \quad . \quad (24)$$

Then, considering the three surfaces with parameters ξ_1, η_1, ζ_1, which pass through the point x_1, y_1, z_1 we must have

$$z_1=\eta_1, \quad y_1=x_1f(\xi_1)+g(\xi_1), \quad F(x_1, y_1, z_1)=\zeta_1, \quad . \quad . \quad (25)$$

and, since the surfaces are orthogonal

$$\frac{\left(\frac{\partial F}{\partial x}\right)_{x=x_1}}{1}=\frac{\left(\frac{\partial F}{\partial y}\right)_{y=y_1}}{f(\xi_1)}=\frac{\left(\frac{\partial F}{\partial z}\right)_{z=z_1}}{0}, \quad . \quad . \quad . \quad . \quad (26)$$

Hence the surfaces ζ=const. are, in general, cylinders with generators parallel to the z axis ; they include as a special case (when $f(\xi)=0$) planes.

We may conclude therefore that it is only for boundary layers attached to cylinders and planes that the curvature effects vanish from the equations of motion. Moreover, in these cases, the boundary layer equations may be taken in Cartesian form. This is obvious for the case of the plane. For the cylinder it follows from eqn. (12) that h_1 is independent of η and h_2 is independent of ξ and therefore by condition (ii.) of p. 240 that *in the surface S* the length elements h_1, h_2 can each without loss of generality be transformed into unity. Thus in the case of the cylinder the equations may be written in Cartesian form with ξ as distance measured around a right section, η as distance measured along the generators and ζ as distance measured normal to S. We thereby recover the standard result in two dimensional flow and obtain the result already justified in particular by previous investigators that the equations in this form are valid for three dimensional flow past a yawed cylinder.

Finally we may obtain the forms taken by K_1 and K_2 when the surface S is one of revolution. The lines of curvature of S are then the meridian curves m and the " parallels " p. Thus the surfaces ξ=const. are the meridian planes and hence

$$K_1=0.$$

The surfaces η=const. are the right circular cones generated by the normals to S along the curves p. Let us consider a particular surface η=const. generated by the normals to S along a particular parallel p_1. Then if R is the length of the normal *to this cone* intercepted between p_1 and the axis of rotation

$$|K_2|=1/R.$$

XXVI. *A Covariant Formulation of the Bloch-Nordsieck Method.*

By W. Thirring and B. Touschek,
Department of Natural Philosophy, The University, Glasgow*.

[Received November 29, 1950.]

Summary.

The results of the Bloch-Nordsieck method are derived in a covariant manner, based on a covariant form of the commutation-relations in momentum space.

§ 1.

In this paper we shall give a covariant derivation of the well known Bloch-Nordsieck (1937) results on the multiple production of low energy quanta. A full proof will be based on the interpretation of the field theoretical set of equations recently given by Yang and Feldman 1950. In § 3 a derivation of the same result from the Dyson-Feynman form of the S-matrix will be outlined.

Though the results obtained here are not new, and have in fact been discussed by several authors, the importance of the Bloch-Nordsieck problem as the only problem in the theory of fields which admits an accurate solution seems to justify a general reformulation of the procedure. The simplification which enables one to find an accurate solution rests on the neglect of the recoil of the source particles, the motion of which is assumed to be given. The theory of fields contains a second problem of this kind in which the rôles of Fermi- and Bose-particles are interchanged. Though this problem can be solved in principle, no manageable form of solution has been found so far. If the solutions of both problems could be handled with equal ease they could be made the basis of a new approximation method. An approximation of this type would have the advantage that the trivial effects of higher powers of the interaction constant (unitarity of the S-matrix) would be considered in every step of the procedure, and only the genuine higher order effects expressing the intrinsic non-linearity of the system would be subjected to gradual approximation. It seems essential for such a programme that the Bloch-Nordsieck result should be given in a covariant form, though its immediate practical applications are of course non-relativistic.

§ 2.

We consider a system of coupled fields. The Bose field will be described by a wave operator $\phi(x)$, and we shall restrict the first part of this discussion to scalar particles. The extension to more general Bose fields is

* Communicated by the Authors.

straight-forward. The source particles are summarily described by a source density $\rho(x)$; x denotes a point in space-time. The field equations are written in the Yang-Feldman form :

$$\phi(x)=\phi^{\text{in}}(x)+\int dx'\ \rho(x')\mathrm{D}_r(x-x')$$
$$=\phi^{\text{out}}(x)+\int dx'\ \rho(x')\mathrm{D}_a(x-x'),$$

where the functions $\mathrm{D}_r(x)$ and $\mathrm{D}_a(x)$ are the retarded and advanced solutions of the Poisson equation

$$(\Box^2-\mu^2)\mathrm{D}_{r,a}(x)=\delta(x). \quad . \quad . \quad . \quad . \quad . \quad . \quad . \quad . \quad (1)$$

Since both ϕ^{in} and ϕ^{out} are solutions of the homogeneous wave equation $(\Box^2-\mu^2)\phi^{\text{in}}=0$ and, therefore, satisfy identical commutation relations of the form

$$[\phi^{+\text{in}}(x),\ \phi^{\text{in}}(x')]=-i\mathrm{D}(x-x') \quad . \quad . \quad . \quad . \quad . \quad . \quad . \quad (2)$$

they must be connected by a unitary transformation

$$\phi^{\text{out}}(x)=\phi^{\text{in}}(x)+\int(\mathrm{D}_r-\mathrm{D}_a)\rho(x')dx'=\mathrm{S}^{-1}\phi^{\text{in}}_{(x)}\mathrm{S}, \quad . \quad . \quad . \quad . \quad . \quad (3)$$

and it has been shown by Yang and Feldman that the unitary matrix S thus defined is identical with the Feynman-Dyson S-matrix.

Since ϕ is a c-number—the motion of the source particles is fixed—ϕ^{out} differs from ϕ^{in} only by a multiple of the unit matrix. $\mathrm{D}_a-\mathrm{D}_r$ is an odd invariant solution of the homogeneous wave equation, and actually

$$\mathrm{D}_a(x)-\mathrm{D}_r(x)=\mathrm{D}(x).$$

The further calculation is considerably facilitated by transforming to k-space. This gives

$$\phi^{\text{out}}(x)=\frac{1}{(2\pi)^3}\int dk\delta(k^2-\mu^2)\phi^{\text{out}}(k)e^{ikx}$$
$$=\frac{1}{(2\pi)^3}\int dk\delta(k^2-\mu^2)[\phi^{\text{in}}(k)-\rho(k)\epsilon(k)]e^{ikx}, \quad . \quad . \quad . \quad . \quad . \quad (4)$$

where the first equation is a definition of the Fourier transform $\phi^{\text{out}}(k)$. Use has been made of the Fourier representation

$$\mathrm{D}(x)=-\frac{i}{(2\pi)^3}\int dk\delta(k^2-\mu^2)\epsilon(k)e^{ikx}$$

of the D-function; $\epsilon(k)$ is ± 1 according to $k_0\gtrless 0$ and $\rho(k)$ is defined by

$$\rho(x)=\frac{1}{(2\pi)^4}\int dk\rho(k)e^{ikx}. \quad . \quad . \quad . \quad . \quad . \quad . \quad . \quad (5)$$

In the following the abbreviation $\delta\phi(k)=-\rho(k)\epsilon(k)$ will be used.

The energy momentum 4-vector for the incoming wave is given by

$$\mathrm{P}^{\text{in}}_{\nu}=\frac{1}{(2\pi)^3}\int_{k_0>0} dk\delta(k^2-\mu^2)k_\nu\phi^{\text{in}}(k)^{+}\phi^{\text{in}}(k),$$

and a similar expression holds for the outgoing wave. The number of quanta in the incoming wave is

$$N^{in}=\frac{1}{(2\pi)^3}\int_{k_0>0} dk\delta(k^2-\mu^2)\phi^{in}(k)^+\phi^{in}(k). \quad . \quad . \quad . \quad (6)$$

In the present case we want to consider an experiment in which quanta are only observed over a limited range of frequency. We shall therefore introduce an interval Δ in k-space which contains only this range of frequencies. It is then easily seen that N_Δ—resulting from equation (6) by integrating only over the interval Δ—is still an integral positive number. This follows from the commutation relations

$$\delta(k'^2-\mu^2)\delta(k^2-\mu^2)[\phi^+(k)\phi(k')]=-(2\pi)^3\delta(k-k')\epsilon(k)\delta(k'^2-\mu^2) \quad . \quad (7)$$

for the free fields, which can be derived from equation (2). Using (7), one obtains

$$\delta(k^2-\mu^2)[N_\Delta\phi(k)] \;=-\phi(k)\delta(k^2-\mu^2)$$

$$\delta(k^2-\mu^2)[N_\Delta\phi^+(k)]=+\phi^+(k)\delta(k^2-\mu^2)$$

for any $k \subset \Delta$.

Since we want to determine the probability for the production of a certain number n of quanta in Δ, we shall assume that the incoming wave does not carry any quanta at all in Δ. Then if χ_0 is the eigenvector ($|\chi_0|^2=1$) describing such a state, we have

$$\delta(k^2-\mu^2)\phi^{in}(k)\chi_0=0 \quad . \quad . \quad . \quad . \quad . \quad . \quad . \quad (8)$$

for every $k \subset \Delta$. For the outgoing wave χ_0' is the corresponding vacuum state and the basis-vectors for the 1, 2, . . . n particle states are

$$\chi_1'(k_1)=\frac{1}{\sqrt{1!}}\phi^{out}(k_1)^+\chi_0'\delta(k_1^2-\mu^2),$$

$$\chi_2'(k_1k_2)=\frac{1}{\sqrt{2!}}\phi^{out}(k_1)^+\phi^{out}(k_2)^+\chi_0'\delta(k_1^2-\mu^2)\delta(k_2^2-\mu^2),$$

$$\chi_n'(k_1 \ldots k_n)=\frac{1}{\sqrt{n!}}\phi^{out}(k_1)^+ \ldots \phi^{out}(k_n)^+\chi_0'\prod_i\delta(k_i^2-\mu^2).$$

The most general n-particle state can then be described by a Hilbert vector,

$$F_n^r=\frac{1}{(2\pi)^{3n}}\int_\Delta dk_1 \ldots \int_\Delta dk_n u_n^r(k_1 \ldots k_n)\chi_n(k_1 \ldots k_n), \quad . \quad . \quad (9)$$

where $u_n^r(k_1, \ldots k_n)$ is a symmetric "Schrödinger-function" and the index r indicates one particular distribution of the quanta over the element Δ of k-space. To normalize F_n^r such that $F_n^r N_\Delta F_n^r=n$ we have to make

$$\frac{1}{(2\pi)^{3n}}\int_\Delta dk_1 \ldots \int_\Delta dk_n \prod_r \delta(k_i^2-\mu^2)|u_n^r|^2=1.$$

The proof of this is analogous to that for the well known case of oscillator eigenfunctions and can be carried out simply by using the method developed by Becker and Leibfried (1946). We shall use a complete set of orthogonal functions u_n^r, *i.e.* such a set that every symmetric function $f_n(k_1, \ldots k_n)$ defined in Δ can be expanded in terms of the u_n^r. The u's will then satisfy the completeness relation

$$\frac{1}{(2\pi)^{3n}} \sum_r \Pi_i \delta(k_i^2-\mu^2) u_n^r{}^*(k_1 \ldots k_n) u_n^r(k_1' \ldots k_n') = \frac{1}{n!} \sum_P \Pi_i \delta(k_i-k_i'). \quad (10)$$

The symmetrized δ-function on the right-hand side of this equation can be replaced by the ordinary δ-function whenever it occurs multiplied by a function symmetric in the $k_1, \ldots k_n$.

The probability amplitude for the creation of n particles in a state r is now given by

$$(\mathrm{F}_n^r \chi_0) = \frac{1}{(2\pi)^{3n}} \times \frac{1}{\sqrt{n!}} \int_\Delta dk_1 \ldots \int_\Delta dk_n \Pi_i \delta(k_i^2-\mu^2)$$
$$\times u_n^r{}^*(k_1 \ldots k_n)(\chi_0'(\phi(k_1)+\delta\phi(k_1)) \ldots (\phi(k_n)+\delta\phi(k_n))\chi_0).$$

On account of equation (8) only the product term $\delta\phi(k_1)\delta\phi(k_2) \ldots \delta\phi(k_n)$ gives a non-vanishing contribution. Since we are not interested in the particular distribution of the quanta inside the interval Δ we have to sum the squared amplitude over all the distributions defined by u_n^r. Thus, by using the completeness relation (10),

$$\sum_r |\mathrm{F}_n^r \chi_0|^2 = \frac{1}{n!} \bar{n}^n |\chi_0' \chi_0|^2 = \omega_n(\Delta), \quad . \quad . \quad . \quad . \quad . \quad (11)$$

where

$$\bar{n} = \frac{1}{(2\pi)^3} \int_\Delta dk \delta(k^2-\mu^2) |\delta\phi(k)|^2. \quad . \quad . \quad . \quad . \quad . \quad (12)$$

Since the total probability must be one we have

$$|\chi_0' \chi_0|^2 = e^{-\bar{n}}. \quad . \quad . \quad . \quad . \quad . \quad . \quad . \quad . \quad (13)$$

$\bar{n}$ is the average number of quanta produced: $\bar{n} = \sum_n n\omega_n(\Delta)$. It can also be found by considering the vacuum expectation value $\chi_0 \mathrm{N}^{\mathrm{out}} \chi_0$ of $\mathrm{N}^{\mathrm{out}}$.

Since the interval Δ is arbitrary, this—in a sense—is a generalization of the Bloch-Nordsieck result. It shows how redundant information, *e.g.* the distribution of energy and momentum over the quanta in Δ, can be eliminated by the use of the completeness relation. Another link with the case of infinitesimal intervals considered by Bloch and Nordsieck lies in the addition theorem of Poisson distributions: Let the interval Δ be divided into two subintervals, Δ_1 and Δ_2. Then $\bar{n} = \bar{n}_1 + \bar{n}_2$ and

$$\omega_n(\Delta) = \frac{(\bar{n}_1+\bar{n}_2)^n}{n!} \exp\{-(\bar{n}_1+\bar{n}_2)\} = \sum_{m=0}^{n} \omega_m(\Delta_1)\omega_{n-m}(\Delta_2).$$

The validity of the Poisson distribution in two subintervals therefore insures the validity of a Poisson distribution for the whole interval, and the proof can be easily extended to cover the case of an arbitrary number of subintervals.

It remains to define the source function $\rho(k)$ for the particular case where a source particle is scattered at $x=0$. Transcribing the above argument to a Maxwell field, we replace $\rho(x)$ by a vector source function $j_\mu(x)$ of a point electron, viz.,

$$j_\mu(x)=e\int_{-\infty}^{+\infty} p_\mu(\tau)\delta(x-\tau p(\tau))d\tau$$

where, e.g., $p_\mu(\tau)=p_\mu$ for $\tau<0$ and $p_\mu(\tau)=p'_\mu$ for $\tau>0$. The sudden change in momentum imposes the restriction that in applying the result to a real scattering process one should limit the admissible frequency range to frequencies $\ll 1/\tau$, where τ is the effective time of collision. Otherwise a sudden change of momentum would be too rough an approximation. According to equation (5) we have for the Fourier transform of $j_\mu(x)$

$$j_\mu(k)=e\left(\frac{p_\mu}{(pk)}-\frac{p'_\mu}{(p'k)}\right),$$

The average number of quanta can be determined from equation (12):

$$\bar{n}=\frac{e^2}{(2\pi)^3}\int_\Delta dk\delta(k^2-\mu^2)\left[\frac{(pe)}{(pk)}-\frac{(p'e)}{(p'k)}\right]^2,$$

where e is a polarization vector.

In the case of mesons $\rho(x)$ will be of the form

$$\rho(x)=g\int_{-\infty}^{+\infty}\sigma(\tau)\delta(x-\tau p(\tau))d\tau,$$

where $\sigma(\tau)$ is a function describing an internal degree of freedom of the source particles, as *e.g.* their spin or isotopic spin. Both p and σ can change at $\tau=0$. In this case the Fourier transform of the source density is given by

$$\rho(k)=g\left\{\frac{\sigma(-)}{(pk)}-\frac{\sigma(+)}{(p'k)}\right\}.$$

n can be easily determined from equation (12).

§ 3.

We shall now briefly indicate the derivation of the above results with Dyson's S-matrix

$$S=1-i\int\phi(1)\rho(1)+\frac{(-i)^2}{2!}\int P\phi(1)\rho(1)\phi(2)\rho(2)+\ldots \quad . \quad (14)$$

Here $\phi(1)$ means $\phi(x)$ at the point x_1, P is the operator arranging the factors in the product in order of time, and the integrations are to be extended over the whole $x_1,\ldots x_n$ space. The problem consists in finding the matrix elements of S which lead from the vacuum state to a state where n particles are present. To this matrix element we shall get contributions from the $n+1$st, $n+3$rd, ... terms in the expansion (14). A typical term of $n+2l$th order will contain n factors $\phi(1)$ which create the final particles, l factors

which create l virtual particles, which are finally annihilated by the remaining l factors. In calculating the matrix element one has to keep in mind that one gets a factor

$$\binom{n+2l}{n}$$

corresponding to the number of possibilities of picking n ϕ's out of the total $n+2l$ ϕ's. A further factor $n!$ arises from the permutations of the n created particles among the n creation operators $\phi(1)$. The matrix element will therefore be of the form

$$\langle 0|S|n\rangle=(-i)^n\int P\{\langle 0|\phi|k_1\rangle \ldots \langle 0|\phi|k_n\rangle\rho(1)\ldots\rho(n) \times\left[1+\frac{(-i)^2}{2!}\langle 0|\phi(n+1)\phi(n+2)|0\rangle+\ldots\right], \quad . \quad . \quad . \quad (15)$$

where Dirac's notation for the matrix elements has been used. It should be noted that the expression in the square brackets is independent of n. The relative probabilities for the production of a given number of particles are thus given by the first non-vanishing approximation. Integrating the squared matrix element over all energy momentum vectors of the quanta, we obtain

$$|\langle 0|S|n\rangle|^2=\frac{1}{(2\pi)^{3n}}\times\frac{1}{n!}\int_{\Delta_1\ldots\Delta_n} dk_1\ldots dk_n|\rho(k_1)|^2\ldots|\rho(k_n)|^2 \times\prod_i\delta(k_i^2-\mu^2)\,[\,]^2.$$

The $1/n!$ arises from the fact that one wants to integrate all the k's over the same interval. Since the particles are not distinguishable, one has to divide by $n!$. $[\,]^2$, which is the square of the bracket in equation (15), can be determined as before with the aid of the unitarity of the S-matrix. It gives only a normalization of the probability. The result is again

$$|\langle 0|S|n\rangle|^2=\frac{\bar{n}^n}{n!}e^{-\bar{n}},$$

with $\bar{n}$, as before, defined by equation (12).

One of us (W. T.) is indebted to the Nuffield Foundation for the award of a Fellowship, during the tenure of which this work was carried out.

References.

Bloch, F., and Nordsieck, A., 1937, *Phys. Rev.*, **52**, 54.
Yand, C. N., and Feldman, D., 1950, *Phys. Rev.*, **79**, 972.
Becker, R., and Leibfried, G., 1946, *Phys. Rev.*, **69**, 34.

XXVII. *Absorption of Penetrating Shower Secondaries.*

By D. M. Ritson *,
Dublin Institute for Advanced Studies †.

[Received November 23, 1950.]

Abstract.

Measurements with a penetrating shower set at sea level showed an apparent mean free path for absorption of the secondaries of penetrating showers of 405 ± 30 gr./cm.^{2} for lead and 350 ± 40 gr./cm.^{2} for iron.

Introduction.

Measurements for the absorption of penetrating shower secondaries have been made previously for lead for thicknesses of 100 gm./cm.^{2}—200 gm./cm.^{2} (Walker 1950). A comparison of the differential absorption for lead and iron under a large thickness of lead (150 gm./cm.^{2}) has been made by (Piccioni 1950).

The measurements reported below give results for the absorption of the secondaries in the range 60 gm./cm.^{2}—450 gm./cm.^{2} for lead and 60 gm./cm.^{2}—260 gm./cm.^{2} for iron.

These investigations were started at a time when it was considered that the penetrating particles of a shower were predominantly π mesons. Later results have shown that the particles capable of transversing 20 centimetres of lead will be composed almost equally of protons and π mesons (Camerini *et al.* 1950). Thus such an investigation does not throw direct light on the π mesons interaction.

However, the background data provided by such an investigation of the effect of lead absorber thickness on the counting rate of a "penetrating shower" set and the further data obtained on the penetration of the shower secondaries of an "extensive shower", appeared to make the publication of a brief report of my investigation worth while.

Experimental.

Measurements were made on penetrating showers at sea level with the apparatus shown in fig. 1.

The top six counters (marked either A, B, or C) and the lower ten counters marked either D or E were of active area 3·5 cm. × 50 cm. Each counter in the top tray was separated from its neighbour by 2·5 cm. of lead. The tray was covered by 15 cm. of lead, the side shielding consisted of 10 cm. of lead, and there was a thickness of 2·5 cm. of lead immediately beneath the tray.

---

* Communicated by Professor C. B. A. McCusker.

† Now at Department of Physics, University of Rochester.

The absorber S_1 over the lower ten counters was variable. The side shielding again consisted of 10 cm. of lead.

Coincidences (A B C D E) were recorded. In order to record penetrating showers simultaneously accompanied by air showers, the pulse X_3 was taken from coincidences between three extended trays, and coincidences A B C X_3, A B C D E X_3 were recorded throughout the experiment. (The three extended trays each of area 750 cm.^{2} were simultaneously used in another experiment, in which they were covered with thicknesses of lead, water, carbon, iron, up to one cascade unit, thick.)

Fig. 1.

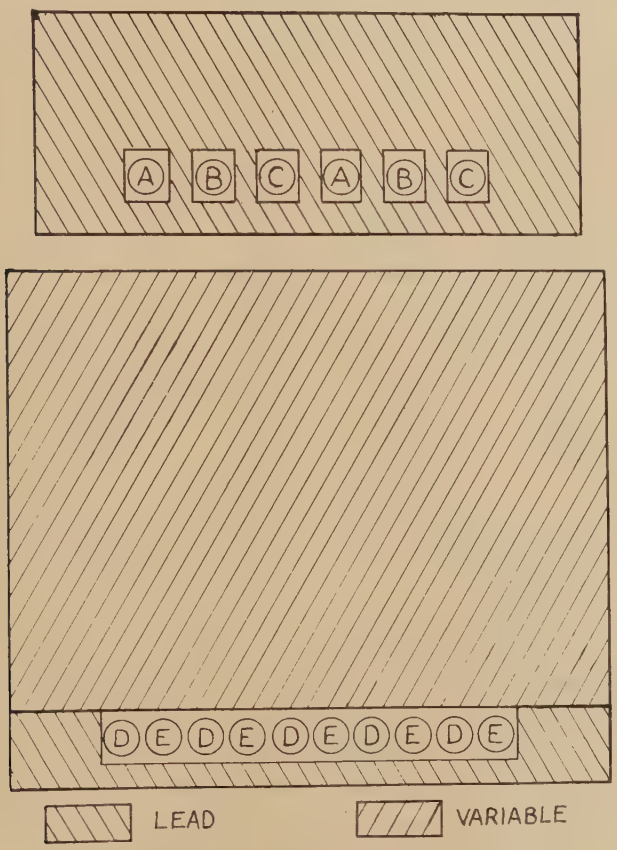

Results.

Fig. 2. plots the logarithm of the rate A B C D E against thickness of the absorber S_1 in g./cm.^{2} of lead. It will be seen that the results can be represented by an exponential absorption for lead with mean free path 405 ± 30 gm./cm.^{2}. (The results were corrected for barometric variations to a pressure of 1015 millibars using a barometer coefficient of -1 per cent per millibar.) A measurement was made with an absorber thickness S_1

composed of 7·5 cm. of lead directly over the counters, and 48 gm./cm.^{2} of carbon above the lead. The observed rate was $0{\cdot}87 \pm 0{\cdot}05$ per hr. Comparison with the lead absorption curve shows that this rate corresponds to a lead absorber thickness of 90 ± 40 gm./cm.^{2}.

Measurements made with absorber S_1 composed of 260 gm./cm.^{2} of iron gave an observed rate corrected to 1015 mbs atmospheric pressure, of $0{\cdot}52 \times {\cdot}03$ c.p.h.r. corresponding to a lead absorber thickness of 300 gm./cm.^{2} thus giving the stopping power of iron relative to lead as $1{\cdot}15 \pm 0{\cdot}15$.

Fig. 2.

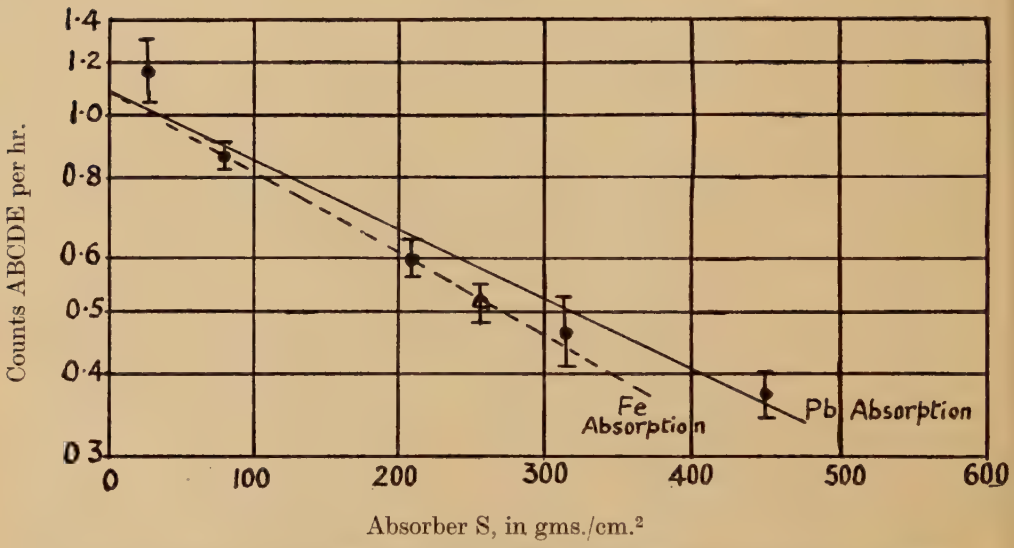

Fig. 2 shows the counting rate A B C D E plotted against absorber thickness in gm./cm.^{2}. The triangular point at 260 gm./cm.^{2} refers to iron absorber. The full line is the best curve for lead absorber, and the dotted line is the best for iron absorber.

Table I. gives the rate of accompanied showers. As the absorber over the extended trays was varied during the course of the experiment we compare the ratios

$$\frac{\mathrm{A\,B\,C\,D\,E\,X_3}}{\mathrm{A\,B\,C\,X_3}}.$$

Including all results for small absorber thicknesses we obtained a value of

$$\frac{\mathrm{A\,B\,C\,D\,E\,X_3}}{\mathrm{A\,B\,C\,X_3}}$$

of $0{\cdot}71 \pm 0{\cdot}10$. If the absorption of the accompanied showers was the same as for non-accompanied showers we should expect a ratio of $0{\cdot}31 \pm 0{\cdot}04$ for 450 gm./cm.^{2} of lead absorber. The observed value of $0{\cdot}55 \pm 0{\cdot}10$ gives an indication that the accompanied penetrating showers are more penetrating than the non-accompanied, though the statistical weight is poor.

Discussion and Comparison with other Experiments.

Similar penetrating shower measurements have been made by Piccioni (1950), Walker (1950). The number of penetrating secondaries, however, necessary to cause a count varied in the two experiments. The data of Walker (1950), also Piccioni (1950) show that the repartition of shower size under various thicknesses of absorber does not appear to alter. Accordingly the absorption curves obtained in the different experiments should be similar.

The values obtained for the apparent mean free paths in Lead by Piccioni and Walker, are respectively, 360 ± 40 gm./cm.^{2} and 405 ± 110 gm./cm.^{2}. Our value of 405 ± 30 gm./cm.^{2} is in good agreement. Further Piccioni obtained a ratio for the stopping powers of Iron and Lead of $1{\cdot}02\pm0{\cdot}13$ in agreement with our value of $1{\cdot}15\pm0{\cdot}15$.

TABLE I.

Data on Penetrating Showers Accompanied by Extensive Air Showers.

Thickness of S_1 Absorber	Time (hrs.)	Number of Counts A B C X_3	Number of Counts A B C D E X_3
26 gm./cm.^{2} of lead	97	3	3
78 gm./cm.^{2} of lead	140	9	7
105 gm./cm.^{2} of lead	128	11	5
78 gm./cm.^{2} of lead plus 50 gm./cm.^{2} of carbon	339	18	14
210 gm./cm.^{2} of lead	284	21	12
315 gm./cm.^{2} of lead	137	8	3
450 gm./cm.^{2} of lead	500	31	17
260 gm./cm.^{2} of iron	444	29	18

The interpretation of these results is not straightforward, but it is now clear from the results with both cloud chambers and photographic plates, (Brown and Mckay 1950, Camerini *et al.* 1950) that the high energy secondaries of penetrating showers are a mixture of protons, neutrons and π-mesons.

At any level in the absorber there will be simultaneous absorption and production of ionizing particles, the measured absorption thus being only indirectly related to the actual absorption processes taking place in the material.

Stress has been laid (Piccioni 1950, *cf.* Greisen 1950 for discussion of Piccioni's results) on the fact that if nuclear processes predominate for absorption and production the stopping powers of iron and lead should be in the ratios of the geometric cross sections *i. e.* 1·55 : 1, and not in the ratios of the stopping powers for ionization losses of 1·1 : 1. This, however,

is too simple an approach to the problem. In the presence of some degree of transparency such as would be expected for nucleons with energies of the order of 1 Bev, and for π-mesons in the 100 Mev—1 Bev range, the ratio of the cross sections for nuclear interactions would be considerably lower. In addition ionization loss processes will play some role and a ratio of the order of 1·2—1·4 would not therefore be in contradiction with present views as to the relatively strong interactions of π-mesons and nucleons.

It is to be expected that the nucleons forming part of the extensive showers will have a harder energy spectrum than those nucleons not accompanied by extensive showers, and thus those nucleons should give rise to higher energy events with greater penetrating power.

Acknowledgments.

The author is indebted for helpful discussion throughout this work with Profs. Janossy and McCusker and to very considerable assistance by Mr. Millar in running the experiment.

References.

Brown and Mckay, 1950, *Phys. Rev.*, **77**, 342.
Camerini, Fowler, Lock and Muirhead, 1950, *Phil. Mag.*, **41**, 413.
Greisen, 1950, *Phys. Rev.*, **77**, 713.
Piccioni, 1950, *Phys. Rev.*, **77**, 6.
Walker, 1950, *Phys. Rev.*, **77**, 686.

XXVIII. *The Conditions at a Sharp Leading Edge in Supersonic Flow.*

By O. Bardsley,
Fluid Motion Laboratory, University of Manchester*.

[Received January 10, 1951.]

[Plates IX.—XII.]

Summary.

Schlieren photographs have been taken to show the supersonic flow past a sharp wedge placed at an incidence large enough to give an expansion region on one side. In addition to the flow phenomena predicted by inviscid theory, the photographs show a weak shock wave immediately upstream of the expansion region. Various possible explanations of this are considered and it is shown that the shock wave is caused by the slight bluntness of the leading edge, although the thickness of the leading edge is only about $8\,\mu$. It cannot be explained by considering the growth of the boundary layer, neither is there any evidence of boundary-layer separation.

§ 1. Introduction.

According to inviscid theory, the supersonic flow past a perfectly sharp wedge consists of two independent regions separated by the wedge. If the angle of incidence of the wedge is sufficiently large there is a centred expansion on one side and a shock wave on the other. It was expected that this theoretical flow pattern might not be found in practice, either because of viscous effects or because of bluntness of the leading edge. Some experiments were therefore made to investigate the supersonic flow past a wedge at a high incidence.

§ 2. Notation.

M, Mach number.
p, pressure before shock wave.
Δp, rise of pressure in shock wave.
R, Reynolds number.
$s = \Delta p/p$, shock-wave strength.
T, absolute temperature.
t, thickness of body near leading edge.
u_1, velocity outside boundary layer.
x, distance from leading edge.

* Communicated by W. A. Mair.

y, distance from axis.
δ_1, displacement thickness of boundary layer in compressible flow.
δ_1^*, displacement thickness of boundary layer in incompressible flow.
γ, ratio of specific heats.
θ^*, momentum thickness of boundary layer in incompressible flow.
μ, coefficient of viscosity.
ν, coefficient of kinematic viscosity.
σ, Prandtl number.

§ 3. Experimental Details.

The intermittent supersonic wind tunnel, the two-mirror schlieren system, and the technique for measurement of humidity have already been described by Bardsley and Mair (1951). The mean Mach number in the working section during the present experiments was 1·965. An alternative optical system which produced a magnified image was used for figs. 6–8 (Pls. XI. & XII.). In this system the object lens was removed and the second mirror arranged to give an enlarged image of a selected area of the working section on the screen. Measurements of the humidity of the air passing through the tunnel showed that the water-vapour content was always less than 1 part in 2000 by weight.

The wedge used was 1·27 cm. long in the direction of the stream, had an apex angle of 10·0° and extended across the whole width of the tunnel. It was made of high-carbon steel, ground and lapped to make the leading edge as nearly perfect as possible, with a constant apex angle. An estimate of the thickness of the leading edge was obtained using a shadowgraph technique. The profile of the wedge was illuminated and a short-focus convex lens was used to form an image magnified 25 times on a screen. Several typical parts of this image were photographed before and after the experiments. Before the experiments about 90 per cent of the span had a profile similar to that shown in fig. 1 (Pl. IX.); the remaining 10 per cent was similar to that shown in fig. 2 (Pl. IX.). After the experiments about 50 per cent of the span had deteriorated to the condition shown in fig. 2, the remainder being unaltered. The deterioration was probably caused by dust in the air stream, although the total running time of the tunnel was only about 2 minutes.

Fig. 9 is a diagrammatic representation of the indentations shown in figs. 1 and 2. The average depth of the indentations (h) was measured on the photographs. Assuming that the wedge angle was constant and that the thickness at a point A was very small (2 μ), the thickness at a point B was calculated. This thickness was found to be 5 μ for the parts of the edge in better condition (fig. 1) and 12 μ for the deteriorated parts (fig. 2). The same method and assumptions were used previously on a similar wedge and gave good agreement with the thickness as measured by a calibrated microscope.

The wedge was supported in the wind tunnel by two arms on the downstream side. The position of these arms was altered, as required, to change the angle of incidence of the wedge.

The knife edges in the schlieren system were horizontal and were arranged so that in all the photographs increasing density in an upward direction was represented by a dark region.

Preliminary visual observations, using a mercury-vapour lamp, showed that the flow on the lower side of the wedge was rather unsteady when the deflection angle at the upper surface was greater than about 7°. This unsteadiness appeared to be due to the interaction between the shock wave on the lower side of the wedge and the boundary layer on the bottom wall of the tunnel. Because of this unsteadiness a short-duration flash (effective exposure about 5 microseconds) was used as the light source for photography. Photographs of the flow are shown in figs. 3–5 (Pls. X. & XI.) for positions of the wedge giving stream deflection angles (on the expansion

Fig. 9.

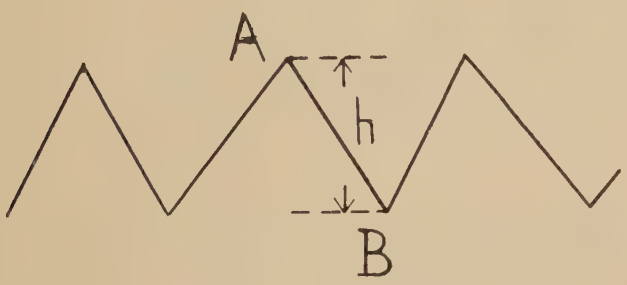

Indentations in leading edge.

side) of 0, 5, and 10°. (The possible error in these angles is $\pm\frac{1}{4}°$.) At the Mach number of these experiments (1·965) the maximum deflection at an attached shock wave is 22·3°, so that with this wedge (10° apex angle) the deflection at the expansion could not exceed 12·3°.

§ 4. Discussion of the Photographs.

The arms supporting the wedge continue downstream beyond the field of view ; the position of the back of the wedge is revealed by the expansion region on the lower side. The wake is clearly visible in figs. 4 and 5, and shock waves can be seen where the direction of flow changes to that of the wake. The bump that appears about two-thirds of the way along the upper surface of the wedge is a small piece of rubber sealing-material at one of the glass side plates. In figs. 3–5 the region representing the shock wave on the high-pressure side of the wedge is fan-shaped in appearance. This is caused by curvature of the shock wave as it enters the turbulent boundary layers on the glass side-walls of the tunnel.

In each photograph the flow past the wedge is similar to that predicted by inviscid theory, but in addition there is a shock wave immediately upstream of the expansion region. This must be caused either by viscosity or by the slight bluntness of the leading edge. Three alternative explanations are considered below.

Firstly, consider the rate of growth of the boundary layer. In the experiments the shock wave occurs for a stream deflection angle (measured at the surface of the wedge) as large as 10°. The boundary layer is therefore considered at the point where its rate of growth is equal to 10°. Blasius' solution (1908) of the laminar boundary-layer equations for incompressible flow past a flat plate shows that the displacement thickness is

$$\delta_1^* = 1{\cdot}72(\nu x/u_1)^{\frac{1}{2}},$$

and the momentum thickness θ^* is given by

$$\theta^*/\delta_1^* = 0{\cdot}386,$$

where ν is the kinematic viscosity, u_1 is the velocity outside the boundary layer and x is the distance from the leading edge of the plate. It follows from Howarth's solution (1948) for a flat plate (assuming $\sigma = 1$ and $\mu \propto T$) that for compressible flow the displacement thickness is

$$\delta_1 = \delta_1^* \left[1 + \frac{\gamma - 1}{2} \left(1 + \frac{\theta^*}{\delta_1^*} \right) M^2 \right].$$

Hence in our case an approximate value of the displacement thickness of the boundary layer on the surface of the wedge is given by

$$\delta_1 = 4(\nu x/u_1)^{\frac{1}{2}}.$$

The rate of growth of the boundary layer is then

$$\frac{d\delta_1}{dx} = 2\left(\frac{\nu}{u_1 x}\right)^{\frac{1}{2}} = 2R^{-\frac{1}{2}},$$

where $R = u_1 x/\nu$, the Reynolds number at the station x.

At the point where the rate of growth is equal to 10° ($\approx 0{\cdot}2$ radians),

$$\frac{d\delta_1}{dx} = 0{\cdot}2 = 2R^{-\frac{1}{2}},$$

therefore $R = 100$.

The boundary-layer theory is not strictly applicable for such a small Reynolds number. However, since the theory would make $d\delta_1/dx \to \infty$ as $x \to 0$ it follows that the actual rate of growth near the leading edge must be smaller than that given by the theory. Hence at the point where the rate of growth of the boundary layer is 10°, x is not greater than the value given by $R = 100$. The stagnation conditions are atmospheric, so

that the Reynolds number in the test section can be expressed as $1{\cdot}34\times10^5$ per cm. Therefore when R=100,

$$x=\frac{100}{1{\cdot}34\times10^5}\approx 8\times10^{-4}\text{ cm.},$$

and at this point

$$\delta_1=4\mathrm{R}^{-\frac{1}{2}}x\approx 3\times10^{-4}\text{ cm.}$$

Thus if there were a point at which the boundary layer grew so rapidly that the sign of the stream deflection was consistent with the presence of a shock wave, the values of x and δ_1 at this point would be of the same order

Fig. 10.

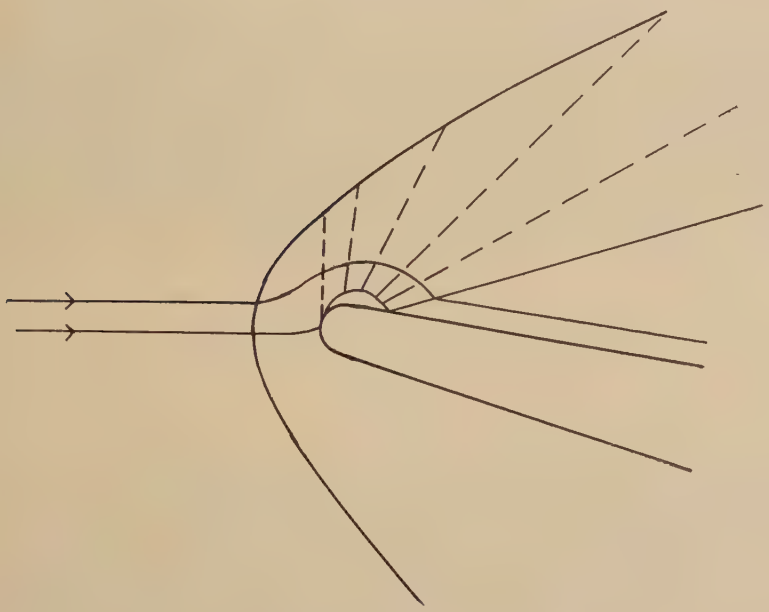

Flow with separation of boundary layer.

of magnitude as the thickness of the leading edge itself. This suggests that the effect of the boundary layer on the formation of the shock wave in front of the expansion is small compared with the effect of the bluntness of the leading edge.

Secondly, consider the possibility of boundary-layer separation. This is a well known phenomenon in the case of flow past blunt-nosed bodies and has been observed, for example, by Liepmann (1950) and by Holder, Tomlinson and Rogers (1949). In their experiments the bodies were at zero incidence and it was found that for sufficiently blunt noses there was a separation of the boundary layer near the nose, followed by re-attachment with an oblique shock wave at the point of re-attachment. If this type of flow occurred on the expansion side in the present experiments the pattern observed would be similar to that shown in fig. 10. In particular, a shock

EXPLANATION OF THE PLATES.

Plate IX.

Fig. 1.

Leading edge in good condition.

Fig. 2.

Leading edge in deteriorated condition.

Plate X.

Fig. 3.

Stream deflection angle 0°.

Fig. 4.

Stream deflection angle 5°.

Plate XI.

Fig. 5.

Stream deflection angle 10°.

Fig. 6.

Stream deflection angle 0°.

Plate XII.

Fig. 7.

Stream deflection angle 5°.

Fig. 8.

Stream deflection angle 10°.

Fig. 1.

Fig. 2.

To face page 260

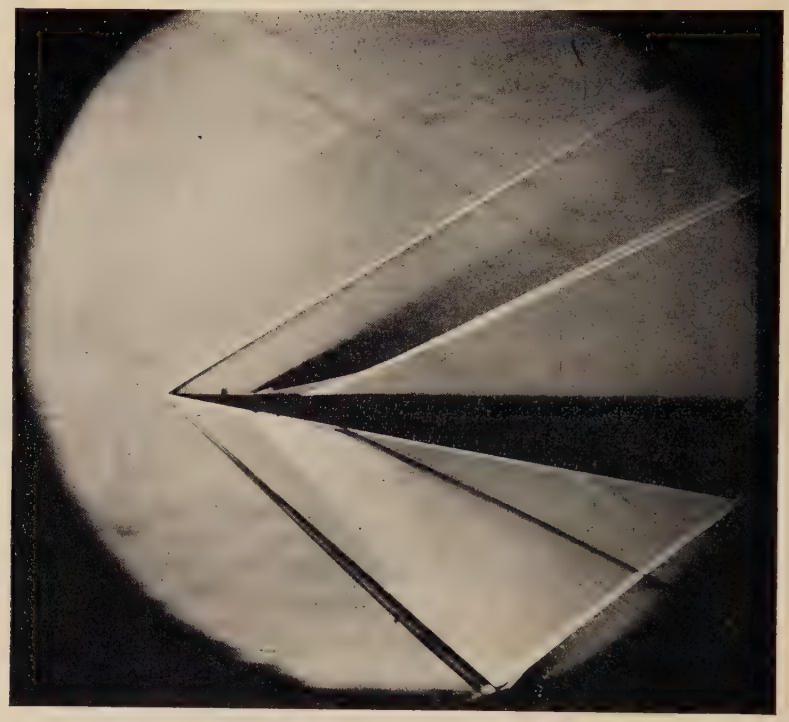

Fig. 3.

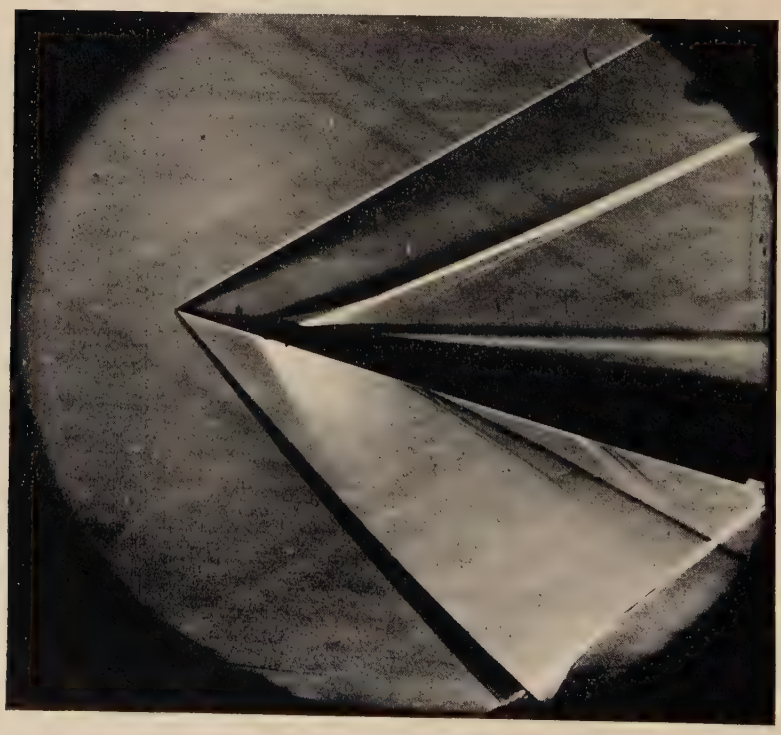

Fig 4.

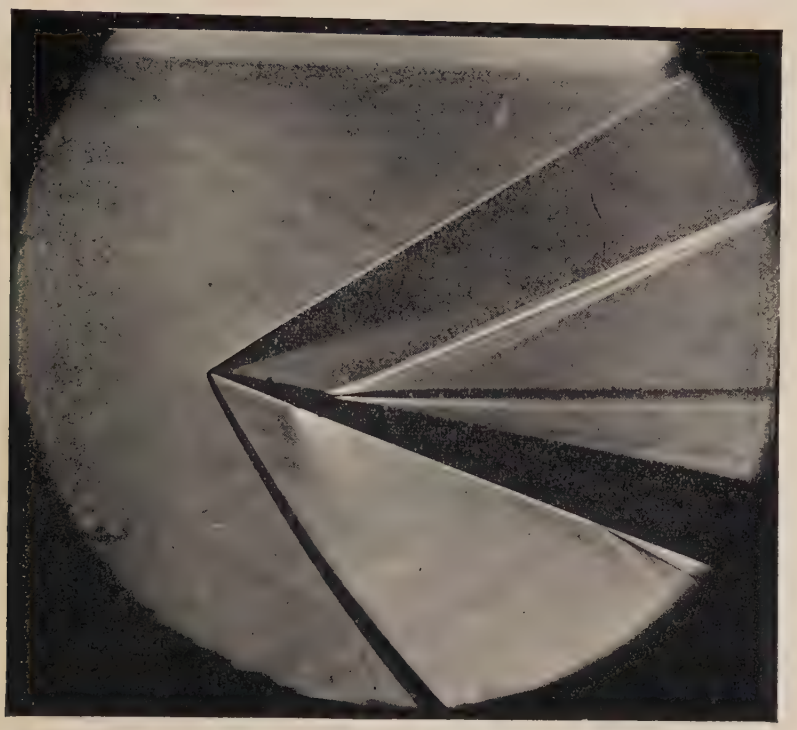

Fig. 5.

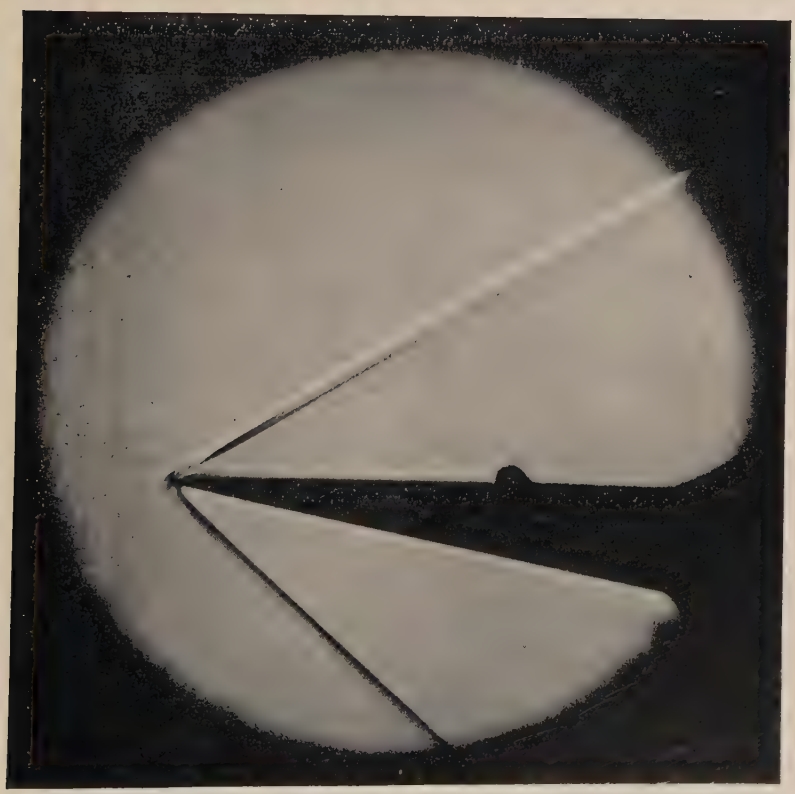

Fig. 6.

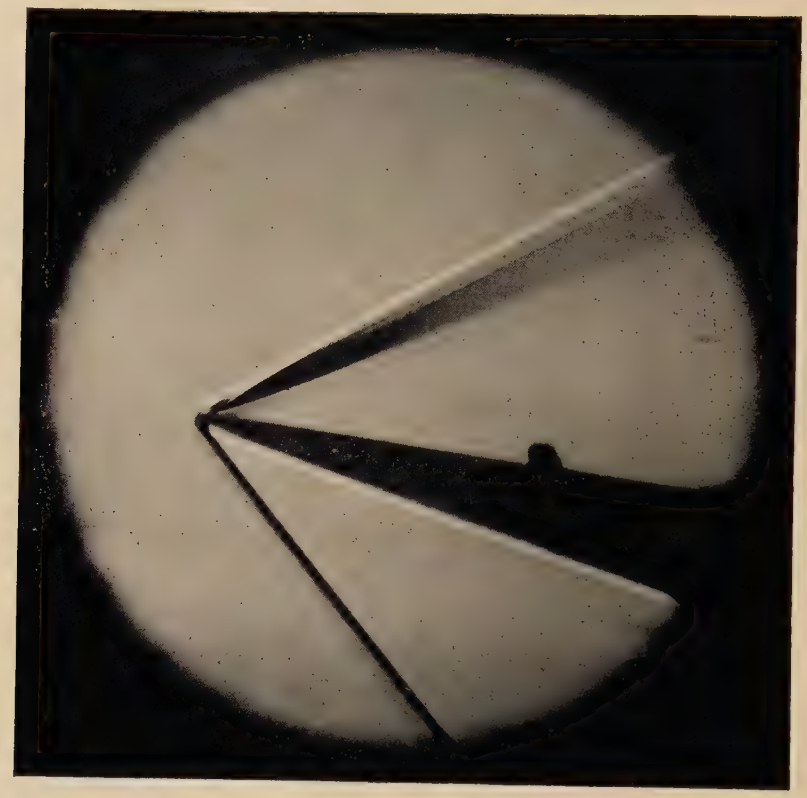

Fig. 7.

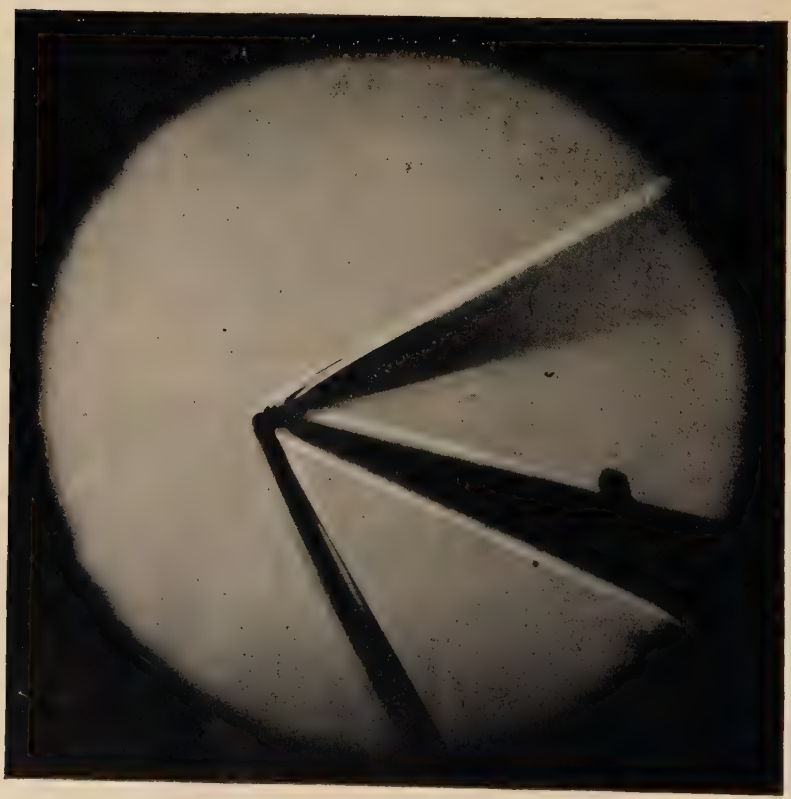

Fig. 8.

wave would be visible on the downstream side of the expansion. No shock wave can be seen in this position in figs. 3–5, but to investigate this further the schlieren system was modified, as described earlier, to give an enlarged image. Photographs produced by this system are shown in figs. 6–8 ; the scale of these is such that the wedge chord is approximately three-quarters of the diameter of the field of view. These show the flow for stream deflection angles of 0, 5, and 10°, and correspond to figs. 3, 4, and 5 respectively. Again, there is no sign of a second shock wave that would indicate boundary-layer separation. Moreover, a theoretical investigation by Mair (not yet published) has shown that a shock wave having a strength ($s=\Delta p/p$) as small as about 0·01 should be detectable with this schlieren apparatus. The deflection of the stream at a shock wave of this strength is only about 0·2°.

Lastly, consider the effect of the finite thickness of the leading edge. The inclination of the shock wave at a large distance from the leading edge was measured and found to be about 31·7° in all the photographs. This corresponds to a shock-wave strength (s) of 0·08. Since the possible error in measuring the shock-wave angle is about $\pm\frac{1}{2}°$, the corresponding error in s is $\pm 0{\cdot}035$, so that only the order of magnitude of the shock-wave strength can be found by this method. As already mentioned, a shock wave having a strength of this order should be easily visible in the photographs.

Now consider the theoretical relation between the shock-wave strength and the thickness of the leading edge of the wedge. For inviscid flow, Friedrichs (1948) has shown that the strength of the shock wave from the leading edge of a thin two-dimensional body with a rounded nose is inversely proportional to the square root of the distance from the axis, for large values of this distance. This can be written in the dimensionless form

$$s=k(t/y)^{\frac{1}{2}},$$

where k is a constant (for geometrically similar bodies), y is the distance from the axis, and t is a length defining the size of the body, taken as the thickness near the leading edge. Applying this result to the photographs of the flow past a flat plate with a blunt nose, obtained by Holder, Tomlinson and Rogers (1949), the constant k is found (by measuring the shock-wave angles) to be about 3. If it is assumed that the irregularly shaped edge of the wedge (figs. 1 and 2) gives a flow at large distances similar to that produced by a two-dimensional blunt nose of thickness t, the equation $s=3(t/y)^{\frac{1}{2}}$ can be applied to the present experiments.

Putting $t=8\times10^{-4}$ cm. (an average value) and $y=6$ cm., we get $s=0{\cdot}035$. Since the value of y at the upper boundary of figs. 3–5 is only about 5 or 6 cm., this calculation shows that a shock wave having a strength of the same order of magnitude as that observed can be explained by the known slight bluntness of the leading edge, without any consideration of viscosity.

§ 5. Conclusions.

It has been shown that the difference between the observed flow past a wedge (as sharp as possible) and that predicted by the idealized theory can be explained by the bluntness of the leading edge. There is evidence that viscosity has no significant effect on the formation of the shock wave upstream of the expansion region.

If experiments of this kind were made with a leading edge of greater thickness, the strength of the shock wave for a given value of y would be greater. The effect of the growth of the boundary layer would then be even less important, and only if the boundary layer separated could viscosity have any significant effect.

It may be noted that in these experiments the Reynolds number, based on the thickness of the leading edge, was very small compared with that in most other experiments on flow past blunt-nosed bodies. It is suggested that this difference in Reynolds number is important and may explain the absence of boundary-layer separation in the present experiments.

Acknowledgments.

The author wishes to thank Professor M. J. Lighthill and Mr. W. A. Mair for their suggestions, and for the interest they have taken in the work. During the course of the research the author was assisted by a grant from the Aeronautical Research Council.

References.

Bardsley, O., and Mair, W. A., 1951, *Phil. Mag.*, **52,** 1.

Blasius, H., 1908, *Zeit. Math. Phys.*, **56,** 4–13.

Friedrichs, K. O., 1948, *Communications on Applied Mathematics*, Vol. 1, pp. 211–245.

Holder, D. W., Tomlinson, R. C., and Rogers, E. W. E., 1949, A.R.C. 12418 (to be published).

Howarth, L., 1948, *Proc. Roy. Soc.* A, **194,** 16.

Liepmann, H. W., 1950, U.S. Naval Ordnance Laboratory Report 1133.

XXIX. *Matrix Elements for Octupole Radiative Transitions.*

By A. P. French,
Cavendish Laboratory, Cambridge *.

[Received December 11, 1950.]

During the analysis of some recent experiments on the angular correlation between alpha particles and gamma rays (Barnes, French and Devons 1950) it was necessary to find values of the matrix elements for certain octupole transitions. These were derivable from general formulæ obtained by Fierz (1949) by group-theoretical methods. Although Fierz deals with multipole radiation of any order, his formulæ do not cover all possible transitions. If j represents the total angular momentum of the initial state, which goes over to a state of angular momentum $j+\Delta j$ with the emission of radiation of multipole order 2^l, then the cases treated by Fierz are limited to $\Delta j=\pm l$ or $\pm(l-1)$. It was thought to be of interest to extend calculations to all possible values of Δj for the particular case of octupole radiation, since radiation of this order (or even higher) seems to appear rather frequently in nuclear problems.

The method used was a simple extension of that applied by Condon and Shortley (1935) to the problem of quadrupole transitions. We assume that the initial state is characterized by j, by its component m along some specified axis (which we shall take as the polar axis Oz in spherical polar coordinates, and by other observables α, with which we are not immediately concerned. The final state is characterized in a similar way by (j', m', α'). The matrix element of electric octupole moment for a transition between the states may then be written as follows :

$$(\alpha jm \,|\, \mathbf{rrr} \,|\, \alpha' j' m') = \sum_{\alpha'' j'', \alpha''' j'''} \sum_{m'', m'''} (\alpha jm \,|\, \mathbf{r} \,|\, \alpha'' j'' m'')(\alpha'' j'' m'' \,|\, \mathbf{r} \,|\, \alpha''' j''' m''') \times (\alpha''' j''' m''' \,|\, \mathbf{r} \,|\, \alpha' j' m').$$

For given values of (α'', j'') and (α''', j''') this summation has for all (m'', m''') a common factor $G(j'', j''')$ given (in the Condon and Shortley notation) by

$$G(j'', j''') = (\alpha j \,\vdots\, r \,\vdots\, \alpha'' j'')(\alpha'' j'' \,\vdots\, r \,\vdots\, \alpha''' j''')(\alpha''' j''' \,\vdots\, r \,\vdots\, \alpha' j').$$

In order to perform a final summation over the (j'', j''') and so obtain the octupole matrix element in manageable form, it is necessary to relate the various $G(j'', j''')$. This can be done through the requirement that $\mathbf{r}\times\mathbf{r}$ shall be zero. If we put

$$\mathbf{r}=\mathbf{i}x+\mathbf{j}y+\mathbf{k}z,$$

$$\mathrm{R}=x-iy,$$

then one must have $$z\mathrm{R}-\mathrm{R}z=0.$$

* Communicated by Professor D. R. Hartree.

This equation can be multiplied through from the left or from the right with z or R, and one can then demand that matrix elements such as $(\alpha jm \mid zz\mathrm{R}-z\mathrm{R}z \mid \alpha' j' m')$ shall be zero. The matrix elements of R and z in the (j, m) scheme are tabulated (Condon and Shortley, p. 62), so it is an easy matter to obtain a set of equations connecting the $\mathrm{G}(j'', j''')$. Once this is done, a matrix element of octupole moment can be expressed in the form

$$(\alpha jm \mid \mathbf{rrr} \mid \alpha' j' m') = g(j, m, j', m') \times \mathrm{G},$$

where G is the same for all transitions $m \rightarrow m'$ having (α, j) and (α', j') the same. g is then a definite function of the j's and m's and can be found.

The radiation field is obtained from the electric moment by writing

$$\mathbf{E}(\theta, \phi) = \text{const} \times (\boldsymbol{\theta}_0\boldsymbol{\theta}_0 + \boldsymbol{\varphi}_0\boldsymbol{\varphi}_0) \,.\, (\alpha jm \mid \mathbf{rrr} \mid \alpha' j' m') : \mathbf{r}_0\mathbf{r}_0,$$

where $\mathbf{r}_0$, $\boldsymbol{\theta}_0$, $\boldsymbol{\varphi}_0$ are the unit vectors of a spherical polar system. The double dot product here denotes a scalar product of $\mathbf{r}_0$ with each of the two right-hand members of every triad of vectors appearing in the octupole moment. The form of the field depends, of course, only on Δm. The possibilities are listed below for convenience, normalized to an outgoing intensity of $4\pi/7$.

$$\mathbf{E}(0) \quad = \frac{\sqrt{3}}{4}\boldsymbol{\theta}_0 \sin\theta(5\cos^2\theta - 1) \qquad = \frac{\sqrt{3}}{4}\mathbf{L}(0) \quad \text{say,}$$

$$\mathbf{E}(\pm 1) = \frac{1}{8}[\boldsymbol{\theta}_0 \cos\theta(15\cos^2\theta - 11) \pm i\boldsymbol{\varphi}_0(5\cos^2\theta - 1)]e^{\pm i\psi} = \frac{1}{8}\mathbf{L}(\pm 1) \quad ,,$$

$$\mathbf{E}(\pm 2) = \frac{\sqrt{10}}{8}[\boldsymbol{\theta}_0 \sin\theta(3\cos^2\theta - 1) \pm i\boldsymbol{\varphi}_0 \sin 2\theta]e^{\pm 2i\psi} = \frac{\sqrt{10}}{8}\mathbf{L}(\pm 2) \quad ,,$$

$$\mathbf{E}(\pm 3) = \frac{\sqrt{15}}{8}[\boldsymbol{\theta}_0 \sin^2\theta \cos\theta \pm i\boldsymbol{\varphi}_0 \sin^2\theta]e^{\pm 3i\psi} = \frac{\sqrt{15}}{8}\mathbf{L}(\pm 3) \quad ,,$$

The matrix elements for all possible types of electric octupole transition are set out below. The corresponding formulae for magnetic transitions are obtained by rotating **E** through 90° about $\mathbf{r}_0$ in the usual way. The matrices are, of course, Hermitian, but for convenience in use a complete tabulation is given. The coefficients A, B, C, etc., are the quantities G mentioned above.

$\underline{\Delta j = +3}$

$$(j, m \mid \mathbf{E} \mid j+3, m \pm 3) = \mp \tfrac{1}{4}\mathrm{A}\sqrt{\{(j \pm m + 1)(j \pm m + 2)(j \pm m + 3)(j \pm m + 4) \times (j \pm m + 5)(j \pm m + 6)\}}\mathbf{L}(\pm 3),$$

$$(j, m \mid \mathbf{E} \mid j+3, m \pm 2) = -\tfrac{1}{2}\mathrm{A}\sqrt{\{(j + m + 1)(j - m + 1)(j \pm m + 2)(j \pm m + 3) \times (j \pm m + 4)(j \pm m + 5)\}}\mathbf{L}(\pm 2),$$

$$(j, m \mid \mathbf{E} \mid j+3, m \pm 1) = \mp \tfrac{1}{4}\mathrm{A}\sqrt{\{(j + m + 1)(j - m + 1)(j + m + 2)(j - m + 2) \times (j \pm m + 3)(j \pm m + 4)\}}\mathbf{L}(\pm 1),$$

$$(j, m \mid \mathbf{E} \mid j+3, m) \quad = -\mathrm{A}\sqrt{\{(j + m + 1)(j - m + 1)(j + m + 2)(j - m + 2) \times (j + m + 3)(j - m + 3)\}}\mathbf{L}(0).$$

$\underline{\Delta j=+2}$

$$(j, m \mid \mathbf{E} \mid j+2, m\pm 3)=\tfrac{3}{4}\mathrm{B}\sqrt{\{(j\mp m)(j\pm m+1)(j\pm m+2)(j\pm m+3)} \times(j\pm m+4)(j\pm m+5)\}\mathbf{L}(\pm 3),$$

$$(j, m \mid \mathbf{E} \mid j+2, m\pm 2)=\mp\tfrac{1}{2}\mathrm{B}(2j\mp 3m)\sqrt{\{(j\pm m+1)(j\pm m+2)(j\pm m+3)} \times(j\pm m+4)\}\mathbf{L}(\pm 2),$$

$$(j, m \mid \mathbf{E} \mid j+2, m\pm 1)=\tfrac{1}{4}\mathrm{B}(j-3m)\sqrt{\{(j+m+1)(j-m+1)(j\pm m+2)} \times(j\pm m+3)\}\mathbf{L}(\pm 1),$$

$$(j, m \mid \mathbf{E} \mid j+2, m) \quad =-3\mathrm{B}m\sqrt{\{(j+m+1)(j-m+1)(j+m+2)} \times(j-m+2)\}\mathbf{L}(0).$$

$\underline{\Delta j=+1}$

$$(j, m \mid \mathbf{E} \mid j+1, m\pm 3)=\pm\tfrac{1}{4}\mathrm{C}\sqrt{\{(j\mp m-1)(j\mp m)(j\pm m+1)(j\pm m+2)} \times(j\pm m+3)(j\pm m+4)\}\mathbf{L}(\pm 3),$$

$$(j, m \mid \mathbf{E} \mid j+1, m\pm 2)=-\tfrac{1}{6}\mathrm{C}(j\mp 3m-2)\sqrt{\{(j\mp m)(j\pm m+1)(j\pm m+2)} \times(j\pm m+3)\}\mathbf{L}(\pm 2),$$

$$(j, m \mid \mathbf{E} \mid j+1, m\pm 1)=\mp\tfrac{1}{4}\mathrm{C}\left[\frac{j(j+7)}{15}\pm\frac{m(2j-1)}{3}-m^2\right]\sqrt{\{(j\pm m+1)} \times(j\pm m+2)\}\mathbf{L}(\pm 1),$$

$$(j, m \mid \mathbf{E} \mid j+1, m) \quad =-\mathrm{C}\left[\frac{j(j+2)}{5}-m^2\right]\sqrt{\{(j-m+1)(j+m+1)\}}\mathbf{L}(0).$$

$\underline{\Delta j=0}$

$$(j, m \mid \mathbf{E} \mid j, m\pm 3)=-\tfrac{1}{4}\mathrm{D}\sqrt{\{(j\mp m-2)(j\mp m-1)(j\mp m)(j\pm m+1)} \times(j\pm m+2)(j\pm m+3)\}\mathbf{L}(\pm 3),$$

$$(j, m \mid \mathbf{E} \mid j, m\pm 2)=\mp\tfrac{1}{2}\mathrm{D}(1\pm m)\sqrt{\{(j\mp m-1)(j\mp m)(j\pm m+1)(j\pm m+2)\}} \times\mathbf{L}(\pm 2),$$

$$(j, m \mid \mathbf{E} \mid j, m\pm 1)=\tfrac{1}{4}\mathrm{D}\left[\frac{(j-1)(j+2)}{5}\mp m-m^2\right]\sqrt{\{(j\mp m)(j\pm m+1)\}} \times\mathbf{L}(\pm 1),$$

$$(j, m \mid \mathbf{E} \mid j, m) \quad =-\mathrm{D}m\left[\frac{(3j^2+3j-1)}{5}-m^2\right]\mathbf{L}(0).$$

$\underline{\Delta j=-1}$

$$(j, m \mid \mathbf{E} \mid j-1, m\pm 3)=\mp\tfrac{1}{4}\mathrm{E}\sqrt{\{(j\pm m+1)(j\pm m+2)(j\mp m)(j\mp m-1)} \times(j\mp m-2)(j\mp m-3)\}\mathbf{L}(\pm 3),$$

$$(j, m \mid \mathbf{E} \mid j-1, m\pm 2)=-\tfrac{1}{6}\mathrm{E}(j\pm 3m+3)\sqrt{\{(j\pm m+1)(j\mp m)(j\mp m-1)} \times(j\mp m-2)\}\mathbf{L}(\pm 2),$$

$$(j, m \mid \mathbf{E} \mid j-1, m\pm 1)=\pm\tfrac{1}{4}\mathrm{E}\left[\frac{(j+1)(j-6)}{15}\mp\frac{m(2j+3)}{3}-m^2\right] \times\sqrt{\{(j\mp m)(j\mp m-1)\}}\mathbf{L}(\pm 1),$$

$$(j, m \mid \mathbf{E} \mid j-1, m) \quad =-\mathrm{E}\left[\frac{(j-1)(j+1)}{5}-m^2\right]\sqrt{\{(j-m)(j+m)\}}\mathbf{L}(0).$$

$\underline{\Delta j=-2}$

$$(j, m \,|\, \mathbf{E} \,|\, j-2, m\pm 3)=\tfrac{3}{4}\mathrm{F}\sqrt{\{(j\pm m+1)(j\mp m)(j\mp m-1)(j\mp m-2)} \times(j\mp m-3)(j\mp m-4)\}\mathbf{L}(\pm 3),$$

$$(j, m \,|\, \mathbf{E} \,|\, j-2, m\pm 2)=\pm\tfrac{1}{2}\mathrm{F}(2j\pm 3m+2)\sqrt{\{(j\mp m)(j\mp m-1)(j\mp m-2)} \times(j\mp m-3)\}\mathbf{L}(\pm 2),$$

$$(j, m \,|\, \mathbf{E} \,|\, j-2, m\pm 1)=\tfrac{1}{4}\mathrm{F}(j\pm 3m+1)\sqrt{\{(j+m)(j-m)(j\mp m-1)} \times(j\mp m-2)\}\mathbf{L}(\pm 1),$$

$$(j, m \,|\, \mathbf{E} \,|\, j-2, m) \quad =-3\mathrm{F}m\sqrt{\{(j+m)(j-m)(j+m-1)(j-m-1)\}}\mathbf{L}(0).$$

$\underline{\Delta j=-3}$

$$(j, m \,|\, \mathbf{E} \,|\, j-3, m\pm 3)=\pm\tfrac{1}{4}\mathrm{G}\sqrt{\{(j\mp m)(j\mp m-1)(j\mp m-2)(j\mp m-3)} \times(j\mp m-4)(j\mp m-5)\}\mathbf{L}(\pm 3),$$

$$(j, m \,|\, \mathbf{E} \,|\, j-3, m\pm 2)=\tfrac{1}{2}\mathrm{G}\sqrt{\{(j+m)(j-m)(j\mp m-1)(j\mp m-2)(j\mp m-3)} \times(j\mp m-4)\}\mathbf{L}(\pm 2),$$

$$(j, m \,|\, \mathbf{E} \,|\, j-3, m\pm 1)=\pm\tfrac{1}{4}\mathrm{G}\sqrt{\{(j+m)(j-m)(j+m-1)(j-m-1)} \times(j\mp m-2)(j\mp m-3)\}\mathbf{L}(\pm 1),$$

$$(j, m \,|\, \mathbf{E} \,|\, j-3, m) \quad =-\mathrm{G}\sqrt{\{(j+m)(j-m)(j+m-1)(j-m-1)} \times(j+m-2)(j-m-2)\}\mathbf{L}(0).$$

References.

Barnes, C. A., French, A. P., and Devons, S., 1950, *Nature, Lond.*, **166**, 145.

Condon, E. U., and Shortley, G. H., 1935, *The Theory of Atomic Spectra* (Cambridge : University Press).

Fierz, M., 1949, *Helv. Phys. Acta.*, **22**, 489.

XXX. *Fluctuations in the Intensity of Radio Waves from Galactic Sources.*

By C. G. Little and A. Maxwell,
Jodrell Bank Experimental Station, University of Manchester*.

[Received January 18, 1951.]

Summary.

It has been shown previously that the fluctuations in the intensity of radio energy from the galactic sources have a local terrestrial origin. This paper describes further observations of the two most intense sources, in the constellations of Cygnus and Cassiopeia, taken over a wide range of angles of elevation. At high angles of elevation the radio fluctuations are shown to be correlated with the occurrence of "spread" ionospheric echoes from the F region. When the sources are low on the northern horizon fluctuations are always observed; these are probably introduced by the passage of radio waves through the continuously disturbed ionospheric regions at high magnetic latitudes. Spaced receiver observations taken over base lines of 0·1, 4 and 11 km. enable the scale of the radio energy diffraction pattern across the ground to be determined.

§ 1. Introduction.

Fluctuations in the galactic radio emissions from the region of Cygnus were first observed by Hey, Parsons and Phillips (1946). They concluded that these fluctuations originated in a high intensity variable source of small angular diameter. Subsequently Bolton and Stanley (1948), using an interference technique, discovered a localized source of angular width $<8'$ in the Cygnus region, from which they recorded a variable component of radiation at 100 Mc./s. At this time it was generally assumed that the variable component was due to true variations in the source emission. Recent combined work by Smith (1950), Little and Lovell (1950), has shown, however, that the fluctuations in the radio emission from a galactic source are not inherent in the source itself, but are impressed on the incoming radiation as it passes through the earth's ionosphere.

The occurrence of fluctuations at night when the electron density of the lower ionospheric layers is small suggests that the F region is the most probable origin of the fluctuations. (The existence of fluctuations when a source is high in elevation indicates that tropospheric refraction is not the cause of the phenomenon.) It was suggested by Little and Lovell that diffraction of the incident radiation by irregularities in the F region

* Communicated by Dr. A. C. B. Lovell.

would suffice to account for the observed fluctuations. An analysis of the occurrence of fluctuations and of "spread" F echoes which are believed to be associated with such irregularities has now been completed and is given in § 4.

The spaced receiver observations referred to above were made at transit of the two most intense galactic sources, in Cygnus (Declination approximately $+40° 30'$, Right Ascension $19^h 57^m$) and in Cassiopeia (Declination approximately $+58°$, Right Ascension $23^h 21^m$). This work has now been extended to all angles of elevation by using aerials movable in azimuth and elevation. In this way it has been possible to investigate in more detail the effect of the ionosphere on the radiation.

§ 2. Apparatus.

The apparatus consisted of two equipments working on a frequency of 81·5 Mc./s., each using a directional aerial, movable in azimuth and elevation, a sensitive, high gain receiver and a recording meter. One receiver was sited permanently at the Jodrell Bank Experimental Station, Cheshire (Lat. 53° 14′ N., Long. 2° 18′ W.), and was connected to a 30 ft. aperture, focal plane paraboloid aerial (free space beam width $\pm 11°$, $\pm 15°$ to half power). A mobile equipment with an array of two Yagi aerials (beam width $\pm 11°$ $\pm 21°$) was used at spacings up to 11 km. from Jodrell Bank.

The receivers used were of the conventional superheterodyne type, modified to include two preamplification stages of low noise factor, and two stages of post detection amplifcation for recording weak signals. The characteristics of the receivers were: Frequency 81·5 Mc./s., bandwidth 0·6 Mc./s., output time constant 0·2 seconds, noise factor 4, overall gain 10^8. All receiver power supplies were carefully stabilized. Pen recording milliammeters were used as recording instruments, with chart speeds ranging from 12 inches per minute to 3 inches per hour.

In this paper, when it is stated that galactic noise fluctuations were "not observed" it is implied that the fluctuations were less than the ripple in the receiver noise output. For the apparatus used, the minimum detectable level was of the order of 1/500 of the total receiver noise, corresponding to a 5–10 per cent modulation of the source intensity. Strong galactic noise fluctuations showed peak intensities up to 40 times the minimum detectable fluctuation level.

§ 3. Method of Observation.

The experiments were carried out over the period May 1949–December 1950, and may be divided into 3 sections: (i.) Transit observations to investigate the correlation between the fluctuations and local ionospheric phenomena. (ii.) Continuous observations to investigate the changes in amplitude and period of the fluctuations with elevation of the source. (iii.) Spaced receiver observations to determine the linear dimensions of the ionospheric irregularities responsible for the fluctuations.

§ 4. Observations at Transit —Correlation with Spread F.

The experiments of Smith, Little and Lovell, referred to in § 1, showed that the fluctuations must originate in a local medium. An analysis of a series of transit observations, taken over the period May 1949–December 1950, has now been made to establish the extent of the correlation of the fluctuations with the ionospheric discontinuities which give rise to a " spread " in the critical frequency and height of F region echoes.

Table I. compares the occurrence of galactic noise fluctuations and spread F conditions during the transit of the Cygnus and Cassiopeia sources. The galactic noise observations, made at Jodrell Bank, refer to the period ± 1 hour from transit, whilst the ionospheric observations were made at Slough, some 230 km. to the South, and refer to the period transit ± 2 hours.

Table I.

Correlation of galactic noise fluctuations with spread F.

Radio source	No. of occasions when spread F and galactic noise observations were made	No. of occasions when spread F and noise fluctuations were		Spread F observed but no galactic noise fluctuations	Galactic noise fluctuations observed but no Spread F
		(i.) Both observed	(ii.) Both absent		
Cygnus	205	53 (26%)	106 (52%)	16 (8%)	30 (14%)
Cassiopeia	195	69 (35%)	74 (38%)	36 (19%)	16 (8%)

Transit observations May 1949 to December 1950.

It is seen that the galactic noise fluctuations and spread F were simultaneously present, or absent, for 75 per cent of the observations, *i. e.* only 25 per cent of the runs indicate the presence of the one without the other. (Smith, Little and Lovell have shown that there is a 10 per cent chance that fluctuations will be observed at only one of two sites 210 km. apart and hence a correlation figure higher than 90 per cent cannot be expected.)

§ 5. Spaced Receiver Experiments.

Previous work with spaced receivers showed that there was no correlation between (transit) fluctuations observed on two receivers separated by a distance of 210 km. but that a fairly good correlation existed for a spacing of 4 km. These experiments have been continued and extended to all angles of elevation to discover where correlation ceases. The results may be summarized as follows :

(i.) Two receivers located at the same site, observing the same source, record identical fluctuations.

(ii.) For a separation of 110 m., the correlation coefficient is still extremely high (>·98). The deviation from unity is within the range of the experimental limitations.

(iii.) As already reported (Little and Lovell 1950), at 4 km. the correlation between the fluctuations is not complete, but remains high with a correlation factor varying between 0·5 and 0·95.

(iv.) Over an 11·2 km. North–South base line there is no correlation between transit fluctuations. However, when a source is near lower culmination the "effective" base line (*i. e.* the projection of the actual base line on a plane normal to the line of sight) becomes small,

Fig. 1.

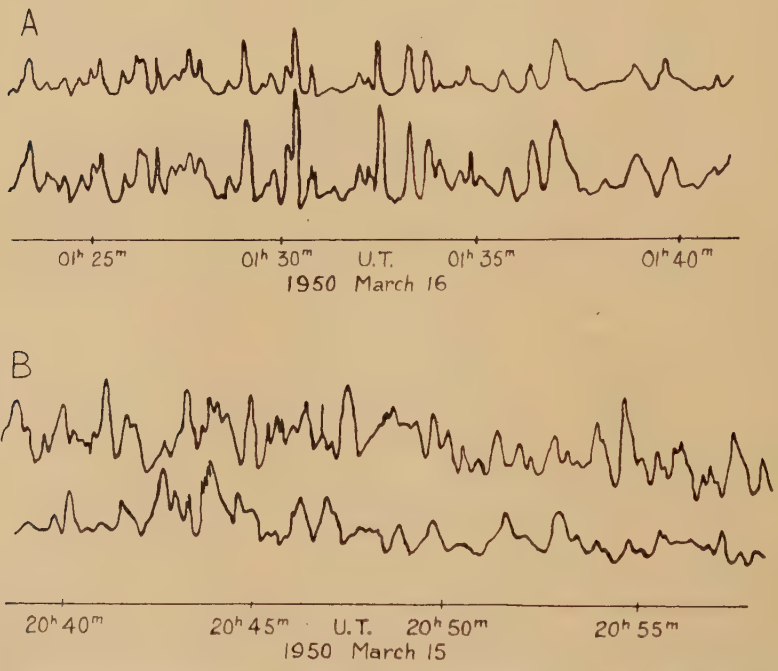

Cassiopeia fluctuation records taken simultaneously by two receivers 11 km. apart on a North–South base line.
Records A: Correlation 0·9 (effective base line 4·1 km.).
Records B: No correlation (effective base line 7·7 km.).

and the correlation factor may rise to as much as 0·95. This is illustrated in fig. 1, in which correlations between fluctuations for different effective base lines are compared, and in Table II., which shows the change in the correlation as the Cassiopeia source nears lower culmination. (The base line used was actually 10° E. of North so that the effective base line is given by $11{\cdot}2 \sin [\cos^{-1} (\cos \alpha \cos \overline{\beta - 10})]$, where α is the angle of elevation and β the azimuth angle.)

(v.) At 210 km., between Cambridge and Jodrell Bank, there is no correlation between transit fluctuations,

TABLE II.

Change of cross-correlation coefficient between fluctuation records with change of effective base line.

Hours after transit	Elevation degrees	Azimuth degrees	Effective base line Kilometres	Correlation between fluctuation records
0–9	85–23		11·2–6·4	correlation not significant
10	23	344	6·4	0·4
11	22	352	5·3	0·6
12	21	0	4·4	0·7
13	22	8	4·1	0·9
14	23	16	4·6	0·8
15	27	24	5·6	0·5
16	31	32	6·8	correlation not significant
17–24	31–85		6·7–11·2	correlation not significant

§ 6. CONTINUOUS OBSERVATIONS.

During the year November 1949–November 1950 some 3000 hours of observations were made on the Cygnus and Cassiopeia point sources by following them with steerable aerials. These observations usually took the form of a 24-hour run on each source once or twice per week throughout the year. Daytime observations were limited during some months by strong radio emissions from active areas on the Sun (of the order of 10^3 intensity of the galactic source radiation), by atmospherics from thunderstorms during the summer months, and occasionally by strong local interference.

The results of this series of observations may be summarized as follows :—

(i.) For a source at high angles of elevation the fluctuations are very closely related with the presence of spread F, and as this latter is essentially a night time phenomenon, fluctuations at high angles of elevation are usually confined to the hours of darkness. Thus, near upper culmination fluctuations were observed on 35 per cent occasions when transit occurred during the hours 1800–0600, but on less than 5 per cent for transit during the daylight hours 0600–1800.

(ii.) At low angles of elevation when the line of sight crosses the ionosphere at high magnetic latitudes, fluctuations were always observed, independent of the hour of day. These fluctuations were in general less marked in the case of Cassiopeia (minimum elevation 21°) than for Cygnus (minimum elevation 4°).

(iii.) The amplitude of the fluctuations of the Cygnus source (corrected for aerial ground lobes) plotted against the elevation of the source is shown in fig. 2 (*a*). It is seen that for angles below 20° the average amplitude of the fluctuations, expressed as a fraction of the mean intensity of the radiation from the source, increases rapidly, reaching a maximum

of about 90 per cent at lower culmination. It will also be seen that for lower culmination in daylight the maximum amplitude of the fluctuations is significantly less than for lower culmination at night.

(iv.) The marked elevation effect associated with fluctuations from the Cygnus source is further illustrated in fig. 3. In this diagram the " onset " and " cessation " of the fluctuations (taken here as the time at which the fluctuations respectively increase or decrease to an amplitude of 25 per

Fig. 2.

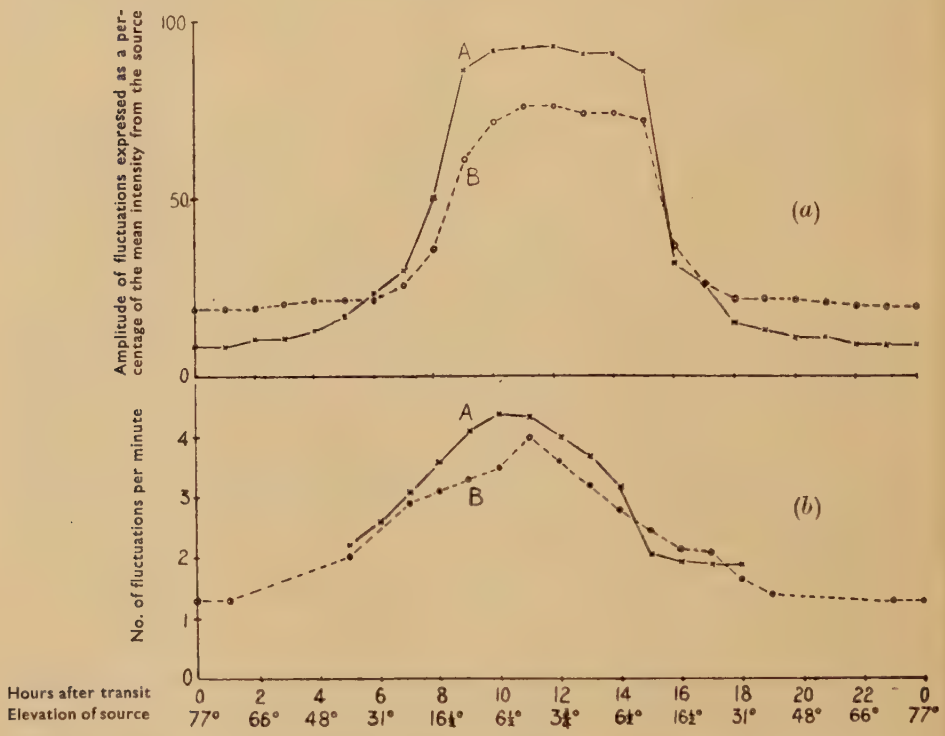

(Upper diagram). Average amplitude of Cygnus fluctuations plotted against elevation of the source.

(Lower diagram). Average number of Cygnus fluctuations per minute plotted against elevation of the source.

In each case curve A represents the average values during the six winter months (October–March), and curve B the average values during the six summer months (April–September). Cygnus lower culmination occurs in daylight during the summer, and in darkness during the winter.

cent) is plotted throughout the year. It is seen that the onset of the fluctuations occurs at approximately the same *sidereal* time each day, about 5 hours before lower culmination, corresponding to an elevation of 23°, and that the fluctuations cease approximately 5 hours after lower culmination. The spread of points during the August–November period

on the onset curve, and during March–June on the cessation curve, correspond to fluctuations at high angles of elevation during the hours of darkness.

(v.) The duration of individual fluctuations at any given angle of elevation and azimuth varies considerably from night to night. For example, individual fluctuations at transit of the sources may last for 2 or 3 minutes on some nights, whilst on other nights for only 20 seconds. Typical durations, however, range from about 1 minute at high angles of elevation to about 15 seconds at low angles of elevation. The number of fluctuations of the Cygnus source per minute plotted as a

Fig. 3.

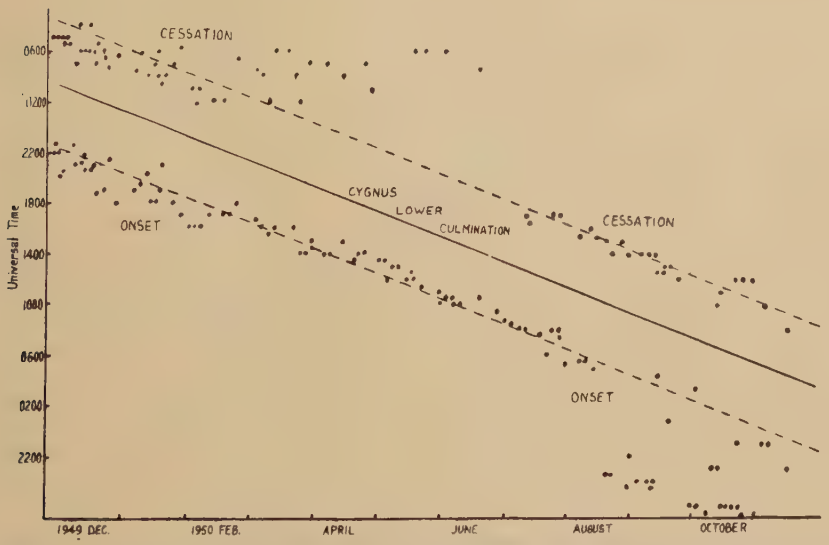

Times of " onset " and " cessation " of Cygnus fluctuations. The two dotted lines correspond to a source elevation of 23° (*i. e.* 5 hours before and after lower culmination respectively).

function of the angle of elevation is shown in fig. 2 (*b*) ; it will be seen that the number of fluctuations per minute for lower culmination in daylight is somewhat less than for lower culmination at night.

§ 7. Discussion.

(i.) *The Mechanism of Fluctuations : Diffraction in the Ionosphere.*

It was suggested by Little and Lovell that the galactic noise fluctuations could be caused by diffraction of the incident radiation by localized irregularities in the refractive index of an ionospheric layer. These irregularities would cause a distortion of the incident wavefront due to the different optical path lengths in the ionosphere, and the resultant diffraction pattern would be observed as an irregular distribution of amplitude across the ground. This distribution would not be constant with time,—due to

the presence of winds and turbulence in the ionosphere, and to the apparent change in position of the star as the Earth rotates,—and hence a fixed receiver would observe fluctuations in the intensity of the incident radiation.

The detailed implications of these ideas have been discussed by Little (1951) on the basis of a theorem by Booker, Ratcliffe and Shinn (1950), in which it is shown that the auto-correlation function of the diffraction pattern across the ground is the same as that of the distortions of the wavefront emerging from the ionosphere ; that is, the scale of the pattern at ground level is the same as that of the distortions in the emergent wavefront. On the assumption that the scale of the distortions in the wavefront is the same as that of the irregularities in the 3-dimensional ionospheric screen, then the experimental results described in this paper will give some indication of the lateral dimensions of the irregularities.

(ii.) *Correlation between records from spaced receivers.*

In § 5 it is shown that the correlation between fluctuation records begins to fall off at spacings of approximately 4 km., and it would appear, therefore, that the ionospheric irregularities causing the fluctuations have lateral dimensions of the order of 4 km.

If we now compare the observations made at the transit and the lower culmination of, say, Cassiopeia by two receivers 11·2 km. apart on a North–South base line, then allowance must be made for the changes in the "effective" base line (§ 5 (iv.)). Thus at transit, when the source is at an elevation of 85° and the effective base line is nearly 11·2 km., we should expect poor correlation if the F region irregularities are of diameter approximately 4 km. Towards lower culmination, however, when the source is at an elevation of 21°, and the effective base line tends toward a minimum of 4·1 km., the correlation would be expected to be good. This is in agreement with the experimental observations.

The above correlation results indicate that the scale of the diffraction pattern, in a plane normal to the incident radiation, is independent of the elevation of the source for elevations greater than 20°. In the case of Cygnus lower culmination (elevation 4°), the sight line crosses the ionosphere at high magnetic latitudes, and the correlation only becomes significant when the effective base line is 1 km. or less. This suggests that the ionospheric irregularities at these high magnetic latitudes are appreciably smaller than those at medium latitudes.

(iii.) *Fluctuations at low angles of elevation.*

There are clearly two important differences between transit observations and those taken near lower culmination : (*a*) as shown in fig. 4, the sight line from Jodrell Bank to the Cassiopeia and Cygnus sources at lower culmination crosses the F region of the ionosphere at latitudes of 62° N. and 71° N. respectively,—the latter well within the auroral zone. At these high latitudes the ionospheric structure is not well defined and fluctuates rapidly with time ; sporadic F is much more intense and occurs during the day as well as at

night ; sporadic E densities are also greatly in excess of the densities at lower magnetic latitudes. (*b*) When the sources are low in elevation the depth of ionosphere along the line of sight is increased. The variation of the amplitude of the Cygnus fluctuations with the change in the effective thickness of the ionosphere is shown in fig. 5. (This latter has been plotted for a disturbing region of two assumed heights and thicknesses : viz., between 300 and 500 km. and between 250 and 1000 km. ; owing to the curvature of the earth the thickness factor does not follow a simple cosecant law.) It is seen that the effective thickness and

Fig. 4.

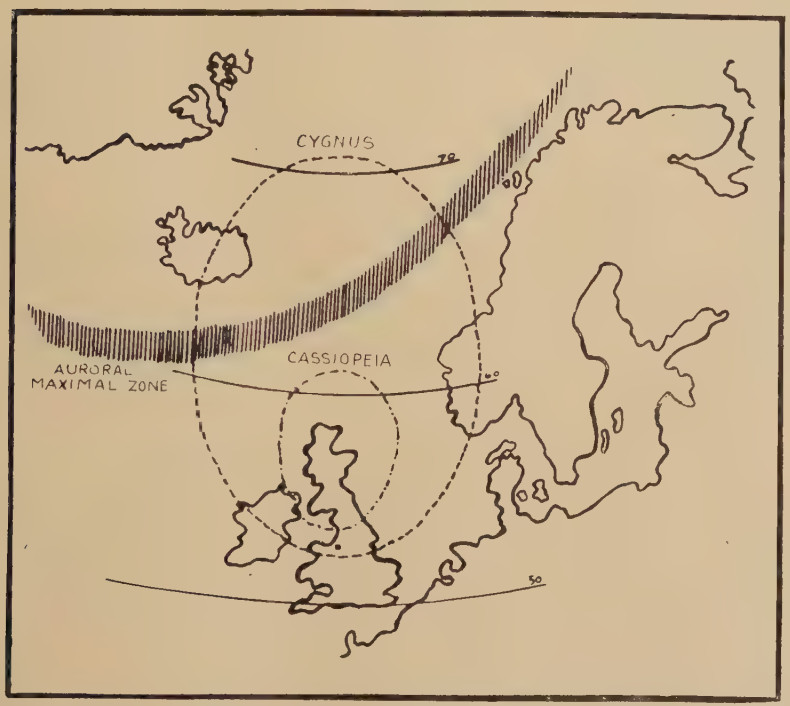

Diagram showing positions at which radiation from the Cygnus and Cassiopeia sources incident at Jodrell Bank crosses the F region of the ionosphere (assumed at a height of 400 km.). At low angles of elevation the sight lines cross the F region near the auroral zone.

amplitude curves follow each other closely for elevations greater than 20°, and it would therefore appear that down to an amplitude of about 20° the increase in fluctuation amplitude could be accounted for in terms of increased thickness of the disturbing region. Below 20°, however, where the rate of increase in the amplitude of the fluctuations is much greater than the corresponding rate of increase in effective thickness, it would seem that the disturbed nature of the ionosphere at high magnetic latitudes is the main contributing factor.

The effect of the troposphere at these low angles of elevation is not readily determinable. However, on metre wavelengths, and for a minimum elevation of 4°, it is unlikely that fluctuations of the type observed could be introduced by the troposphere, because (*a*) the variations in the refractive index of the troposphere are too small : of the order of 10^{-6} (*cf.* Booker and Gordon 1950), compared with 10^{-4}–10^{-3} for the ionosphere, and (*b*) the effective thickness of the troposphere traversed at 4° elevation is about 100 km., compared with 1000 km. for the effective thickness of the F region of the ionosphere.

Fig. 5.

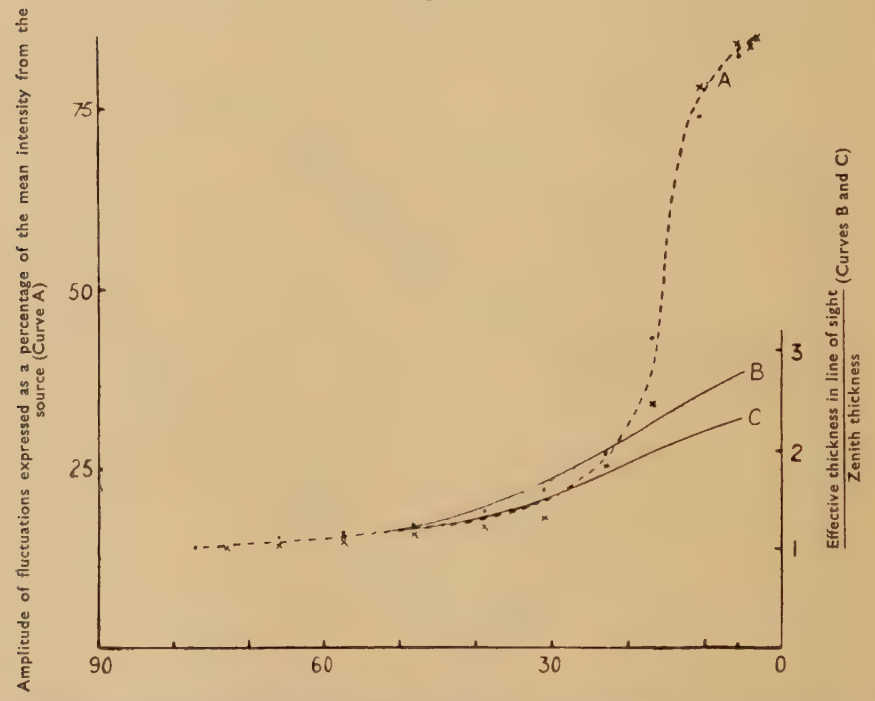

Curve A : Amplitude of Cygnus fluctuations with elevation. × source setting, • source rising (averages over 12 months).

Curves B and C : Ratio of effective thickness of disturbing region in line of sight to zenith thickness—(Curve B for a disturbing region of assumed minimum height 300 km. and maximum height 500 km. ; curve C for assumed minimum height 250 km. and maximum height 1000 km.).

(iv.) *The duration of individual fluctuations.*

Time variations in the intensity of the galactic radiation could be brought about in several ways : (*a*) a random growth and decay of the irregularities, (*b*) a turbulent motion of the irregularities, (*c*) the movement of the ionospheric irregularities as a whole under the influence of an ionospheric wind, (*d*) the apparent motion of the star relative to the ionospheric irregularities due to the rotation of the earth.

Ionospheric observations have shown that changes in the electron density of the F region are of periods very much longer than 30 seconds, the average duration of an individual fluctuation. This, together with the observation that correlation between fluctuation records is high over base lines of 4 km., suggests that fluctuations are not introduced to any great extent by turbulence, or by random growth and decay.

The duration of individual fluctuations should therefore be determined by the ratio of the size of phase irregularities in the ionosphere to the components of wind and star velocity in their plane. Wind velocities of approximately 7 km./min. have been found by Munro (1948), and for 4 km. irregularities would lead to fluctuations with a period of the order of 30 seconds. In the absence of winds, the apparent motion of the star due to the rotation of the earth would lead to fluctuations with a period of approximately 3 minutes. These figures agree fairly well with the observed limits of from about 20 seconds to 5 minutes for the fluctuations at transit.

The results described in § 6 (v.) and illustrated in fig. 2 (*b*) show that the period of the fluctuations is significantly less near lower culmination (decreasing steadily for elevations less than about 20°) than at transit. This effect is to be expected for three reasons: (*a*) the radiation then traverses the ionosphere near the disturbed auroral regions, (*b*) the depth of the ionosphere along the line of sight is considerably increased, and (*c*) ionospheric winds of 20 km./min. are reported to exist at high latitudes (Meek 1949).

§ 8. Conclusion.

The main conclusion to be drawn from the experiments described above is that the fluctuations in intensity of the radio emission from the galactic sources are introduced when the radio waves pass through an inhomogeneous ionospheric region, and spaced receiver experiments suggest that these inhomogeneities are of the order of 4 km. in size. Correlation with ionospheric phenomena indicates that the F region is mainly responsible, but it is not possible to exclude other ionospheric effects in cases where the radiation passes through disturbed auroral regions.

Further investigation of galactic noise fluctuations on various frequencies, and over varying base lines, should yield valuable information on the structure of the upper regions of the ionosphere.

Acknowledgments.

The work described in this paper forms part of the research programme of the Jodrell Bank Experimental Station. The authors wish to express their thanks to Dr. A. C. B. Lovell, Director of the station, for his helpful advice and criticism, to Dr. A. F. Wilkins and the Director of the Radio Research Station, Slough, for the ionospheric information, to the Air Ministry for permission to locate a mobile equipment at the Mobberley Direction Finding Station of Ringway Airport and to Mr. C. Hazard for

assistance in making the radio observations. A considerable portion of this work has been made possible by the grant from the Department of Scientific and Industrial Research for the development of the experimental work at Jodrell Bank. The authors are personally indebted to the Department of Scientific and Industrial Research for the award of a maintenance grant (C.G.L.) and a research grant (A.M.).

References.

Bolton, J. G., and Stanley, G. J., 1948, *Nature*, **161,** 312.
Booker, H. G., and Gordon, W. E., 1950, *Proc. I.R.E.*, **38,** 401.
Booker, H. G., Ratcliffe, J. A., and Shinn, D. H., 1950. *Phil. Trans. Roy. Soc.* A, **262,** 579.
Hey, J. S., Parsons, S. J., and Phillips, J. W., 1946, *Nature*, **158,** 234.
Little, C. G., 1951 (in publication).
Little, C. G., and Lovell, A. C. B., 1950, *Nature*, **165,** 423.
Meek, J. H., 1949, *J. Geophys. Res.*, **54,** 339.
Munro, G. H., 1948, *Nature*, **162,** 886.
Smith, F. G. 1950, *Nature*, **165,** 422.

XXXI. *The Electric Quadrupole Moment and the Magnetic Moment of the Bromine Nucleus.*

By J. D. Ranade*,
Royal Holloway College†.

[Received January 9, 1951.]

Abstract.

Deviations from the interval rule have been observed in the hyperfine structure of the bromine arc spectrum. These are attributable to an electrical quadrupole moment of the bromine nucleus. Coupling constants are determined for the term involved. The nuclear quadrupole moment is calculated to be $0{\cdot}28\times10^{-24}$ cm.^{2}, and the magnetic moment 1·8 nuclear magnetons.

§ 1. Introduction.

Deviations from the interval rule in the BrI spectrum were first observed in the term $5s^4P_{5/2}$ by Tolansky and Trivedi (1940). These can be attributed to the nuclear electrical quadrupole moment. The separations in this term were measured accurately from lines in the red and the infra-red regions where the resolving power of the Fabry–Perot interferometer is high. There is no evidence of any possible perturbation from another configuration. Table I. shows the observed positions of the hyperfine structure levels as compared with those calculated from the interval rule.

Table I.

F value	4	3	2	1
Observed.....	417	218	83	0
Calculated..... (Interval rule)	417	232	93	0

At the time the quadrupole moment was not evaluated for want of the coupling constants of the term. Hence, here, following a method similar to that used by Schmidt (1939) for iodine, coupling constants of the term involved and thus the quadrupole moment are determined.

§ 2. Quadrupole Moment.

The interaction between the angular momentum J of a non-spherically symmetrical configuration and the spin I of a non-spherically symmetrical nucleus takes the form

$$E=a_0+\frac{a_1}{2}c+bc(c+1),$$

where

$$c=F(F+1)-I(I+1)-J(J+1).$$

* At present, at the Institute of Science, Bombay, India.
† Communicated by Professor S. Tolansky.

In this interaction law a_0, a_1 and b are constants, a_0 being the displacement of the centre of gravity of the hyperfine structure pattern from the position the term would have occupied if the spin had been zero, a_1 is the hyperfine structure interval factor which is a function of the nature of the electron configuration and is also proportional to the nuclear magnetic moment, b is a measure of the deviation from the interval rule. The quantity b is a function of the nuclear electrical quadrupole moment of the nucleus.

The values of the interaction constants given by the observed intervals are (units cm.$^{-1}\times10^{-3}$)

$$a_0=223,$$
$$a_1=\ 47{\cdot}1,$$
$$b=\ \ 0{\cdot}17.$$

For the calculation of the quadrupole and the magnetic moments, it is necessary to know the coupling constants for the configuration electrons. For these, first, the coupling constants of the $4p^4$ electron group in the singly ionized bromine atom is calculated, then the attachment of a 5s electron to this group, giving rise to the $4p^4\,.\,5s$ configuration of the neutral atom is considered. It is assumed that the attachment of a 5s electron to the $4p^4$ group does not alter the coupling constants in the group. The p^4 electron group can be treated as equivalent to the p^2 group. Hence for calculation $p^4.\,s$ can be treated as $p^2.\,s$. The effect of this on the quadrupole moment formula is a change of sign since the spin–orbit interaction changes sign. The eigenfunctions for the p^2s configuration are written in terms of the single electron functions. The term $^4P_{5/2}$ arises from the term $^3P_2$ of BrII. Thus for $J=2$ and $m=2$ the eigenfunctions for the configuration p^2 are, as given by Breit and Wills (1933)

$$\left[\frac{3}{2}\frac{1}{2}\right]^2_2=\frac{1}{\sqrt{2}}(p^{3/2}_{3/2}p'^{1/2}_{1/2}-p^{1/2}_{1/2}p'^{3/2}_{3/2}),$$

$$\left[\frac{3}{2}\frac{3}{2}\right]^2_2=\frac{1}{\sqrt{2}}(p^{3/2}_{3/2}p'^{1/2}_{3/2}-p^{1/2}_{3/2}p'^{3/2}_{3/2}).$$

Here $p^{3/2}_{3/2}$ etc. signify the single electron eigenfunctions, the magnetic quantum number being given by the superscript to the right. The eigenfunction of the $^3P_2$ term is a linear combination of the above functions and is given by

$$\psi(^3P^2_2)=c_1\left[\frac{3}{2}\frac{1}{2}\right]^2_2+c_2\left[\frac{3}{2}\frac{3}{2}\right]^2_2.$$

The coefficients c_1 and c_2 are to be determined from the multiplet structure and from the value of the spin–orbit interaction. The values of the spin–orbit interaction (δ) and the electrostatic energy integral (F_2) are given by Robinson and Shortley (1937). Using the values

$$\delta=2958\text{ cm.}^{-1}\quad\text{and}\quad F_2=1750\text{ cm.}^{-1}$$

and the term values for BrII, leads to

$$c_1=0{\cdot}434\quad\text{and}\quad c_2=0{\cdot}901.$$

The eigenfunctions of the $^4P_{5/2}$ term arising from the attachment of the s-electron to the p^2 group are given by

$$\psi(^4P^{5/2}_{5/2})=s^{1/2}_{1/2}\,.\,\psi(^3P^2_2).$$

The formula for the electrical quadrupole moment q as given by Casimir (1935) for a p-electron is

$$q=-\frac{b\,.\,Z_i\,.\,H}{\delta\overline{(3\cos^2 d-1)}}\,.\,2i(2i-1)j(2j-1)\times 0{\cdot}986\times 10^{-24},$$

where H is a relativity correction. The average value of $\overline{(3\cos^2 d-1)}$ is determined by using the above eigenfunction in conjunction with formulæ given by Schüler and Schmidt (1936). For $^4P_{5/2}$ we have

$$\overline{(3\cos^2 d-1)}=-\tfrac{2}{5}(2\sqrt{2}c_1c_2S_1-c_1^2R_1'),$$

where S_1 and R_1 are the relativity corrections and c_1 and c_2 are the constants already computed. Thus finally

$$q=-\frac{bZ_iH2i(2i-1)j(2j-1)\times 0{\cdot}986\times 10^{-24}}{\delta.-\frac{2}{5}(2\sqrt{2}c_1c_2S_1-c_1^2R_1')]}.$$

With $c_1=0{\cdot}434$, $c_2=0{\cdot}901$, $S=1{\cdot}07$, $R_1'=1{\cdot}045$, $H=1{\cdot}024$, $i=\frac{3}{2}$, $j=\frac{5}{2}$, $Z_i=31$ [(Z−4) for a p-electron] and $\delta=2958$ cm.$^{-1}$ giving

$$q=b\times 1{\cdot}612\times 10^{-24}\text{ cm.}^2$$

and with $b=0{\cdot}17$

$$q=+0{\cdot}28\times 10^{-24}\text{ cm.}^2.$$

No separation of the isotopes is revealed by hyperfine structure. The value obtained here compares well with the values found by the micro-wave technique and reported by Townes, Holden and Merrit (1948), as

$$^{35}Br_{81}\,.\,q=+0{\cdot}28\times 10^{-24}\text{ cm.}^2,$$

$$^{35}Br_{79}\,.\,q=+0{\cdot}23\times 10^{-24}\text{ cm.}^2.$$

§ 3. Magnetic Moment.

Using the earlier data of Tolansky (1932) for the separations of the terms $^4P_{5/2}$, $^4P_{3/2}$ and $^2P_{3/2}$ of BrI, Schmidt (1938) calculated the nuclear magnetic moment of bromine as 2·6 nuclear magnetons. Since then Tolansky and Trivedi (1940) have remeasured and redetermined the separations more accurately. The interval factor for the term $^4P_{3/2}$ is now given to be 20 cm.$^{-1}\times 10^{-3}$ instead of the value 42 cm.$^{-1}\times 10^{-3}$ first given and used by Schmidt (1936). Therefore the nuclear magnetic moment has been re-determined using the improved data now available. The total splittings for the terms $^4P_{5/2}$ and $^4P_{3/2}$ which are now being used are

$$(^4P_{5/2})=417\text{ cm.}^{-1}\times 10^{-3},$$

and

$$(^4P_{3/2})=120\text{ cm.}^{-1}\times 10^{-3}.$$

Breit and Wills (1933) have calculated the interval coupling factors for the $^4P_{5/2}$ and $^4P_{3/2}$ terms, in intermediate coupling, giving

$$A(4P_{5/2})=\tfrac{1}{5}a(s)+\tfrac{1}{5}[(3c_1^2+4c_2^2)a'+c_1^2a''+4\sqrt{2}c_1c_2a'''],$$

$$A(4P_{3/2})=-\tfrac{1}{5}a(s)+\tfrac{3}{10}[(3c_1^2+4c_2^2)a'+c_1^2a''+4\sqrt{2}c_1c_2a'''].$$

Here $a(s)$ is the interval constant for the s-electron and a', a'' and a''' are the interval constants for the p-electrons, c_1 and c_2 are the coupling constants as computed above. The constants a', a'' and a''' are related as follows.

$$a''=a' \,.\, 5F''/F'$$

and

$$a'''=-a' \,.\, 5/16 \,.\, G/F'.$$

Here F′, F″ and G are the relativity corrections.

Using the values $c_1=0{\cdot}434$, $c_2=0{\cdot}901$, F″=1·09 and F′=G=1·02 leads to the interval factors

$$A(4P_{5/2})=0{\cdot}2a(s)+0{\cdot}823a',$$

$$A(4P_{3/2})=-0{\cdot}2a(s)+1{\cdot}235a'.$$

From these relations and the known values of

$$A(4P_{5/2})=47{\cdot}1 \text{ cm.}^{-1}\times10^{-3} \quad \text{and} \quad A(4P_{3/2})=20 \text{ cm.}^{-1}\times10^{-3}$$

given by Tolansky and Trivedi, it follows that

$$a(s)=101{\cdot}3 \text{ cm.}^{-1}\times10^{-3},$$

$$a'=32{\cdot}6 \text{ cm.}^{-1}\times10^{-3}.$$

For $a(s)$, Goudsmit's formula leads to

$$\mu=\frac{a(s) \,.\, i \,.\, n^3_{\text{eff}} \,.\, 0{\cdot}1185}{ZZ_0^2F''(1-ds/dn)} \quad . \quad . \quad . \quad . \quad . \quad . \quad . \quad (1)$$

For a',

$$\mu=\frac{a' \,.\, i \,.\, Z_iH \,.\, 3{\cdot}446}{\delta \,.\, F'} \quad . \quad . \quad . \quad . \quad . \quad . \quad . \quad . \quad (2)$$

In equation (1), n_{eff} is the effective quantum number for the s-electron when it is the only valence electron present. This happens in BrV. The corresponding configuration is $4s^2 \,.\, 5s$. In neutral bromine the configuration is $4s^2 \,.\, 4p^4 \,.\, 5s$. The absolute value of this term of BrV is not experimentally known. It is, however, here determined by extrapolation using the known term values for the $5s^2 \,.\, 5s$, $5s^2 \,.\, 6s$ etc. terms of the iso-electronic sequence gallium I, germanium II and arsenic III. The term values for these are taken from Goudsmit and Bacher (1932). From this $n_{\text{eff}}=3{\cdot}95$ and $(1-ds/dn)=0{\cdot}65$. With $i=\frac{3}{2}$, Z=35, $Z_i=31$, H=1·024, F′=1·02, F″=1·09, $n_{\text{eff}}=3{\cdot}95$, $(1-ds/dn)=0{\cdot}65$, and $Z_0=5$ (Br V), giving

$$\text{from } a(s): \ \mu=1{\cdot}79,$$

$$\text{and from } a': \ \mu=1{\cdot}77,$$

The agreement between these values is perhaps fortuitous and much better than can be expected. One can take closely enough

$$\mu = 1{\cdot}8 \text{ nuclear magnetons.}$$

The determination of the nuclear magnetic moment of bromine has been carried out by the nuclear paramagnetic resonance absorption method and the magnetic beam resonance in CsBr and LiBr. The values given by Pound (1947) are

$$(Br^{81}) = 2{\cdot}2 \text{ nuclear magnetons,}$$

$$(Br^{79}) = 2{\cdot}1 \text{ nuclear magnetons.}$$

When the approximations used here are taken into account the difference is not significant and indeed the two methods give reasonably concordant results.

Acknowledgments.

My thanks are due to Professor S. Tolansky for his constant interest and kind continual encouragement during the progress of this work.

References.

Breit and Wills, 1933, *Phys. Rev.*, **44,** 270.
Goudsmit and Bacher, 1932, *Atomic Energy States.*
Pound, 1947, *Phys. Rev.*, **72,** 1273.
Robinson and Shortley, 1937, *Phys. Rev.*, **52,** 715.
Tolansky, 1932, *Proc. Roy. Soc.* A., **136,** 585.
Tolansky and Trivedi, 1940, *Proc. Roy. Soc.* A., **175,** 366.
Townes, Holden and Merrit, 1948, *Phys. Rev.*, **74,** 370.
Schmidt, 1938, *Zeits. f. Physik*, **108,** 408.
Schmidt, 1939, *Zeits. f. Physik*, **112,** 199.
Schuler and Schmidt, 1936, *Zeits. f. Physik*, **99,** 717.

XXXII. *Hyperfine Structure in the Spectrum of Bromine.*—II.

By J. D. Ranade*,
Royal Holloway College†.

[Received January 9, 1951.]

Abstract.

Measurements for the hyperfine structures of 18 classified and 21 unclassified lines of the first spark spectrum of bromine are reported. The spectrum was excited by a high-frequency electrodeless discharge in pure bromine vapour. The patterns are analysed and interval factors for fourteen terms are given.

§1. Introduction.

Measurements for the hyperfine structures of several lines of the arc spectrum of bromine have been reported earlier by Tolansky (1932) and Tolansky and Trivedi (1940), who proved that both the bromine isotopes 79 and 81 have the same nuclear spin, 3/2, and have practically identical nuclear magnetic moments. Tolansky and Trivedi also reported measurements of the hyperfine structure for four lines of the first spark spectrum of bromine.

The measurements reported here consist of a study of the classified and the unclassified lines of the spark spectrum of bromine. The first spark spectrum of bromine was partially classified by Lacroute (1935), who studied the Zeeman effect but could not exploit them fully due to lack of hyperfine structure data.

§2. Experimental.

The spark spectrum was excited in bromine vapour with an electrodeless high-frequency discharge which is gentle and can be considered essentially as a low voltage excitation in which arc lines tend to predominate. A brilliant arc spectrum can be excited in bromine vapour at a pressure of about 1 mm. As the gas pressure is lowered, the increase in the mean free path enables the ions to acquire higher energies between collisions and spark lines appear. Sharper spark lines result than those excited in a Geissler discharge tube. By reducing the bromine vapour pressure below 1 mm. and by using a capillary more constricted than that necessary for an arc spectrum, strong spark lines were excited.

Oscillations were generated by a 500 watt thermionic valve, the wavelength being of the order of 20 m. The field was applied by means of an external electrode of copper foil to a pyrex discharge tube which

*Communicated by Professor. S. Tolansky.
† At present at the Institute of Science, Bombay, India.

was incorporated in a vacuum circulating system having charcoal and liquid oxygen traps in the circuit. A continuous stream of pure bromine vapour was circulated through the discharge tube from a side limb cooled by immersion in a flask containing liquid oxygen. By adjusting the height of the bottom of the limb above the liquid oxygen surface, the bromine could be cooled to a temperature of $-80°$ C. at which a good excitation of the spark spectrum resulted. Cooling to $-45°$ C. is necessary for the arc spectrum. No carrier gas was used. The portion of the discharge tube emitting the spectrum was cooled by directing on to it a strong blast of air.

The high resolving power instruments used were a variable gap Fabry-Perot interferometer coated either with silver, aluminium or an aluminium-magnesium alloy, and a quartz Lummer plate by Hilger, (20 cm. long and 3.42 mm. thick). The interferometer was used in an external beam mounting crossed with a large Hilger glass-quartz Littrow spectrograph.

§ 3. Observations.

Table I. contains hyperfine structures measured for classified lines of BrII spectrum. The wavelengths and allocations are taken from Lacroute. The units used are cm.$^{-1}\times10^{-3}$ and beneath each component is indicated a visual estimate of its intensity. The lines are classed A, B, C according to whether the resolution in the pattern is good (A), moderate (B) or poor (C). The factors affecting the class are the complexity and the narrowness of the patterns and the widths of the lines. For lines classed as A, the errors are some 1 or 2 cm.$^{-1}\times10^{-3}$. Whenever two components are not completely resolved, the blend is indicated by binding of components with a hyphen. Measurements for a number of unclassified lines are given in Table II.

§ 4. Analysis.

For the singly ionized bromine atom Hund's theory predicts three families of terms arising from the basic terms 4S, 2D and 2P of BrIII. All the lines classified by Lacroute (1935) belong to the 4S system. The analysis of lines involving common terms will now be considered.

Of the three lines λ 5164·4, 5238·2 and 5182·4 one has a term with a zero J value and hence no structure. The three lines have a common lower term $5s^3S_1$, the upper terms being $5p^3P_0$, $^3P_1$, $^3P_2$ respectively. The structure of the line λ 5164·4 $5s^3S_1-5p^3P_0$ gives that of the term $5s^3S_1$. From this, the structures of the upper $5p^3P_1$ and $5p^3P_2$ terms follow as shown by fig. 1. The agreement between the predicted and the observed patterns is reasonably good and $5s^3S_1$ is not fully resolved.

The term $5s^5S_2$ will give rise to regular quartets in lines for which the upper terms have narrow structure. The two lines λ 4193·5 and 4230·0 have a common lower term $5s^5S_2$. Since the structures of the upper terms $5p^3P_1$ and $5p^3P_2$ have been derived above, these lines give the structure of the term $5s^5S_2$. The two central components of λ 4230 are not properly resolved.

The lines λ 4816·7, 4785·5 and 4704·9 have well resolved quartet patterns. The structures in these lines are essentially those of the term $5s^5S_2$ and the number of components directly gives the spin. The analysis is

TABLE I.

Hyperfine structures, of classified Br II lines.
Units cm.$^{-1}\times10^{-3}$.

Wavelength	Allocation	Structure Red		Violet		Class
5238·2	$5s^3S_1-5p^3P_1$	0 (1)	95 (2)			C
5182·4	$5s^3S_1-5p^3P_2$	0 (1)	38 (2)	93 (3)		B
5164·4	$5s^3S_1-5p^3P_0$	0 (1)	48 (2)			C
4848·8	$5p^5P_3-6s^5S_2$	Borad single-width 50				
4816·7	$5s^5S_2-5p^5P_1$	0 (5)	154 (3)	264 (2)	323 (1)	A
4785·5	$5s^5S_2-5p^5P_2$	0 (4)	125 (3)	213 (2)	270 (2)	B
4766·0	$5s^5P_2-6s^5S_2$	0 (2)	65 (1)			C
4735·4	$5p^5P_1-6s^5S_2$	0 (2)	76 (3)			B
4704·9	$5s^5S_2-5p^5P_3$	0 (5)	130 (3)	219 (2)	274 (1)	A
4396·4	$5p^3P_2-4d^5D_2$	0 (1)	— 75 (1)			C
4356·9	$5p^3P_1-4d^5D_2$	Single				
4230·0	$5s^5S_2-5p^3P_1$	0 (3)	188 (2)	270 (1)		B
4193·7	$5s^5S_2-5p^3P_2$	0 (4)	130 (3)	219 (2)	280 (1)	B
3980·4	$5p^5P_3-4d^5D_4$	0 (2)	— 49 (1)			C
3980·0	$5p^5P_3-4d^5D_3$	Single				
3935·2	$5p^5P_2-4d^5D_1$	Width 50				
3914·5	$5p^5P_1-4d^5D_1$	Single				
3914·1	$5p^5P_1-4d^5D_0$	Single				

illustrated in fig. 2 giving the structures of the upper terms $5p^5P_1$. $^5P_2$ and $^5P_3$. The agreement between the predicted and the observed values is good,

TABLE II.

Hyperfine structures of unclassified BrII lines.
Units cm.$^{-1}\times10^{-3}$.

Wavelength	Structure			
	Red		Violet	
4921·3	0	112		
	(1)	(3)		
4802·3	434	337	188	0
	(1)	(2)	(3)	(5)
4742·7	0	122	198	237
	(5)	(3)	(1)	(1)
4728·2	Single			
4719·8	0	59	119	
	(2)	(2)	(5)	
4693·3	0	144	218	384
	(6)	(3)	(1)	(1)
4678·7	Single			
4542·9	0	121	254	362
	(1)	(2)	(5)	(9)
4365·6	0	67	156	
	(2)	(2)	(3)	
4351·2	0	176	344	
	(5)	(3)	(1)	
4297·8	0	156	246	
	(3)	(1)	(1)	
4291·4	0	158	266	364
	(9)	(6)	(4)	(3)
4223·9	118	0	215	341
	(3)	(10)	(5)	(2)
4179·6	0	146	232	
	(7)	(2)	(5)	
4140·4	Single			
4135·9	Single			
3986·3	132	0	205	338
	(1)	(10)	(3)	(5)
3970·6	Single			
3968·3	0	129	224	
	(9)	(6)	(4)	
3955·4	Single			
3950·6	Single			

The lines λ 4766·0, 4735·4 and 4848·8 have complex structures. Except for λ 4735·4, the components are closely packed so that resolution is poor. λ 4848, appears as a broad single line pattern of width 50 cm.$^{-1}\times10^{-3}$. The structure of the $6s^5S_2$ term is obtained from these lines.

The group of $4d^5D$ terms combines with the $5p^3P_{012}$ and $5p^5P_{123}$ multiplets which have narrow structures. Most of the lines from these transitions appear single but λ 3980·9 shows two blended components. Therefore the ^5D terms have all narrow structures. The width of λ 4396·4 enables an estimate to be made of the structure of $5d^5D_1$ while from λ 3980, the total width of $4d^5D_4$ can be estimated. The line λ 3935 gives an approximate structure of the term $4d^5D_1$. There is no check available.

Fig. 1.

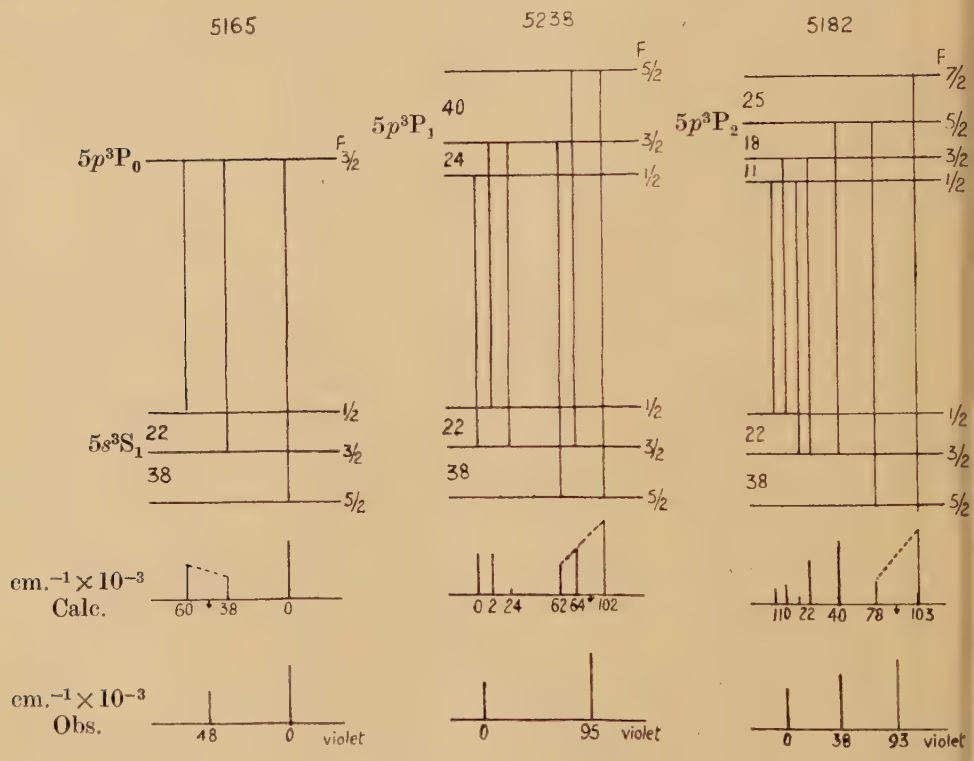

§5. Discussion.

Table III. shows the term hyperfine structures derived. A minus sign before the first interval implies that the whole structure is inverted, the highest F value lying deepest.

The term interval factors derived from these structures are given in the last column of the same table.

The $5s^5S_2$, $6s^5S_2$ and $5s^3S_1$ terms are spherically symmetrical and are not therefore affected by any nuclear electric quadrupole moment which leads to deviation from the interval rule in the arc spectrum of bromine for some lines. For these terms, the interval rule should be strictly obeyed unless perturbations are caused by configuration interaction. The structures of these terms as determined here show that the interval rule is obeyed within the limits of measurement.

Fig. 2.

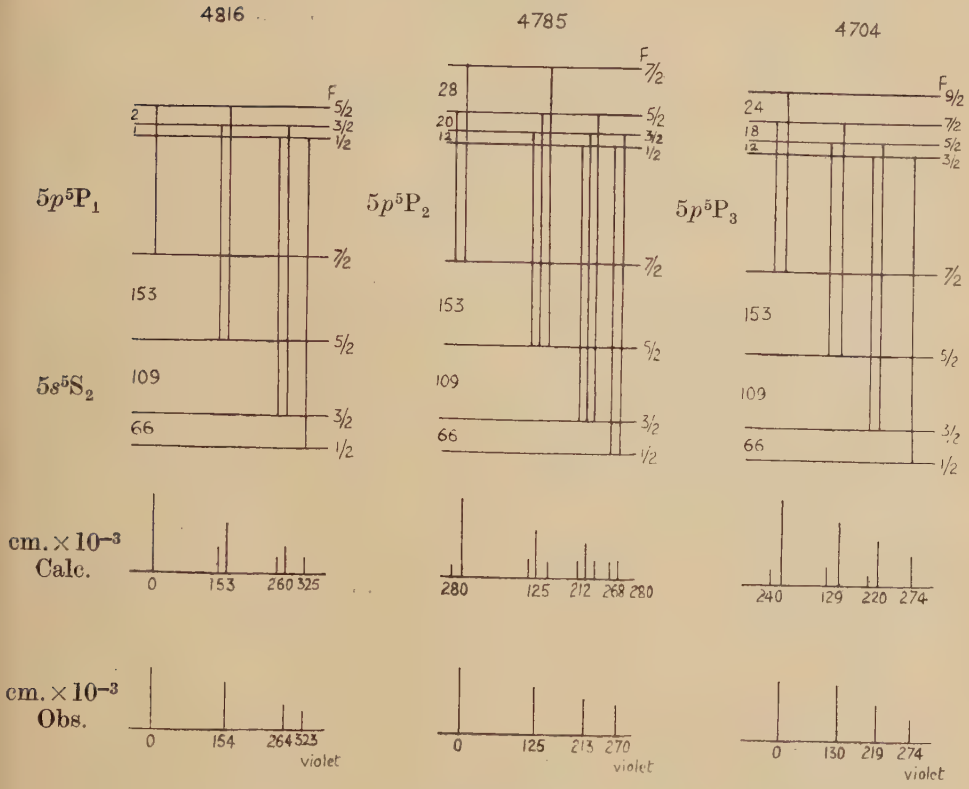

TABLE III.

Hyperfine Structures in the terms of BrII—Intervals.

Configuration	Term	Structure cm.$^{-1}$ × 10^{-3}			Interval factors cm.$^{-1}$ × 10^{-3}
$4s^2.4p^3.5s$	$^5S_2$	153	109	66	44
	$^3S_1$	−38	22		−14
$4s^2.4p^3.5p$	$^5P_3$	24	18	12	5
	$^5P_2$	28	20	12	8
	$^5P_1$	2	1		1
	$^3P_2$	25	18	11	6
	$^3P_1$	40	24		16
	$^3P_0$				0
$4s^2.4p^3.6s$	$^5S_2$	36	27	15	10
$4s^2.4p^3.4d$	$^5D_4$	Very small.			
	$^5D_3$	Very small.			
	$^5D_2$	−21	15	9	−6
	$^5D_1$	10	6		4
	$^5D_0$				0

The interval factor for the term $5s^5S_2$ is about four times that of the term $6s^5S_2$. This is similar to what was found by Tolansky and Forester (1938) for the first spark spectrum of iodine. These terms arise from the

addition in parallel of an s-electron to the electron core of the basic ion term $4p^3.{}^4S_{3/2}$ of the doubly ionized bromine atom, according to the coupling theory of White (1930). Thus from the smallness of the interval factor of the $6s^5S_2$ term, it follows that the coupling of the $4p^3$ group is small. The term $^3S_1$ is formed by the addition of an s-electron, anti-parallel to the $4p^3$ group of BrIII. The interaction energy is proportional to cos JS which is equal to -1 in this case. Thus the interval factor for the $^3S_1$ term should be negative and numerically smaller than the positive interval factor of the term $^5S_2$. The value of the interval factor for $^3S_1$ as found here (-14 cm.$^{-1}\times 10^{-3}$) fits in the above theory. The magnitude, however, suggests that the coupling constant of the $4p^3$ electrons is about 4/7ths that of the $5s$-electron. This is not as small as one would expect from the interval factor of the $6s^5S_2$ term. The interval factors of the $4d^5D$ terms are small and this suggests that the coupling of the $4p^3$ group is not strong since a $4d$ electron is not expected to possess penetrating properties. In contrast to singly ionized iodine, the coupling of the $4p^3$ electron group in BrII is weak and the interval factor of the $5s^3S_1$ term rather larger than would be expected under these circumstances. In BrI, the group $4p^5$ has a large coupling constant. This may mean that there is a change in the nature of the electron coupling, in moving from the $4s^2.4p^3$ to $4s^2.4p^4$ configuration. This can also be inferred from the fact that contrary to expectations the singly ionized bromine atom shows structures which are no wider than those of the neutral bromine atom.

No anomalies appear except for λ 4356·9. It is a transition from the $4d^5D_2$ to the $5p^3P_1$ term. The structure of this line, which appears as a sharp single, does not fit in with the observed structures of the two terms involved. It is possible that the line is wrongly classified.

Regarding the unclassified lines these can be arranged in groups showing similar structures. The two lines λ 4223·9 and λ 3986·3 have similar structure suggesting that they involve the same common term. This is substantiated by the Zeeman splittings given by Lacroute. The lines λ 4719 and λ 4365 both show a triplet structure roughly of the same order while the three lines λ 4297, 4179 and 3968 have similar patterns. From the data on Zeeman effect given by Lacroute, it seems that none of these lines can belong to the classified levels of the 4S system.

Acknowledgments.

My thanks are due to Professor S. Tolansky for his constant interest and kind continual encouragement during the progress of this work.

References.

Lacroute, 1935, *Ann. Phys. Paris*, **3,** 5.
Tolansky, 1932, *Proc. Roy. Soc.* A., **136,** 585.
Tolansky and Forester, 1938, *Proc. Roy. Soc.* A., **168,** 78.
Tolansky and Trivedi, 1940, *Proc. Roy. Soc.* A., **175,** 366.
White, 1930, *Proc. Nat. Acad. Sci.*, **16,** 68.

XXXIII. *The Electrical Resistance of Gold, Silver and Copper at Low Temperatures.*

By E. Mendoza and J. G. Thomas,
H. H. Wills Physical Laboratory, University of Bristol*.

[Received January 19, 1951.]

Abstract.

A brief review of published papers on the subject of electrical resistance at very low temperatures shows that several metals exhibit a feature which has not yet been explained theoretically, namely that the resistance goes through a minimum value as the temperature decreases, whereas present theories indicate that it should remain constant. An apparatus is described for measuring electrical resistance below 1° K.; by means of its use, the effect was confirmed in gold and silver and also found in copper. There was no tendency for the curves to flatten off even at the lowest temperatures. The gold behaved in magneto-resistance experiments as if it contained less than 1 part in 10^6 of ferromagnetic impurity. Slight anomalies in the shapes of some of the curves seem also to exist.

§ 1. Introduction.

At very low temperatures it is regarded as usual behaviour for the electrical resistance of a non-superconducting metal specimen to fall to a value which is constant, independent of temperature. The accepted explanation is that when the thermal vibrations of the lattice are negligible, the mean free path for electron scattering, which determines the electrical resistance, is constant with temperature, being in turn limited only by the imperfections in the crystal lattice. The imperfections include foreign impurity atoms and "physical" impurities such as dislocations, a mosaic crystal structure or other departures from perfect regularity, which do not change with temperature.

A considerable number of exceptions to this rule have however been noted. Among metals whose resistance begins to increase again as the temperature is decreased, the best known is gold which has been the subject of several investigations at liquid helium temperatures (Meissner and Voigt 1930, de Haas, de Boer and van den Berg 1934, de Haas and van den Berg 1936, 1937, Giauque, Stout and Clark 1937, de Haas, Casimir and van den Berg 1938, Stout and Barieau 1939, Nakhimovich 1941, Garfunkel, Dunnington and Serin 1950). Of a number of specimens of silver which have been investigated, one was found to exhibit the same phenomenon (de Haas and van den Berg 1936). Similar behaviour was

* Communicated by Dr. L. C. Jackson.

noted in gallium by Keesom (1933), and in sodium, magnesium, aluminium, molybdenum, cobalt, and cerium by Meissner and Voigt (1930). Sodium had been previously found to exhibit an increase with decreasing temperature by Woltjer and Kamerlingh Onnes (1924); the specimen measured by Justi (1948) exhibited a decrease at low temperatures while MacDonald and Mendelssohn (1950) found "normal" behaviour for a purer specimen. Keesom (1934) and more recently Garfunkel, Dunnington and Serin (1950) and MacDonald and Mendelssohn (1950) have confirmed the effect in magnesium. Keesom (1933) apparently observed a minimum for aluminium, but Boorse and Niewodniczanski (1936) and Garfunkel, Dunnington and Serin (1950) found no minima for their specimens of aluminium, while Steiner and Fünfer (1936) found none for molybdenum.

The phenomenon in gold is regarded as one not merely due to spurious causes; the effects of varying the measuring current, of attaching the electrical leads to the specimens differently, and of varying the heat treatment of the metal were all eliminated by de Haas and van den Berg (1937). The phenomenon still occurred in specimens for which no trace of ferromagnetic impurity was quoted, but the possible effect of such impurities may nevertheless be important and is dealt with later in the present paper.

Among suggestions as to the cause of the phenomenon there are those due to Justi (1942) that it is a size effect and Gorter (1938) that it may be a thermodynamic necessity—both of which have been criticized by MacDonald and Mendelssohn (1950)—while Lane (1949) has suggested that scattering at grain boundaries may play a part, though this mechanism would not seem to lead to a variation of resistance with temperature. The theory of Vonsovsky (1940) apparently refers to electric fields which are many orders of magnitude greater than those encountered experimentally. Sondheimer and Wilson (1947) have treated the problem of electrical resistance using a model more complicated than the free-electron model and have shown that at intermediate temperatures the resistance cannot be split up into two additive components (temperature-variable and temperature-independent). They assume from the outset, however, the existence of a temperature-independent residual resistance at very low temperatures. The interactions introduced by Fröhlich (1950) into the free electron model to account for the phenomena of superconductivity seem to have no bearing on the present problem.

It is an open question whether the rise in resistance continues as the temperature is decreased, particularly below 1° K. The only experiment so far performed in this region is that of Casimir, de Haas and van den Berg (1938) on gold. They showed that the rise did continue but the accuracy of their results was apparently impaired by poor thermal contact between the gold wire and the paramagnetic salt used to attain the low temperature. The present experiments are an attempt to repeat

this work—measurements being also taken throughout the liquid helium range, 4·2° K. to 1° K.—and to extend it to other metals; this report presents preliminary results.

§ 2. Apparatus.

A method has been described (Mendoza 1948) for establishing thermal contact between a metal specimen and a paramagnetic salt cooled by adiabatic demagnetization below 1° K. The metal specimen is joined to copper fins of comparatively large surface area embedded inside the pill of compressed powdered salt. When the salt is demagnetized, the metal cools. If power is then generated in the metal specimen—for instance, by the passage of a measuring current—a temperature difference is set up between the metal and the salt. Other things being fixed, this temperature difference increases rapidly with decreasing temperature; its order of magnitude may be estimated, and it can be made small if the dissipating area of the fins is made large enough. At the same time, the provision inside the salt of layers of metal of comparatively high thermal conductivity is advantageous, reducing the inhomogeneities of temperature which might otherwise persist inside the salt and lead to errors of measurement.

An apparatus embodying these data was constructed for resistance measurements; the low-temperature part, which was immersed in a liquid helium bath, is shown in fig. 1. The salt A—iron or chrome alum—was cylindrical in external form, 12·5 mm. in diameter and about 30 mm. long, and contained four or more copper fins F, 5 mm. wide, 0·1 mm. thick, placed parallel to one another, running the whole length of the salt and projecting from the ends. The fins had a number of small holes cut in them to increase the mechanical strength of the block of salt; their total surface area was approximately 12 cm.^{2}. The assembly was made in one operation by pressing in a suitable die. M was a former, a hollow cylinder of copper, 10 mm. external diameter, 0·5 mm. thick and 16 mm. long. It had a spiral groove on its outside, deep enough to hold, without strain, the wire W whose resistance was to be measured, and the surface was insulated with a thin covering of a bakelite varnish. M was connected by a wire to one of the fins. With this construction consistent results were obtained. The ends of the specimen W were joined to short potential and current leads connected separately to the fins. The other ends of the fins were soldered to superconducting leads (of which one is shown at L), made most conveniently from 0·03 mm. diameter constantan wire, tin plated electrolytically then covered with a thin layer of soft solder. Such leads were found to be robust, flexible and easy to solder and to have a high thermal resistance. They passed from the fins, along the outside of the salt and joined on to platinum wires which passed through platinum seals such as P into the helium bath, the length of lead between the salt and the platinum wire being about 5 cm. The magnetic susceptibility of the salt was measured by a static (Gouy) method, since

this ensured freedom from the eddy current heating in the fins and wire which might have occurred had dynamic methods been used. A was suspended by a nylon thread from a quartz rod Q, attached in turn to

Fig. 1.

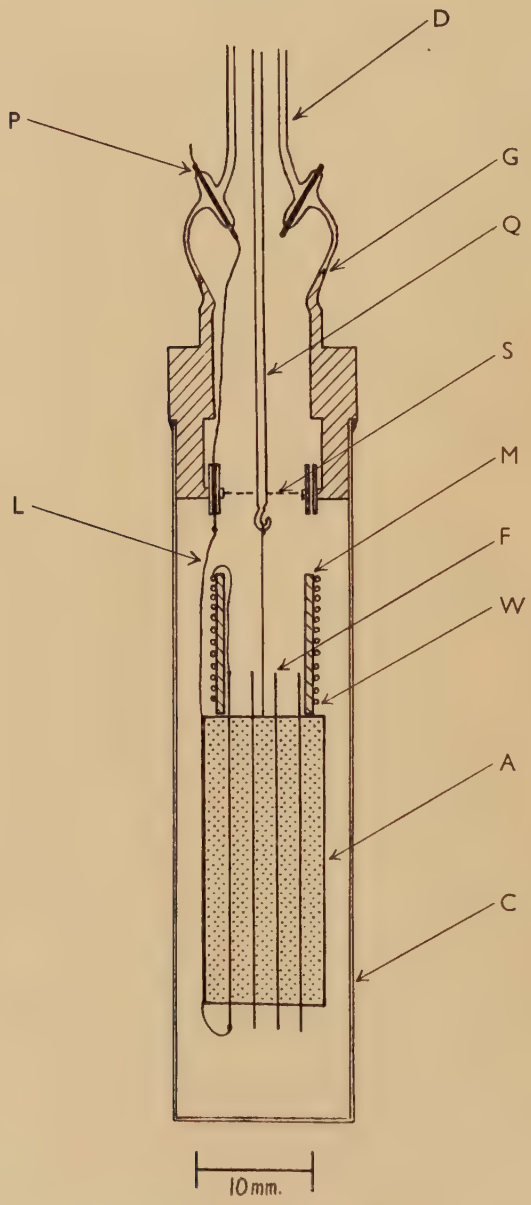

a Sucksmith balance (Sucksmith 1929, Jackson 1933) at the top of the cryostat. A number of flat spiral springs retained the quartz rod centrally inside the glass down-tube D; the lowest of these springs, S, also served

to maintain the top of the nylon thread at the temperature of the helium bath. The assembly was housed in a thin-walled calorimeter C, G being a copper-glass seal. Contact gas could be introduced into the calorimeter and pumped away again.

The dimensions of the wire specimen W were chosen as follows. The smallest voltage that could be measured with the given potentiometer to the required degree of accuracy (50 μV. to 0·2 per cent in our case) was one datum, the other was the need to limit the power dissipation in the wire to a value determined by the area of the fins and the maximum tolerable uncertainty of temperature (in our case, the order of 10^{-1} erg/sec. giving a difference of less than 10^{-3} deg. at 10^{-1} °K. and 3×10^{-3} deg. at 6×10^{-2} °K.; the heat conducted down the leads L also had to be dissipated but this was calculated to be less than 10^{-2} erg/sec. and was negligible). These conditions defined the resistance of W and the measuring current (0·25 ohm and 0·2 ma.), and, when using good conductors like gold, compelled the use of long thin wires. It was then necessary however to check that two further conditions were satisfied. The first was that the diameter so determined was sufficiently great, compared with the mean free path for electron scattering, for the effect on the electrical resistance of scattering by the surface of the wire to be negligible (in our case the diameter was usually at least 10 times the mean free path). The second condition concerned the temperature distribution along the length of the wire; had the wire been thermally isolated from its surroundings, except for ends maintained at the temperature of the fins, its temperature would have varied approximately parabolically along its length because of the generation of Joule heat at all points. In practice, an imperfect thermal contact probably existed with the former M, and the value of the temperature inhomogeneity calculated from estimates of the thermal conductivity of the wire represented an upper limit. Nevertheless the precaution was sometimes taken of connecting one or two points along W to separate fins. (With sections 20 cm. long, the maximum inhomogeneity of temperature was calculated to be of the order of 3×10^{-3} deg. at 10^{-1} °K. and 5×10^{-3} deg. at 6×10^{-2} °K. for most of our specimens.) A final restriction on the experimental conditions was to note that the warming time of the salt after demagnetization was sufficiently long compared with the thermal time-constant of the salt calculated from its known thermal diffusivity (Garrett 1950) and the linear dimension between fins. (This was easily satisfied, even for warming times as low as two hours.)

The above conditions allowed measurements of known maximum uncertainty to be made below 1° K. For measurements on the same specimens at liquid helium temperatures, contact gas was introduced into the calorimeter and the same measuring power introduced negligible errors of temperature. Those specimens which were measured only in the helium range were immersed directly in liquid helium; they were wound on a wax-coated mica cruciform, the wax being later dissolved away to leave the wire hanging freely. Again, during measurement the

rise of temperature of the specimen above that of the bath, due to the Kapitza sub-surface layer of poor thermal conductivity (Kapitza 1941) was kept to a low value with the small power dissipation. (In some measurements done in the past on short, fat specimens of high electrical conductivity, this condition may not always have been satisfied.)

§ 3. Results and Discussion for Gold.

Measurements in Zero Magnetic Field.

The variations of resistance with temperature for three specimens are shown in fig. 2. All were from the same batch of material, the wires being

Fig. 2.

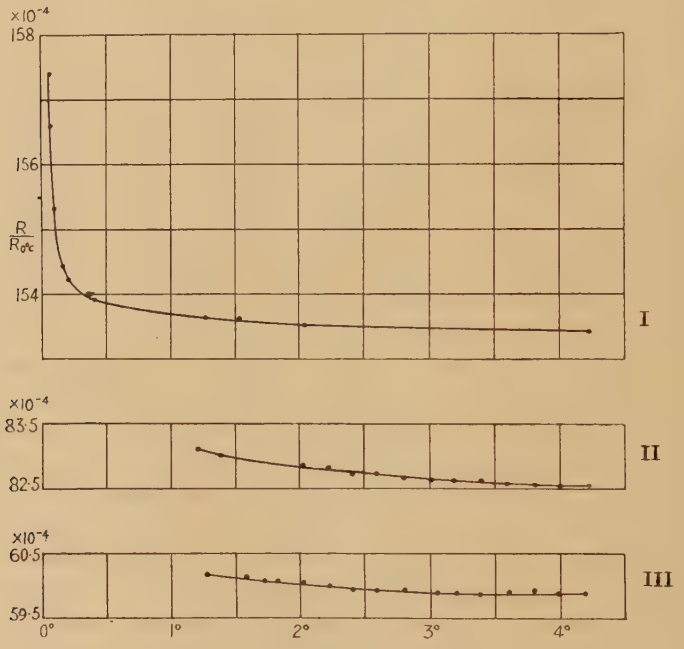

Temperature (deg. absolute).

drawn by Johnson Matthey from their Lab. No. 3459 " by methods where there was virtually no likelihood that they should pick up ferromagnetic impurities ", the spectroscopic analysis of the wire when 0·5 mm. diameter showing the presence of Fe and Ni (all sensitive lines) with Ag, Cu and Mg lines faintly visible and Sn and Na very faintly visible. The specimens were as follows : Curve I., diameter 0·025 mm. not annealed, measuring current 0·18 ma. ; curve II. 0·025 mm. diameter, annealed *in vacuo* for two hours at 500° C., measuring current 5·1 ma. ; curve III., 0·10 mm. diameter, same heat treatment as II., measuring current 20 ma.

It is seen that the resistance still continues to rise at the lowest temperatures reached. van der Leeden (1940) found a term proportional to the concentration of chemical impurity and varying as $T^{-\frac{1}{2}}$ to fit the Leiden results; our results do not fit any simple power law but vary more strongly with temperature than $T^{-\frac{1}{2}}$. Our curves tend to rise more steeply with increasing minimum resistance, in agreement with the observations of previous workers.

Magnetoresistance Experiments.

Magnetoresistive effects are conveniently shown on Kohler diagrams, where the fractional increase in resistance $\Delta R/R$ is plotted as a function of $H \cdot R_{0° C.}/R$, where H is the applied field; curves for different temperatures are then usually superposable (see for example Blom (1950), where however the curve for gold is wrongly drawn). However, Stout and Barieau (1939) found that for a gold wire of high minimum resistance ($R/R_{0° C.} \sim 650 \times 10^{-4}$), which exhibited a marked rise of resistance in the helium range, the magnetoresistance curve for transverse fields at 1·5° K. lay well below that at 4·2° K. The indication was that the effect would have been zero at approximately 1° K.; below this temperature it would presumably have changed sign and a negative magnetoresistance effect was in fact found at 1·5° K. in another specimen by Giauque and Stout (1938). Previously Meissner and Scheffers (1929) noted a negative effect at one temperature, 4·2° K., with a gold wire in small fields. The anomaly was attributed to ferromagnetic impurity in the wire and this was confirmed by Nakhimovich (1941) who made a careful study of the effect of adding iron impurity to the gold. He found that the deviations from Kohler's rule, including a negative magnetoresistance effect, could be observed with gold wires in which of the order of 10^{-2} per cent of iron was dissolved; the presence of the iron made the metal paramagnetic at low temperatures, and of high minimum resistance. The magnetoresistive change could be considered as consisting of two approximately additive components: a "normal" positive component, and an "anomalous" negative component, which was due to the presence of the iron; the positive component could be increased with respect to the other by annealing.

We have measured the transverse magnetoresistance effect in fields up to 10 kilogauss with gold wires from the same batch as those used for measurements in zero field. No anomalous effects were noted, curves from 14° K. down to 1·2° K. being shown in fig. 3; the facts that these are closely superposable and that plotted on a reduced Kohler diagram (Blom 1950) they join on to high-temperature curves for gold and silver seem, in view of the results of Nakhimovich, to indicate that the specimens were free from ferromagnetic impurity—even more free than Nakhimovich's purest specimens. It is possible to make a rough estimate of an upper limit of the concentration of iron in our specimens, by assuming first that Kohler's rule holds for iron-free specimens, and secondly that the

percentage difference between the magnetoresistance effects at approximately 4·2° K. and 1·3° K. for specimens containing iron is proportional to the concentration. On the basis of the trend of the points in fig. 3, compared with the data for Nakhimovich's specimen 13 and Stout and Barieau's specimen, 10^{-4} per cent is set as this upper limit. Though this does not demonstrate that the rise of resistances in zero field takes place in the absence of all ferromagnetic impurity, it would nevertheless seem surprising if 1 part in 10^6 of dissolved iron impurity were the cause of increases plotted in fig. 2.

Fig. 3.

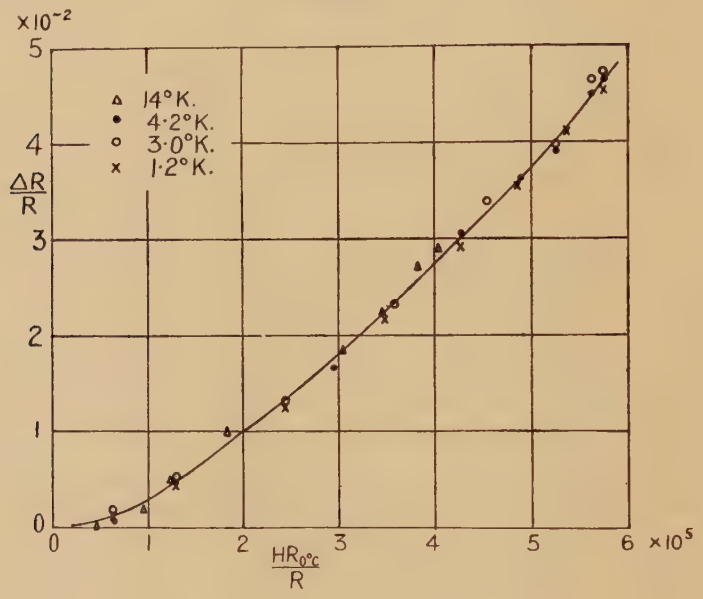

§ 4. Results and Discussion for Silver.

Measurements in Zero Magnetic Field.

The silver specimens were all 0·05 mm. diameter, drawn by Johnson Matthey from their Lab. No. 3406. Spectrographic analysis of the original silver showed the presence of Fe, Mg, Mn, Pb, Si, Cd (faintly visible) and Sn, Na, Cu (very faintly visible). Some resistance-temperature curves are shown in fig. 4. Details of the specimens are as follows: Curves I., II. and III., specimens not annealed; measuring currents 14·5, 2·5, and 0·18 ma. respectively. Another specimen Ag3 gave a curve which coincided within very small limits with curve III. between 4·2 and 1·23° K., (12 ma. measuring current.) It was then annealed for two hours at 450° C. in a vacuum of better than 10^{-5} mm.; curve IV. was then obtained with 14·5 ma. measuring current. It was then given three further heatings to 600° C. in helium gas; curve VI. was later observed using 14·7 ma. measuring current. This specimen was also used for magnetoresistance

Fig. 4.

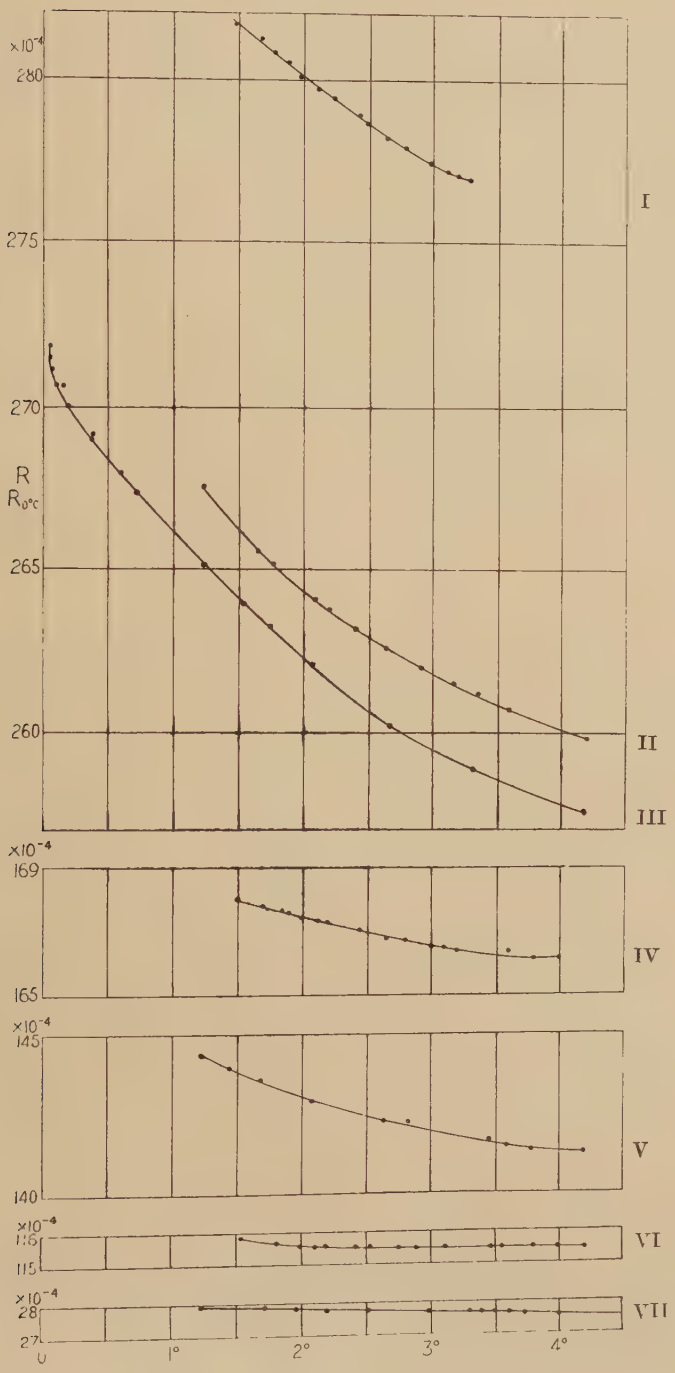

Temperature (deg. absolute).

experiments. Curve V. was for a specimen given the same heat treatment as that for curve IV., with 21 ma. measuring current. Curve VII. is taken for comparison from de Haas and van den Berg (1936) and is for a specimen of Hilger silver drawn down to 0·06 mm. diameter, annealed *in vacuo* at 450–500° C. for three hours ; measuring current not stated.

The increase of resistance with decreasing temperature occurs with all specimens, implying minima in the curves above the helium range. The curves do not fit any simple power law. There is a general tendency for them to rise more sharply as the minimum value of the resistance increases, but this is not observed exactly. As remarked by de Haas and van den Berg (1937) concerning their work on gold, variations in the shape of the curves for unannealed specimens are not unexpected but there exists also a lack of homogeneity between the curves for the annealed specimens, which one might have expected all to have belonged to the same family. The anomalies observed by MacDonald and Mendelssohn (1950) in the resistance-temperature curves of potassium and cæsium may be in some way analogous to these variations. It is also possible that the effects of dissolved gases, undetected spectroscopically, but capable of varying in amount and distribution on annealing, may be important.

Magnetoresistance Experiments.

The specimen measured by Stout and Barieau (1939) (which in zero field gave $R/R_{0^\circ C.}=194{\cdot}2\times10^{-4}$, constant throughout the helium range) followed Kohler's rule in its transverse magnetoresistive behaviour, their curves for temperatures from 20·3° K. down to 1·54° K. being closely superposable ; the dotted line in fig. 5 is for this specimen.

Our specimen Ag3 however gave different results, similar in some but not all respects to the results for gold contaminated with iron. In fig. 5 are shown the curves in transverse fields at 4·2° K. and 1·23° K. for the specimen before annealing. After the first annealing however the effect plotted in this way was quite unchanged, though the resistance at any temperature had been greatly reduced. As mentioned above Nakhimovich noted a different result for gold, namely a tendency to reduce the departures from Kohler's rule after annealing. It is conceivable that this difference of behaviour is in some way connected with the fact that iron, though it can dissolve in gold, is insoluble in silver (Constant 1945) so that the effects of annealing on the impurity are likely to be very different.

§ 5. Results and Discussion—Copper.

Three samples of enamel-covered commercial copper wire were investigated, and the results are shown in fig. 6. All samples showed traces of Ca, Cd, Mg, Si, Pb, Mn and Zn on spectroscopic analysis, the total impurity content being estimated at less than 10^{-2} per cent. The wire for Curve I. was 0·035 mm. diameter, and the measuring current 0·2 ma. ; for Curve II. 0·05 mm., 0·18 ma. ; for Curve III. 0·10 mm., 4·5 ma. None was annealed. The comparative lowness of the residual

Fig. 5.

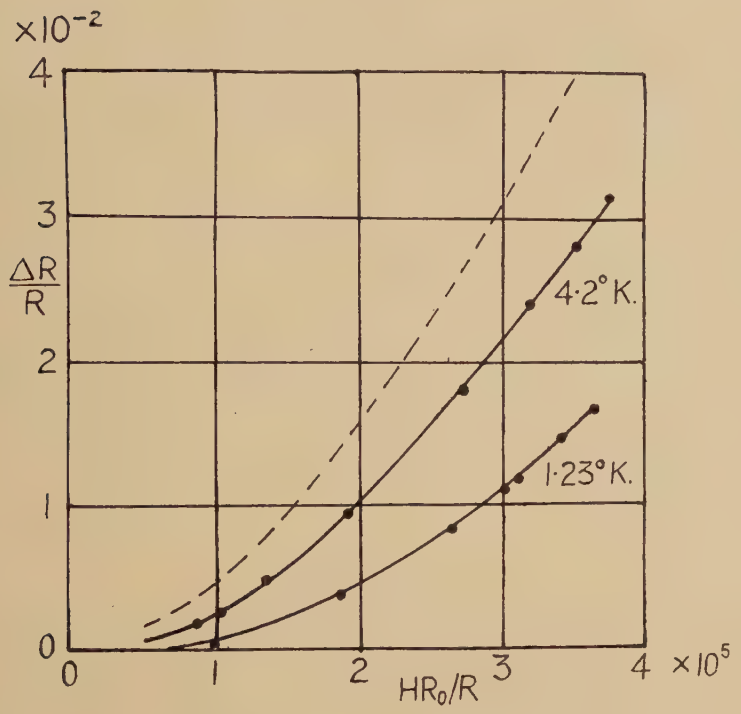
×10⁻²
4
3
ΔR/R
2
1
0
0
1
2
3
4
×10⁵
HR₀/R
4·2° K.
1·23° K.

Fig. 6.

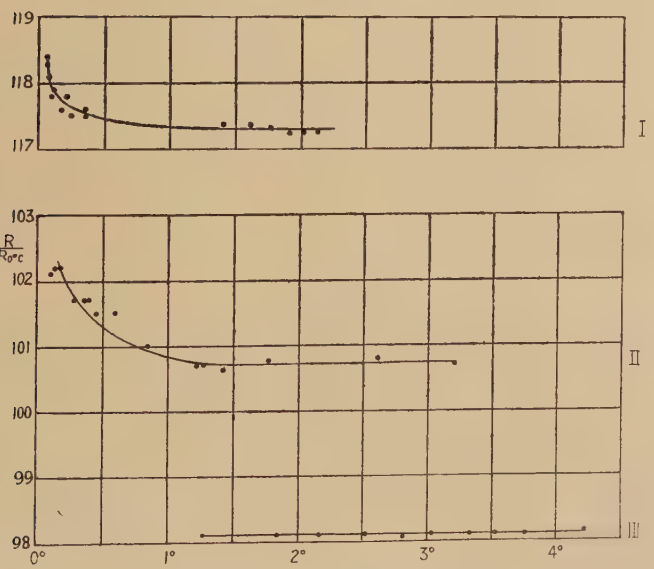
119
118
117
I
103
R/R₀°c
102
101
100
99
98
II
III
0°
1°
2°
3°
4°
Temperature (deg. absolute).

resistances was unexpected when Curves I. and II. were measured, with the result that the measuring accuracy for both these curves was not high. The rise of resistance at the lowest temperatures is nevertheless outside experimental error.

One further sample from a reel of copper wire, 0·035 mm. in diameter, of curious composition was also investigated. It contained 0·94 per cent of Sn, and also showed traces of Mn. It had a very high resistance at helium temperatures (Allen 1933), and the following values of $R/R_{0°C}$ were noted: 4·19° K., 0·4322; 2·50° K., 0·4324; 1·46° K., 0·4325; 0·418° K. 0·4326; 0·067° K., 0·4327.

Previous investigations of copper have given the following results. The readings of Meissner and Voigt (1930) show variations at liquid helium temperatures which are probably due to experimental error. de Haas and van den Berg (1934) found that the curves for several samples of pure copper were not parallel at liquid hydrogen temperatures; van den Berg (1948) found that unannealed technical copper wires gave constant residual resistances at liquid helium temperatures.

No magnetoresistance measurements have so far been taken on copper.

§ 6. Conclusion.

It appears from previously published work and from our own experiments that the rise of resistance at very low temperatures is a phenomenon occurring in a fairly large number of metals. It has only been noted so far in specimens which were far from being ideally pure, but in any case theory gives no indication as to the cause of the rise in connection either with pure or impure metals. It remains undecided, however, whether the rise is to be associated with the presence of small amounts (less than 1 part in 10^6 in our gold specimens) of ferromagnetic impurity. It also appears to be a fairly common occurrence that resistance-temperature curves for different specimens of a given metal do not always vary from one to another in a simple manner as the impurity is varied (see for example the curves for copper given by de Haas and van den Berg (1934) and our own curves for silver (above)). Presumably this means that different impurities may produce curves of the same minimum value of resistance but of different shapes.

Acknowledgments.

The thanks of the authors are due to Dr. L. C. Jackson for much help and advice at all stages of the work, to the other members of the low temperature Group for assistance during experiments, and to Professor N. F. Mott for discussions.

The analyses of the copper wires were kindly carried out by the Research Department of the National Smelting Co., Avonmouth, and by the City Analyst, Bristol.

One of us (J. G. T.) is in receipt of a grant from the Department of Scientific and Industrial Research.

References.

Allen, J. F., 1933, *Phil. Mag.* [7], **16,** 1005.
Blom, J. W., 1950, *Physica*, **16,** 152.
Boorse, H. A., and Niewodniczanski, H., 1936, *Proc. Roy. Soc.* A, **153,** 463.
Constant, F. W., 1945, *Revs. Mod. Phys.*, **17,** 81.
de Haas, W. J., de Boer, J., and van den Berg, G. J., 1934, *Physica*, **1,** 1115.
de Haas, W. J., Casimir, H. B. G., and van den Berg, G. J., 1938, *Physica*, **5,** 225.
de Haas, W. J., and van den Berg, G. J., 1936, *Physica*, **3,** 440 ; 1937, *Ibid.*, **4,** 683.
Fröhlich, H., 1950, *Phys. Rev.*, **79,** 845.
Garfunkel, M. P., Dunnington, F. G., and Serin, B., 1950, *Phys. Rev.*, **79,** 211.
Garrett, C. G. B., 1950, *Phil. Mag.* [7], **41,** 621.
Giauque, W. F., and Stout, J. W., 1938, *J. Amer. Chem. Soc.*, **60,** 388.
Giauque, W. F., Stout, J. W., and Clark, C. W., 1937, *Phys. Rev.*, **51,** 1108.
Gorter, C. J., 1938, *Physica*, **5,** 483.
Jackson, L. C., 1933, *Proc. Roy. Soc.* A, **140,** 695.
Justi, E., 1942, *Forschungen u. Fortschritte, Berlin*, **18,** 7 ; 1948, *Ann. Phys., Lpz.*, **3,** 183.
Kapitza, P. L., 1941, *J. Phys., U.S.S.R.*, **4,** 181.
Keesom, W. H., 1933, *Commun. Phys. Lab. Univ. Leiden*, No. 224c ; 1934, *J. Phys. Radium*, **5,** 373.
Lane, C. T., 1949, *Phys. Rev.*, **76,** 304.
MacDonald, D. K. C., and Mendelssohn, K., 1950, *Proc. Roy. Soc.* A, **202,** 103, 523.
Meissner, W., and Scheffers, H., 1929, *Phys. Z.*, **30,** 827.
Meissner, W., and Voigt, B., 1930, *Ann. Phys., Lpz.*, **7,** 761, 892.
Mendoza, E., 1948, *Cérémonies Langevin-Perrin, Paris*, 53.
Nakhimovich, N. M., 1941, *J. Phys., U.S.S.R.*, **5,** 141.
Sondheimer, E. H., and Wilson, A. H., 1947, *Proc. Roy. Soc.* A, **190,** 435.
Steiner, K., and Fünfer, E., 1936, *Congrès Int. du Froid, s'-Grav.*, **1,** 388.
Stout, J. W., and Barieau, R. E., 1939, *J. Amer. Chem. Soc.*, **61,** 238.
Sucksmith, W. 1929, *Phil. Mag.* [7], **8,** 158.
van den Berg, G. J., 1948, *Physica*, **14,** 111.
van der Leeden, P., 1940, *Thesis*, Leiden.
Vonsovsky, S. V., 1940, *J. Phys., U.S.S.R.*, **2,** 113.
Woltjer, H. R., and Kamerlingh Onnes, H., 1924, *Commun. Phys. Lab. Univ. Leiden*, No. 173 a.

XXXIV. *On Pair Production by Fast Electrons.*

By J. E. Hooper, D. T. King and A. H. Morrish,
The H. H. Wills Physical Laboratory, University of Bristol *.

[Received January 18, 1951.]

[Plate XIII.]

Summary.

A study has been made of electron " pairs " directly produced by fast electrons in photographic emulsions. Evidence is presented to show that this process is of importance in the development of electromagnetic cascades present in the " soft " component of the cosmic radiation. It is found that the variation with energy of the cross-section for the interaction agrees with that predicted by theory.

§ 1. Introduction.

Observations on the creation of electron " pairs " by fast electrons in photographic emulsions have been reported by Occhialini (1949) and by Bradt, Kaplon and Peters (1950). In this laboratory we have now searched, with immersion objectives, 2·8 cm.^{3} of electron-sensitive emulsion exposed to the cosmic radiation at an altitude of 22 km. ; and we have found 80 examples of these so-called " trident " or " giraffe " events. Of these, the path-length in the emulsion, either of the " primary " or of the three " secondaries ", is in 50 cases of sufficient length to permit a determination of the energy of the primary electron by the scattering method.

In favourable examples it is possible to make measurements of the energy of all the particles associated with a given " trident ". In almost all such cases, we have found that the energy of the primary particle is equal to the sum of the energies of the out-going particles, within the limits of experimental error. Such a conservation of energy is confirmed by the work of Dilworth *et al.* (1950), who have, in addition, found strong evidence that charge is also conserved in the interaction. In those events in which the energy of the primary particle cannot be directly measured we can, in favourable cases, infer it from the total energy of the three secondaries. In determining the energies of particles we have adopted scattering constants and procedures recently developed by our colleagues in this laboratory and shortly to be published.

The formation of secondary electrons as a result of interactions between fast charged particles and the Coulomb field of nuclei was suggested by Oppenheimer. Studies of theoretical aspects of such processes have been made by Furry and Carlson (1933) and many other authors. Bhabha (1935) has extended the treatment to include the effects of screening and gives an extensive bibliography to the earlier work.

* Communicated by Professor C. F. Powell, F.R.S.

§ 2. Identity of the Trident Particles.

Two examples of tridents are shown in Pl. XIII. In A, two of the secondary particles originating at P are of relatively low energy and cannot have a rest-mass greater than $100m_e$. We may, therefore, with confidence, assume them to be electrons. Event B is typical of those in which the energy of the primary is shared almost equally among the three secondary particles. In such tridents, the origin is indicated by an apparent sudden increase in the grain density of the primary track, clearly seen at P. The collimation of the three tracks is so close that they are only just resolvable under high magnification at a point 300 microns from P ; and they are not separated to the extent shown by event A until a point several millimetres from their origin has been reached.

A number of observations give strong support for the view that at least most of the primary charged particles which produce pairs are electrons. It is well known that there are difficulties, in principle, in distinguishing between the tracks of particles, of charge $|e|$ but of different rest-mass, when they are moving with great kinetic energy. Recent evidence from this laboratory strongly suggests, however, that the fast "shower" particles emerging from nuclear interactions are exclusively or almost exclusively, π-mesons or protons (Camerini *et al.* 1950). We have never observed pair-production by such a particle.

Further, the tracks of electrons of great energy can commonly be identified, if the length in the emulsion is greater than 2 cm., as a result of the reduction in energy of the particles through the creation of *bremsstrahlung* ; and we have frequently observed such effects in dealing with the primary particles of tridents.

Finally, tridents are occasionally found to be produced by one of the components of an electron pair created by a photon ; and in favourable cases, when there is a considerable length of path in the emulsion, they may be observed to be associated with electron cascade phenomena. An example of such an event is shown in the line drawing reproduced in fig. 1. In this case the primary particle of the trident is a fast recoil particle, almost certainly an electron, produced by an energetic heavy particle of charge $|e|$. The lateral scale in this diagram has been extended by a factor of 50, relative to the longitudinal, so that the characteristics of the different tracks may be displayed. The evidence for the electronic nature of the secondary particles is easier to obtain. They are frequently of such low energy that their rest-mass can be shown, as a result of scattering measurements, to be less than $100m_e$. We therefore regard the evidence as very strong that both the primary and secondary particles of the trident events are electrons.

§ 3. Tridents as a Distinct Physical Process.

It has been suggested to us by Professor Peierls that the trident events might be due, not to the direct production of a pair of electrons by the charged primary particle, but to *bremsstrahlung* γ-rays, which by chance,

have converted to electron pairs at points very close to the track of the parent electron (Hooper and King 1950). In order to examine this point we have made the following observations :—In the searched area of the plates we have found 150 pairs which evidently occur as a result of the cascade process in the emulsion-glass assembly. Events of this type may be seen in fig. 1. The perpendicular distance R, from the point of origin of the pair to the nearest parallel track, has been measured in each of these examples, and the distribution in R is shown in fig. 2.

Fig. 1.

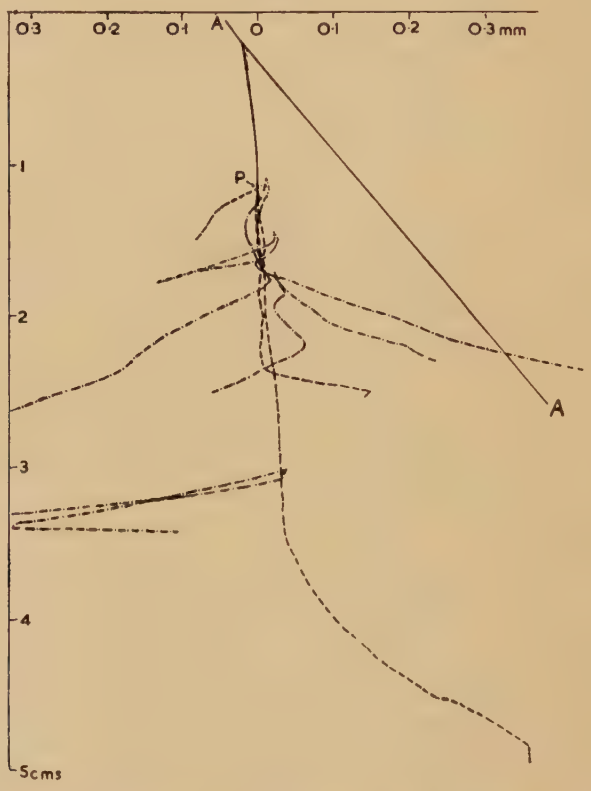

A reproduction of the tracks of a cascade shower plotted on a scale greatly extended laterally. AA represents the track of the heavy particle, and a trident is formed at P on the recoil electron track. The dashed lines indicate trident secondaries and the dot-dash lines the tracks of electrons from pairs.

The magnitude and shape of this distribution at small values of R appears to be inconsistent with the view that the 80 tridents ($R<0{\cdot}25\,\mu$), are due to the same process. In such a case the distribution in the values of R would include those for the tridents ($R<0{\cdot}25\,\mu$) and would show a very sharp peak for very low values of R, followed by a slowly decreasing frequency from $R=0{\cdot}5\,\mu$ to $20\,\mu$. We have not calculated the distribution in the values of R to be expected from cascade theory, for it involves

extensive integrations, but it appears certain that it could not yield a distribution such as is obtained if the tridents are attributed to the conversion of photons. We therefore regard the observations as providing very strong evidence that most of the tridents are due to the direct production of pairs of electrons in the interactions of fast electrons with atomic nuclei.

§ 4. The Cross-Section for Trident Production.

It appears to be possible, in principle, to determine the cross-section for the interaction leading to production of tridents, and its variation with energy, by measuring the total length in the searched area of the plates of electrons in different energy intervals ; and by comparing the results thus obtained with the corresponding numbers of observed tridents. Such an experiment demands, however, a very extensive investigation, for it depends on an identification of the electrons by the methods to which we have already referred. For this purpose only particles of great range in the emulsion can be employed and they are rarely observed.

Fig. 2.

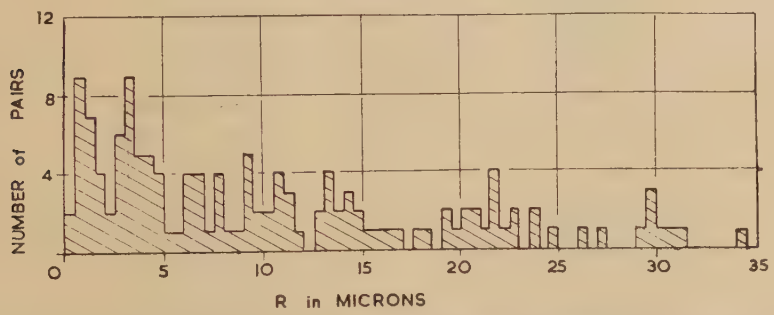

Distribution in the values of the perpendicular distance, R, from the pair origin to the nearest parallel track. There are 14 events with $R > 35$ microns. The 80 tridents ($R < 0{\cdot}25\,\mu$), found in the same volume, would contribute a peak in the first interval.

In these circumstances, we have determined the relative values of the cross-section as a function of the energy of the primary electrons. This can be done since the distribution in energy of the electrons in the plates employed has already been determined (Carlson *et al.* 1950). We assume the track length L—in the total volume of emulsion examined—due to electrons with energy between E and E+dE to be represented by the equation

$$L(E)\,dE = aE^{\gamma}\,dE, \quad . \quad . \quad . \quad . \quad . \quad . \quad . \quad . \quad (1)$$

where a is a constant, and $\gamma = -1{\cdot}7$.

The distribution in the values of the energy of the primary particles of the 50 tridents on which it has been possible to make measurements, are shown in fig. 3. Fig. 4 shows the corresponding relative values of the cross-section for six energy intervals between 60 and 16,000 MeV.

It is possible to determine a mean, absolute, value of σ over a very large energy interval, by considering those tridents which occur on one of the tracks of an electron pair created in the emulsion. These are then compared with the total track length of electrons, in the same energy interval, which originate in pair events in the emulsion.

Fig. 3.

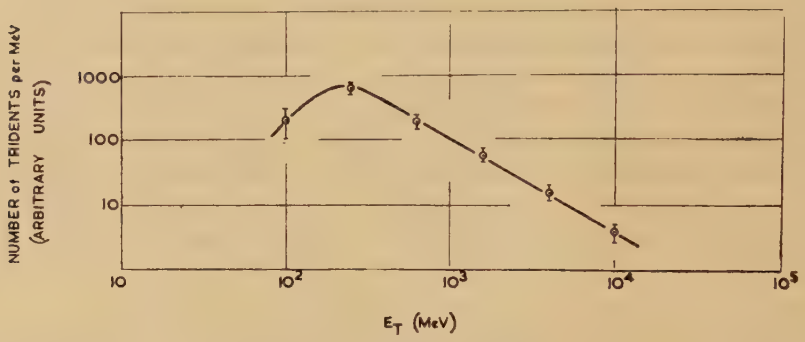

The distribution, per unit energy interval, of the frequency of occurrence of tridents observed in Ilford G5 emulsions.

Fig. 4.

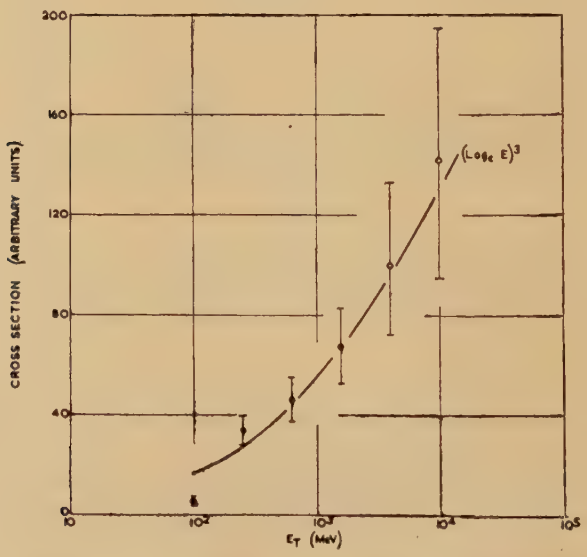

The observed variation with energy of the trident cross-section. The curve represents the theoretical variation normalized to the point at 1600 MeV.

It may be shown that the expected number of tridents in the energy interval from E_1 to E_2 is given by the relation

$$N_{E_1}^{E_2} = aK \int_{E_1}^{E_2} E^{\gamma} \left\{ \log \frac{E}{mc^2} \right\}^3 . dE, \qquad . . . . . \quad (2)$$

Examples of two tridents. The creation by a fast electron of a pair (A) of low energy and wide divergence may be contrasted with one (B) of high energy and marked collimation. In both events the primary energy is about $1{\cdot}3 \times 10^4$ MeV.

where a is defined in (1) and K is a constant depending on the absolute cross-section. Since we have observed only four tridents to originate on an arm of a pair, the value of 80 cm. obtained for the trident " mean free path " at $E=10^3$ MeV. is subject to a large statistical error, of the order of 70 per cent. The observed value is, however, consistent with that calculated by Ravenhall; viz. 99 cm. It will presumably be possible, for values of E up to 300 MeV., to determine an accurate absolute value for the trident cross-section in experiments with electrons from high energy accelerators.

Acknowledgments.

We are indebted to Professor C. F. Powell, F.R.S., for extending to us the hospitality and facilities of this laboratory. We also wish to thank Mrs. J. Cowie, Mrs. D. M. Ford, Miss J. Jones, Miss M. Jones and Miss J. Witchell for their assistance in collecting the data. The authors were supported by grants from the Department of Scientific and Industrial Research, the Medical Research Council and the National Research Council of Canada, respectively. This work has been carried out as part of a research programme supported by the Department of Scientific and Industrial Research.

References.

Bhabha, 1935, *Proc. Roy. Soc.* A, **152,** 559.
Bradt, Kaplon, and Peters, 1950, *Helv. Phys. Acta.*, **24,** 23.
Camerini, Fowler, Lock, and Muirhead, 1950, *Phil. Mag.*, **41,** 413.
Carlson, Hooper, and King, 1950, *Phil. Mag.*, **41,** 701.
Dilworth, Goldsack, Goldschmidt-Clermont, and Levy, 1950, *Phil. Mag.*, **41,** 1032.
Furry, and Carlson, 1933, *Phys. Rev.*, **44,** 237.
Heitler, 1944, *Quantum Theory of Radiation*, 2nd. Ed. (Oxford: University Press).
Hooper, and King, 1950, *Phil. Mag.*, **41,** 1194.
Occhialini, 1949, *Nuovo. Cim. Supp.*, **6,** 3, 413.
Ravenhall, 1950, *Proc. Phys. Soc.* A, **63,** 1177.

XXXV. CORRESPONDENCE.

Intrinsic Crystalline Structure and the Strength of Metals.

By W. A. Wood,
The Baillieu Laboratory, University of Melbourne*.

[Received January 1, 1951.]

In his paper "On the Strength of Quasi-Isotropic Solids", Fürth (1949) makes use of the idea that a solid contains an intrinsic block structure and derives a relation, similar to one obtained by Bragg, in which the strength varies inversely as the size of the blocks. Discussing the source of the structure, he suggests that the blocks might be accounted for by a recent theory due to Born, and goes on to imply that this theory would also explain the block structure in metals proposed by my colleagues and myself on the basis of X-ray diffraction work. This paper has been followed by a note by Paterson (1950) who queries these suggestions on the grounds that Born's theory predicts a decrease in size of the blocks with increase of temperature. According to Paterson it ought then to follow from Fürth's hypotheses that a metal is stronger at higher temperatures, and that the X-ray diffraction lines from a deformed metal show greater broadening at higher temperatures of deformation. But, in practice, both these effects usually go the other way.

It would be unfortunate, however, if the matter were allowed to rest at that, for the block theory of strength is the only one of any promise, being the only one that can be substantiated by direct observation. It might be worthwhile pointing out therefore that the arguments advanced by Paterson are less conclusive than they might seem at first sight. The essential point of the block theory should be that the strength, and the X-ray pattern, depend on the production in the structure of elements that are "dislocated" or "disoriented"; for only when they are dislocated or disoriented sufficiently can they provide sub-boundaries that are effective barriers to slip, or become incoherent X-ray reflectors. But there is no reason why these disoriented elements should always coincide with the ultimate blocks in any and every type of mechanical test; they could be multiples of ultimate blocks; and this aspect, as indicated below, is especially relevant in tests at higher temperatures.

We think it is so important to distinguish between the actual "disoriented elements" and the intrinsic ultimate blocks that it might be useful to illustrate the point by referring to the X-ray results. In

---

* Communicated by the Author.

these, the fundamental observation is that the process of deformation reduces the grains of a metal to disoriented elements. If the deformation is drastic enough the elements become very small, but for a given metal they do not become smaller than a characteristic minimum size. Now it is evident that the breakdown could not be produced at all unless the grains in the first place contained enough lines of planes of weakness. Whether these faults form a static or dynamic pattern in the grain it is impossible to say. Nor, so far as the strength is concerned, does it matter ; for the only way of measuring the strength is by deforming the metal and as soon as the metal is deformed an observable disoriented substructure is produced at once. Therefore, for all practical purposes, we may speak of an intrinsic sub-structure, and this sub-structure has a lower limiting size.

The next observation is that the size of the actual disoriented elements into which the grain breaks up is determined by the conditions of deformation, and in particular by the temperature and rate of strain. Thus, to quote from actual experiment : if aluminium of grain size 10^{-2} cm. is strained at 300° C. at a rate of 0·1 per cent per hour, the resulting sub-structure is coarse ; the size of the elements is about 10^{-3} cm., as against an ultimate crystallite or block size of less than 10^{-4} cm. for deformation at room temperature. At first sight it might appear that at the higher temperature the pattern of faults in the grain before deformation is spaced more widely, so that the grains could break down to correspondingly coarse elements only. But this is not so ; for we can break the grains down to a finer sub-structure merely by increasing the rate of strain at the same temperature, and there is no doubt that by a sufficiently fast rate of strain we could break them down to the characteristic lower limiting size.

Further, direct observations show clearly that the strength exhibited by the metal under given conditions of deformation is primarily determined by the size of the actual disoriented elements produced by that deformation. Using the aluminium again as example, we find that during deformation at 300 ° C. at an extremely slow rate the grains do not break down at all ; this is because the deformation presumably occurs mainly by viscous flow at the grain boundaries, but this aspect here is immaterial. The relevant point is the parallel observation that in the absence of breakdown the metal exhibits little or no resistance to the applied strain ; its strength is negligible. This is one extreme. But if we increase the rate of strain at the same temperature we break down the grains and the sub-structure becomes increasingly finer as the rate of strain is greater ; and at the same time we find that the resistance or strength of the metal increases in proportion. Conversely, we can change the fine sub-structure back into a coarse sub-structure, still at the same temperature, by reducing the rate of strain again ; then we find the strength exhibited by the metal is again reduced. Because of this interdependence of sub-structure, temperature and strain-rate, it can be shown that a

specimen strained rapidly at an elevated temperature may be stronger than one strained slowly at a lower temperature. By experiments such as these it is not difficult to demonstrate that the strength follows the size of the sub-structure.

These illustrations will therefore serve to indicate that the block theory of strength is on the right lines. It is true that in the form usually advanced by theoretical workers it is often open to criticism, of which the remarks by Paterson on the Fürth theory are an example. But the weakness of this theory as it stands (and of the corresponding Bragg theory) is not in the assumption of an intrinsic block structure, but in failing to take into account the experimental observation that the operative elements are not always the ultimate blocks ; they may contain a group of blocks. It is also clear, however, that the block theory can easily be brought into line with experiment if so desired.

Quadruple Moments and the Nuclear Shell Model.

By B. Touschek,
Department of Natural Philosophy, The University, Glasgow*.

[Received January 22, 1951.]

It has been pointed out by Hill (1949) that the quadrupole moments of atomic nuclei are in reasonable qualitative agreement with the nuclear shell model recently suggested by Haxel, Jensen and Süss (1949, 1950) and M. G. Mayer (1949, 1950). We want to show that this model makes quite definite predictions about the quadrupole moments of a certain category of odd nuclei and that on the whole these predictions are in good agreement with experiment. One should expect that the quadrupole moments of nuclei of the form $(A-Z, Z)=(M, M\pm1)$, where M is one of the magic numbers 8, 20, (28, 40), 50, 82, 126 should be determined by the odd proton alone, since the contribution to the quadrupole moment of the closed shells is zero. The periodic table shows two nuclei of this type : ${}_{19}K^{41}_{20}$ and ${}_{83}Bi^{209}_{126}$. The quadrupole moment from a proton in a state with spin j should be

$$Q=\pm C\frac{2j-1}{2j+2}\overline{r^2}\ ,$$

where the $-$ sign corresponds to a nucleus $(M, M+1)$ as ${}_{82+1}Bi$ the $+$ sign to a nucleus $(M, M-1)$ as ${}_{20-1}K$. $C=(1-(2A-Z)/A^2)$ is a factor correcting for the motion of the mass centre and $\overline{r^2}$ is the average square distance of the odd (or missing) proton. It is obvious that the sign of the quadrupole moment predicted for K^{41} is wrong (as noticed by Hill), but the present experimental value is hardly more than an estimate.

---

* Communicated by the Author.

Determining $(\overline{r^2})^{\frac{1}{2}}$ for Bi one finds a value $7{\cdot}4\times10^{-13}$ cm. which is fairly near to the fast neutron radius ($\sim9{\cdot}10^{-13}$ cm.). A further category of nuclei for which simple predictions can be made are odd proton nuclei with spin 3/2. Since the neutrons can only contribute very little to the quadrupole moment (via the centre of gravity motion, their contribution being $Z/A^2\times$smaller than that of a free proton) the quadrupole moment must stem from the protons. According to the shell theory the spin 3/2 should only occur in connection with a shell of spin 3/2, so that an odd proton can only mean one or three protons in a 3/2 shell. The prediction of the shell theory is therefore

$$Q=\pm\frac{2}{5}C\overline{r^2}$$

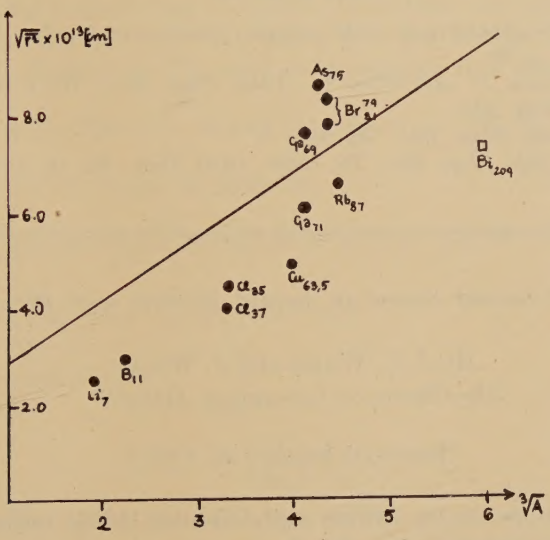

the $+$ sign holding for the case of three odd protons. In the figure $\sqrt{(\overline{r^2})}$ for such nuclei is plotted against $A^{1/3}$ and it is seen that the general trend of the curve is in good agreement with the curve (drawn out) representing the nuclear radii as measured by fast neutron experiments (Gamow and Critchfield 1949). It is worth noting that the positions of isotopes are according to their neutron numbers. Thus Cl^{37} with a magic neutron number (20) lies lower than Cl^{35}, Ga^{71} (40) lower than Ga^{69} (38), and the positions of the Bromine isotopes may be due to the approach of the magic number 50. Bi with 126 neutrons lies comparatively low, and the high quadrupole moment of As may be due to the small no. (2) of neutrons in the $g_{9/2}$ shell. That the fluctuations in the case of quadrupole moments tend to be greater than those for the fast neutron radii seems to be a confirmation of a one particle picture, which will naturally lead to larger fluctuations than the statistical picture applicable to the determination of neutron radii.

That the odd neutron nuclei should have quadrupole moments comparable in size with the odd proton nuclei need not be a contradiction to the shell model, since the cancellation of the proton spins in pairs does not imply a simultaneous cancellation of the quadrupole moments. The check of these moments would require the determination of the contribution to the quadrupole moment of an arbitrary number of particles in an unfinished shell. A few quadrupole moments (as those of Eu) are very large (about three times the size of the moments shown in the figure), and it is quite plausible to assume that they are the result of collaboration between three or more protons. This is further enhanced by the fact that none of the nuclei with "abnormal" quadrupole moments has a spin $<5/2$.

REFERENCES.

GAMOW, W., and CRITCHFIELD, 1949, *Atomic Nuclei and Nuclear Energy Sources* (Oxford), p. 10.
HAXEL, O., JENSEN, J., and SÜSS, H., 1949, *Phys. Rev.*, **75**, 1766; 1950, *Zeits f. Phys.*, **128**, 294.
HILL, R. D., 1949, *Phys. Rev.*, **76**, 998.
MAYER, M. G., 1949, *Phys. Rev.*, **75**, 1969; 1950, *Ibid.*, **78**, 16, 22.

The Velocity of Second Sound in Liquid Helium near the Absolute Zero.

By J. C. WARD and J. WILKS,
The Clarendon Laboratory, Oxford*.

[Received January 25, 1951.]

RECENT measurements by Atkins and Osborne (1950) indicate that the velocity of second sound in liquid helium approaches the value 150 m./sec. at absolute zero, which is in agreement with Landau's prediction of $C/\sqrt{3}$ where C is the velocity of ordinary sound. Landau (1941) obtained this expression from the usual two fluid formula for second sound $C_2=(TS^2/C)(\rho_s/\rho_n)$ where (ρ_s/ρ_n) was calculated in a rather obscure way from a model in which liquid helium at sufficiently low temperatures is represented by a phonon gas. However it is possible to derive the expression $C/\sqrt{3}$ directly from the phonon gas model without having recourse to the two fluid theory at all.

We follow Landau in representing liquid helium near the absolute zero by a phonon gas consisting of the elementary (Debye) excitations, for which $E=pC$ where C is the velocity of ordinary sound and may be taken as constant. We also assume that at these temperatures interactions in the helium are very small so that the collisions between phonons are elastic and conserve momentum. Actually Landau makes all these

---

* Communicated by the Authors.

assumptions in calculating (ρ_s/ρ_n). Suppose now that a compressional "sound" wave is propagated through this phonon gas, then there will be periodic variations of the phonon density. These periodic variations in the model will correspond to temperature variations in liquid helium, that is to second sound.

Hence the velocity of second sound is the velocity of a sound wave in a phonon gas where the conservation laws of energy and momentum hold and also the relation $E=pC$. The expression for this velocity will be similar to that for the velocity of a sound wave in a photon gas for that too depends only on the two conservation laws and the relation $E=pC_l$.

The velocity of sound in a relativistic gas has been given by Hoffmann and Teller (1950) for the general case when a magnetic field is present. We may derive the same answer for the velocity in a phonon gas more directly by using a result due to Curtis (1950) that the velocity of sound in general relativity is $\sqrt{(\partial P/\partial \eta)}$ where η is the energy density. In a photon gas η is defined by $\Sigma E=\eta C_l^2$ so by analogy in a phonon gas

$$\eta C^2=\Sigma E=v\int_0^\infty A\{\exp(pc/kT)-1\}^{-1}.pc.dp. \quad . \quad . \quad . \quad . \quad (1)$$

Now the pressure of the gas is given by

$$P=\iint(\tfrac{1}{2}vc\sin\theta\cos\theta\,d\theta)(2p\cos\theta.A\{\exp.(pc/kT)-1\}^{-1}dp)$$

$$=\tfrac{1}{3}vc\int_0^\infty Ap\{\exp.(pc/kT)-1\}^{-1}dp. \quad . \quad . \quad . \quad . \quad . \quad . \quad . \quad . \quad (2)$$

Comparing (1) and (2)

$$P=\tfrac{1}{3}\eta C^2,$$

$$C_2=\sqrt{\left(\frac{\partial P}{\partial \eta}\right)}=C/\sqrt{3}.$$

This derivation gives no indication of the region in which we may expect this expression to be valid. Clearly it will fail if (*a*) the collisions between phonons do not satisfy the conservation laws of energy and momentum and (*b*) if the excitations of the liquid cannot be adequately represented by phonons. All we can say is that if at a sufficiently low temperature the specific heat of the liquid varies as T^3 then we should expect the velocity of second sound to be $C/\sqrt{3}$. It seems possible that this method could be used to predict the velocity at higher temperatures provided we knew a satisfactory expression for the other types of excitation which may occur. Landau in his theory covers the region above 0·6° by introducing excitations called rotons but we can see no theoretical basis for his expression for them.

As this model could also be used to represent a crystalline solid at low temperatures, it emphasizes a suggestion by Peshkov (1947) that second sound might be observed in crystals*. As he points out it will be necessary

* It is interesting to note that Nernst (1917) suggested that in good thermal conductors at low temperatures heat might have sufficient inertia to give rise to an oscillatory discharge.

to experiment with a crystal in which the scattering of phonons by inhomogeneities and irregularities is a minimum. In a pure crystal however the essential criteria for second sound are probably that the number of elastic collisions between the phonons should be sufficient to ensure that the phonon gas is not in the Knudsen region while at the same time very few collisions of the umklapp type should occur. (This is important because in this kind of collision it is inadmissable to apply the momentum conservation law (Peierls 1929)). Measurements of thermal conductivity by Berman *et al.* (1950) and Wilkinson and Wilks (1951) have shown that the number of umklapp type collisions rapidly decreases as the temperature falls and should be negligible in the region where the conductivity is limited by size effect. Therefore we intend to look for second sound in a corundum crystal at helium temperatures where umklapp collisions should be rare.

References.

Atkins, K. R., and Osborne, D. V., 1950, *Phil. Mag.*, **41**, 1078.
Berman, R., Klemens, P. G., Simon, F. E., and Fry, T. M., 1950, *Nature, Lond.*, **166**, 864.
Curtis, A. R., 1950, *Proc. Roy. Soc.* A, **200**, 248.
Hoffmann, F. de, and Teller, E., 1950, *Phys. Rev.*, **80**, 692.
Landau, L., 1941, *J. Phys. U.S.S.R.*, **5**, 71.
Nernst, W., 1917, "*Die theoretischen . . . . Grundlagen des n. Wärmesatzes*" (Halle : Knapp).
Peierls, R. E., 1929, *Ann. Phys. Lpz.*, **3**, 1055.
Peshkov, V., 1947, *Report on Cambridge Low Temperature Conference* (London : Physical Society), p. 19.
Wilkinson, K. R., and Wilks, J., 1951 *Proc. Phys. Soc.* A, **64**, 89.

[*The Editors do not hold themselves responsible for the views expressed by their correspondents.*]